The Role of Early Autocrine IL-2 Signals in Programming Antigen-Specific CD8 T cell Responses

Yevgeniy Yuzefpolskiy

A dissertation

submitted in partial fulfillment of the

requirements for the degree of

Doctor of Philosophy

University of Washington

2019

Reading Committee:

Surojit Sarkar, Chair

Vandana Kalia, Co-Chair

Margaret Sedensky

Program Authorized to Offer Degree:

Pathology

University of Washington

Abstract

The Role of Early Autocrine IL-2 Signals in Programming Antigen-Specific CD8 T cell Responses

Yevgeniy Yuzefpolskiy

Chair of the Supervisory Committee:
Associate Professor Surojit Sarkar, Ph.D.

IL-2 is a potent cytokine in mediating antigen-specific CD8 T cell responses. Following antigen priming, IL-2 signals drive the differentiation of resting cytotoxic T cells into potent effector cells to elicit rapid expansion, and the expression of effector molecules critical for eradicating intracellular infections. Antigen-specific CD8 T cells more sensitive to early IL-2 signals undergo pronounced effector expansion as they differentiate into terminal effector cells that subsequently undergo substantial contraction following antigen clearance. Conversely, cells expressing lower levels of the high affinity IL-2 receptor, CD25, exhibit lesser expansion and preferentially form long-lived memory CD8 T cells, which provide protection from future infections. Interestingly, one of the hallmark features of these memory CD8 T cells is their retained function of autocrine IL-2 production. This suggests that autocrine IL-2 is intrinsically linked to the differentiation and maintenance of effector and memory cells. In our studies we have utilized a murine model of acute infection in which we studied the effects of autocrine IL-2 ablation on antigen-specific CD8 T cells. We were able to show that autocrine IL-2 signals were dispensable to antigen-specific CD8 T cells for mounting a primary immune response; the T cells showed no defect in effector expansion or function, and were capable of forming long-lived, polyfunctional memory CD8 T cells. However, upon antigenic rechallenge memory cells deficient in autocrine IL-2 signals underwent increased cell-death resulting in a compromised secondary response. We then used temporal ablation of autocrine IL-2 to determine that these signals were critical during the initial priming of antigen-specific CD8 T cells.

Unlike acute infections, where antigen is cleared by the effector response, during chronic infections antigen persists in the host exhausting the antigen-specific T cells via constant stimulation. However, the initial priming events are similar in both acute and chronic IL-2 infections. Thus, we wanted to determine if autocrine IL-2 signals also program survival in CD8 T cells in a system where the cells are continuously stimulated with antigen. We discovered that in the absence of autocrine IL-2, antigen-specific CD8 T cells undergo lower expansion but are not affected in their ability to elicit effector function. Following establishment of exhaustion, CD8 T cells lacking autocrine IL-2 over-expressed inhibitory receptor PD-1, and had a pronounced defect in maintenance. Surprisingly, T cells lacking autocrine IL-2 underwent significantly better expansion following PDL1 checkpoint blockade therapy, expanding to levels similar to their WT counterparts. These data show for the first time a critical role for autocrine IL-2 during chronic infections. Furthermore, this research suggests that it is possible to tune exhausted CD8 T cells using IL-2 signals, to boost their responsiveness to checkpoint blockade therapy.

Acknowledgements

I'd like to thank my advisors Surojit Sarkar and Vandana Kalia who have helped me in every step through my graduate education both intellectually as well as a family while being far from home. Thank you also to the rest of my committee: Ram Savan, Matt Kaeberlein and Margaret Sedensky, for coming together and being so supportive for a student who transferred randomly in the middle of his education.

I'd like to thank Laura Anne Penny and Arif Azam Khan for all the time they invested in teaching me as an undergraduate, and Julie Cheung a fellow undergrad at the time that bounced research ideas with me, even when we had no idea what we were talking about.

Special thank you to Florian Martin Baumann, a fellow graduate student in the lab. We made a great team and I definitely couldn't have done it without you. Thank you also to Kiki Mullikin and Rebekah Dadey the most hardworking undergrads I've ever met.

Finally, I'd like to thank my Mama (Lucy Goldstein) and Papa (Yakov Yuzefpolskiy) and the rest of my family for supporting me through all the ups and downs of graduate school. Also, thank you to my extended family Ian Wolff and Nina Rao who try to keep me grounded and sane.

Thank you Mr. Breidenbach, you taught me early on that if you understand, you don't have to memorize which sparked my love for math and science.

Table of Contents

Chapter 1: Introduction

Importance of Vaccines

To date one of the largest contributors to worldwide mortality is acquired bacterial and viral infections. Immunology was born from the desire to understand what causes the range of symptoms exhibited during infection- from mild fevers, to debilitating diseases, and death. The investigations into the nature of infections have yielded the understanding of germ theory by Louis Pasteur and disease transmission by Robert Koch. These have lead to the advent of sterile technique, as well as a better understanding of which vectors are critical in spreading diseases. However, one of the greatest advancements in immunology was the characterization and utilization of acquired immunity; the robust protection provided to a host form a disease to which they have already been exposed.

The idea of acquired immunity can be traced as far back as the ancient Greeks who noticed that people who recovered from an infection were protected from reinfection when tending to the sick[1]. While this idea incubated in many societies, it was not until the late 1700s that Edward Jenner was able to implement the development of a technique that provided acquired immunity to smallpox - a disease that had caused disfigurement, blindness and death - by pretreating patients with an innocuous cowpox virus, that we now term a vaccine[2]. The ability to acquire immunity to a debilitating infection without undergoing the dangerous primary infection has created a revolution in the world of medicine. Since the discovery of the vaccine process scientists have been able to advance this process with advancing technologies, leading to the eradication of diseases like smallpox, polio, measles, rubella, and many others, which had caused countless health complications and mortalities. The implementation of these vaccines has markedly decreased the early childhood mortality rate, and boosted the life expectancy of adults[3].

There is still a lot to learn in vaccine design, as a majority of the underdeveloped nations struggle not only with implementing existing vaccines, but also suffer from diseases for which we have not yet been able to design effective vaccines[4]. Thus, it is critical that we continue to deconvolute the mechanisms of the immune system, to create strategies for longer-lasting,

more potent, and farther reaching immune therapies, that can drive down unnecessary suffering, and boost the quality of life, world-wide.

Immune Protection from Invading Pathogens

The mammalian immune system can be widely broken down into two branches: the innate immune system, and the adaptive immune system. These two systems work in concert to prevent the majority of foreign organisms from entering the body, and eliminating those pathogens that were able to establish a foothold.

The innate immune system is a multiplex array of nonspecific defense systems implemented to prevent the entry of external organisms into the body (utilizing skin, mucosal surfaces, and proteolytic and chemical mechanisms of destruction). If entry into the host is not prevented, there are innate immune cells whose function is to recognize any pathogen associated molecular patterns (PAMPs; foreign RNA, DNA, lipid, or sugar moiety detection) and destroy it before it can establish a presence in the host. Unfortunately, nonspecific immune responses have a limit to their effectiveness, and eventually more pathogen-specific response need to be elicited. To achieve a pathogen specific response, a subset of the innate immune system, the professional antigen-presenting cells (APCs), ingest the foreign invaders and break them down into peptide fragments that are specific to the pathogen, because it is comprised of the pathogen itself. The APCs take these fragments and present them to the adaptive immune system, which can then specifically target the pathogen and clear it from the system. These adaptive immune cells are what make vaccines possible, as they are extremely specific to the pathogen and are capable of forming long-lived memory against the pathogen, which prevents reinfection if the host ever encounters it in the future.

The Adaptive Immune System

This adaptive immune response is the current focus for the development of the vaccine strategies that have been developed in the last two centuries[2]. There are two principle components of the adaptive immune response, the humoral response, and the T cell mediated response. The humoral response is performed by B cells, which form soluble factors called

antibodies. These antibodies bind with high-specificity to extracellular pathogens. Being coated by B cell secreted antibodies marks invading pathogens for destruction, as well as neutralizes their mobility and blocks proteins the pathogens utilize to gain entry into the host cells. Humoral immunity is the focus of many vaccines, checking the titers of the antibodies circulating in the blood is one of the primary screening methods to check the potency of an immune response[5]. However, this immune response can only deal with extracellular pathogens, and is ineffective in dealing with somatic cells that have been infected with viruses or bacteria, or cancerous cells that have transformed into a pathogenic entity. Infections in which the host's cells become populated with viruses or bacteria instead rely on the CD8 T cell mediated cytotoxic immune response.

Cytotoxic CD8 T cells can recognize the difference between healthy cells and cells that are pathogenic. These cytotoxic CD8 T cells circulate throughout the body scanning for the presence of foreign invaders. Once these T cells recognize an infected cell, they target it and release cytotoxic mediators that drive the infected cell to apoptosis. Once all the infected cells are eliminated from the body, the T cells continue circulating as memory cells, capable of much faster responses if the same pathogen tries to infect the host[6,7]. Our studies focus on these cytotoxic CD8 T cells, to understand how they are recruited to respond to infection, how they expand to kill infected cells, and following the clearance of the pathogen, how they provide immunity to future reinfection.

Basics of a T cell Immune Response

Cytotoxic CD8 T cells use their T cell receptor (TCR) to scan somatic cells for signs of invading pathogens that would be displayed on the surface of the infected cell via their Major Histocompatibility complex class I (MHCI). All cells in the body express MHCI; healthy cells express MHCI carrying different pieces of proteins found in cells during homeostasis. However, upon intracellular infection, bacterial or viral proteins become expressed intracellularly as the pathogen takes over the infected cell[8]. As the cell is infected, its MHCI will start displaying foreign viral protein fragments on the cell surface. When the TCR of a cytotoxic CD8 T cell

makes contact with the MHCI of an infected cell they form a stable junction, which triggers the release of cytotoxic granules by the CD8 T cell, driving apoptosis in the infected cell[9].

The vast diversity of viruses and bacteria that have evolved to efficiently infect the mammalian host makes it a necessity that the host can produce a wide variety of T cells with unique TCRs to be able to respond to any infection. This process of TCR development by CD8 T cells is performed in the thymus through a process called VDJ gene rearrangement. The thymus is a nursery for developing T cells, where each T cell forms a unique TCR with a total diversity estimated to fall in the range of 10^8 distinct specificities[10,11]. T cells are also trained to ignore healthy cells as to prevent autoimmune responses and focus specifically on their antigen of specificity. These naive antigen-specific T cells circulate throughout the body, ready to be recruited to fight-off invading pathogens[12].

The process of antigen clearance can be divided into three separate stages: recruitment of antigen-specific CD8 T cells, effector expansion and viral clearance, and finalized by the contraction of the effector response and the formation of long-lived memory cells[6,7,13]. As discussed previously, the adaptive immune response is recruited by circulating APCs that are carrying pieces of the pathogen they've ingested, on their MHCI. These APCs scour the body looking for the antigen-specific T cell that can recognize one of the foreign protein fragments displayed on its cell surface. Once an APC finds the antigen-specific T cell that is specific to the virus peptide its presenting, the TCR of the T cell engages with the MHCI of the APC and the T cell is activated and recruited to fight the invading pathogen. Recruitment of the T cell involves the activation of the resting naïve CD8 T cell into an effector CD8 T cell capable of vigorously undergoing up to a 10,000 fold expansion to make more copies of the cells that are specific to the invading pathogen[14]. Furthermore, these effector CD8 T cells acquire the necessary functions to induce inflammation, and cytotoxicity to go throughout the body searching for infected cells carrying the same protein fragment against which it was recruited. Following antigen clearance, these effector CD8 T cells undergo a significant contraction up to 95% of the total effector size. The remaining cells differentiate into long-lived memory cells[7]. The formation of long-lived memory T cells creates a population of antigen-specific cells that are present at a significantly higher frequency compared to their naïve counterparts. Furthermore

the antigen experienced memory cells are significantly faster at responding to secondary infections compared to their naïve counterparts[15]. T cell immunology is centered on understanding the factors necessary for optimal progression through all three stages of the immune response and how these factors can be manipulated to optimize the amount and quality of memory cells formed.

A Model for Studying T cell Immunity

In the past 40 years the study of the adaptive immune system has made significant strides with the development of a robust mouse model. This model makes use of a stable inbred mouse strain, C57BL6, which normalizes the variance created by genetic diversity that would be observed in an outbred population. Furthermore, this model allows for the selective deletion of target genes, while keeping all other variables constant.

One of the best-studied viruses in this model is the Lymphocytic choriomeningitis virus Armstrong strain ($LCMV_{Arm}$). This virus elicits a powerful T cell immune response causing the robust expansion of antigen-specific CD8 T cells. These CD8 T cells are capable of clearing infection, and forming long-lived memory cells, capable of undergoing secondary T cell expansion. The three immunodominant peptides derived from LCMV and presented by APCs are GP33-41, GP276-284 and NP396-404 derived from the glycoprotein (GP) and nuclear protein (NP), respectively[16-18]. In the process of understanding TCR development, Zinkernagel *et al.* cloned the TCR specific for MHCI carrying the viral GP33-41 fragment into B6 mice[19], such that instead of having a diverse array of TCRs the mouse only produced T cells expressing the GP33-41 specific TCR, thus developing the P14 strain. While these mice were instrumental in answering key questions in TCR development, their use has extended far beyond this role. The ability to purify a large, mono-antigen-specific pool of naïve CD8 T cells from these P14 mice has opened the gates to studying the differentiation of effector cells before their logarithmic expansion, when their frequency in the host are low[20-22]. Furthermore, P14 mice can be crossed to any necessary knock-out mouse strains to study the CD8 T cell intrinsic role of the gene during infection and memory maintenance. These genes are studied in a T cells intrinsic manner by transferring P14 KO CD8 T cells into wild-type (WT) recipients, the environment is kept constant, while only the CD8 T cell is knocked-out[23,24].

Our laboratory and countless others, have utilized this dynamic mouse model to understand the factors that drive CD8 T cell immunity. Furthermore, in the studies presented here we will further develop tools for this model by incorporating the new CRISPR/CAS9 technology to more eloquently approach T cell manipulation. We will show how we utilized this model system to develop a high-throughput screen system to test genes critical to T cell mediated tumor clearance.

CD8 T cell Responses to Acute and Chronic infections.

An acute infection, such as $LCMV_{Arm}$, is characterized by establishing a viral load that recruits an effector CD8 T cell response, which is capable of culling the infected cells and clearing the virus from the host. In the past two decades great strides have been made in characterizing the T cell responses throughout the infection, by discovering surface markers and transcription factors necessary for driving powerful effector responses, and then down-regulating those effector responses following viral clearance to drive the formation of long-lived memory cells. Here we will define what markers we have utilized in our study to study the antigen-specific CD8 T cell responses.

Following thymic maturation, naïve CD8 T cells circulate the secondary lymphoid tissues of the host waiting to be recruited to fight an infection[25]. These naïve resting CD8 T cells rely primarily on IL-7, and IL-15 signaling to drive survival, as well as the tonic TCR signal they receive as they scan somatic cells looking for antigen[26]. Due to their reliance on IL-7, these cells express high levels of the IL-7Ra (CD127) and high levels of CD62L, an L-selectin allowing for easy extravasation into secondary lymphoid tissue. Upon contact with an APC carrying their antigen of specificity on its MHCI, CD8 T cells receive a TCR mediated stimulation signal, along with a costimulatory signal through CD28[27,28], which drives the activation of the naïve T cell into an effector CD8 T cell. The initial TCR stimulation and costimulations drive the expression of cMyc as well as the production of inflammatory cytokines (IFN-γ, TNF-α, and IL-2)[29-31], effector molecules (perforins and granzymes including Granzyme B)[32], and activation markers (PD-1, CD69, CD25, etc.)[15]. The production of inflammatory cytokines further drives the activation of themselves (through autocrine signaling) as well as surrounding T cells, via paracrine signaling[30]. The upregulation of effector molecules arms the newly activated T cells to lyse infected cells

that they will encounter, and the remaining activation markers help modulate the T cells' TCR signal strength, sensitivity to cytokine production, and ability to circulate the sites of infection. To fuel these functions CD8 T cells upregulate their mitochondrial oxidative phosphorylation metabolism as well as the unique property of recruitment of aerobic glycolysis which is a less energetically efficient, but anabolically-preferred breakdown of metabolites[33,34]. These CD8 T cells are now primed and ready to undergo effector expansion, and elicit function necessary to clear virus infected somatic cells.

Following recruitment of naïve CD8 T cells and activation into effector CD8 T cells, there are two goals for the antigen-specific cells: the first is to clear the virus from the host, and second is to establish long-lived memory cells that can more rapidly respond to future exposure to the same antigen. Recent studies show that these are two aspects that are inextricably linked to each other[21,35,36]. Upon antigen priming, one of the first instances that show heterogeneity in the antigen-specific response is the differential expression of IL-2Ra (CD25) by effector cells, which occurs early (within the first 3-4 days) following infection[20]. Effector cells that express higher levels of CD25 ($CD25^{Hi}$) undergo significantly greater expansion resulting in a large effector pool that drive viral clearance. However these cells differentiate into terminal effector cells, which will die following antigen clearance. On the other hand, their $CD25^{Lo}$ counterparts undergo significantly less proliferation; rather they differentiate in higher proportion to the central memory (long-lived) T cell fate. As the effector cells continue expanding beyond day 4, CD25 is downregulated in all effector cells and KLRG-1 emerges to differentiate the Terminal Effectors (TE; KLRG-1^{Hi}) from the Memory Precursor Effector cells (MPECs; KLRG-1^{Int})[21]. By the peak of the effector expansion, and clearance of the virus, KLRG-1^{Hi} cells make up the vast majority of the immune response. These KLRG-1^{Hi} cells have potent expression of inflammatory cytokines TNF-α and IFN-γ, and express high levels of Granzyme B, making them potent effector cells. However, as the infection is cleared and the system returns to homeostasis, these cells are unable to return to a functional resting state, and undergo a massive contraction leaving behind only the KLRG-1^{Int} MPECs[21]. Following antigen clearance, MPECs undergo a gradual reversion into a resting state, reducing oxidative phosphorylation and aerobic glycolysis instead preferentially relying on fatty acid synthesis and catabolism for their

energetic needs[37]. While MPECs downregulate the expression of effector molecules and cytokines, the transition through an effector state has left them licensed to upregulate these factors rapidly following restimulation[38]. These cells upregulate their CD127 expression[39,40], and over time upregulate expression of CD62L restoring their sentry function of scanning the body for antigen. While these cells do not proliferate as rapidly as effector cells, they rely on gradual self-renewal through homeostatic proliferation and autophagy. In many cases of acute infection, these cells will continue to persist for the life span of the host. In fact a longitudinal study of the smallpox vaccine observed antigen-specific memory cells still present in patients 70 years following vaccination[41]. The benefit of memory cells is immense, as these cells can react to antigen presence without the APC intermediates. Furthermore, their response to antigen is much faster, and more potent as they are able to quickly access the loci containing the effector molecules and also store mRNA of some of the effector molecules, ready for translation following antigen recruitment.

When the effector T cell response recruited to a viral infection is incapable of clearing the antigen from the host, the virus establishes a chronic infection. In the LCMV model this virus is the CL-13 strain, which is responsible for establishing a chronic infection in which the virus persists indefinitely in the host[42]. During a chronic infection the initial APC mediated recruitment is largely similar to the acute counterpart. However, as the effector T cells undergo rapid expansion, the amount of antigen in the system does not go down as the virus establishes a permanent foothold in the system. This prolonged exposure to virus prevents the classic differentiation into terminal effectors and long-lived memory cells observed during a acute infection. Instead constant stimulation through the TCR causes prolong expression of inhibitory receptor PD-1, and the upregulation of exhaustion programming, resulting in a progressive loss of function in exhausted CD8 T cells the longer they persist in in the presence of antigen[42-44]. This exhaustion is characterized by a loss of metabolic function and decrease in self-renewal[45]. Furthermore, there is a progressive loss-of-function as the T cells lose their ability to produce inflammatory cytokines, followed by effector molecules, and ultimately the fully exhausted T cells are deleted. Chronic infections are established by many diseases such as HBV, HCV, and HIV and cause a severe impact on systemic function. Furthermore, solid tumor environments

filled with pathogenic somatic cells have displayed similar state to a localized chronic infection where T cells recruited into the tumor undergo antigen-mediated exhaustion, leading to an inability to clear the tumor cells. Thus understanding the chronic model and how to restore function to these exhausted T cells has become as important in immunology as understanding the acute T cell kinetics to prepare potent vaccines.

As chronicity establishes in the host, there is still heterogeneity in the effector response, similar to what is observed in the acute responses. During chronic infection, exhausted antigen-specific CD8 T cells contain a subset of cells that are PD-1 intermediate, $Tbet^{Hi}$, $BLIMP^{Lo}$, $Eome^{Hi}$, $TCF\text{-}1^{Hi}$, $CXCR5^{Hi}$ which represent a population that will act as a stemcell-like population that differentiate into a larger pool of fully exhausted T cells, maintaining a homeostasis with the established viral infection[46-50]. These cells are not only formed from the primary immune response, but are also continuously fed by cells being recruited into the chronic infection. One of the primary breakthroughs in the field was the idea that blocking these inhibitory signals imposed on the exhausted CD8 T cells, can rescue the cells driving the proliferation and expansion and restoration of effector function[51,52]. This therapy is now widely known as checkpoint blockade, and has been used extensively in the clinic to drive the regression of tumors as the exhausted T cells regain their cytotoxic properties. In fact, these checkpoint blockade therapies target the stem cell-like population of exhausted cells releasing their breaks by blocking their cell surface inhibitory signals and allowing for the clearance of the pathogen[48,49]. While this has been a landmark therapy welcomed with the Nobel Prize Award in Medicine to James Allison and Tasuku Honjo, there are limitations to its application as it stands. It is necessary to continue deconvoluting the factors that can be manipulated to boost these exhausted T cell responses.

What is the role of IL-2 Signals in driving CD8 T cell differentiation?

Cytokines are extracellular proteins that have a wide variety of function in driving T cell homeostatic maintenance, as previously discussed with IL-7 and IL-15, as well as inflammatory cytokines that drive T cell expansion, and effector differentiation. One of the first cytokines discovered was IL-2, the T cell growth factor[53]. When present in solution it drove massive

expansion of activated CD8 T cells, as well as their production of effector molecules[54]. IL-2 is capable of driving this powerful immune response by driving the engine of the effector T cell response. In fact, depleting activated CD8 T cells of IL-2 signals largely represses the aerobic glycolysis even in the presence of potent TCR stimulation preventing the cells from eliciting any effector function or proliferation[55].

Upon antigen priming, the TCR and costimulatory CD28 signals drive IL-2Rα upregulation, which increases the T cells affinity towards IL-2 by 100 times[56]. However, recent developments have demonstrated that IL-2 has a complex relationship with the differentiation of effector CD8 T cells during acute infections. As discussed previously, one of the first markers of heterogeneity of the effector T cell response is the expression of the IL-2Ra (CD25). Increased IL-2 signaling early during infection drive the differentiation of CD8 T cells into cytotoxic terminal effectors. These terminal effectors not only have decreased survival following antigen clearance, but also lose the capability to produce their own autocrine IL-2[20]. Conversely, cells that receive less IL-2 signals due to lower expression of CD25, largely differentiate into long-lived memory cells, which maintain an increased capacity to produce autocrine IL-2. Interestingly, one of the hallmark features of memory CD8 T cells is their polyfunctionality, the ability of the cell to coproduce IFN-γ, TNF-α and IL-2 following antigenic rechallenge. Following effector differentiation most cells can coproduce IFN-γ and TNF-α, however, the ability to produce IL-2 is tightly correlated with the highest quality of memory CD8 T cells. However, despite being so tightly correlated with increased functionality, it is not understood what role autocrine IL-2 has in the activation, differentiation, or maintenance of antigen-specific CD8 T cells.

The role and function of IL-2 during chronic infection has been less characterized. As exhaustion sets in from chronic antigen stimulation, autocrine IL-2 production is lost, and that functionality is never regained[44]. Thus the assumption is that its impact on the chronic system is quite minimal. However, studies on checkpoint blockade therapy showed that combining exogenous IL-2 concurrently with PDL1 checkpoint blockade therapy significantly boosts the responsiveness of exhausted CD8 T cells[57]. Furthermore, the similar priming environments

during acute and chronic LCMV infections suggest that the early function of IL-2 maybe similar in both modes of infection.

The power of IL-2 to modulate CD8 T cell function makes it an ideal target to mold antigen-specific CD8 T cell responses. The ability for antigen-specific CD8 T cells to make autocrine IL-2 and its intrinsic ties to long-lived memory T cells suggests a greater importance in its role of T cell differentiation, than we currently appreciate. The aim of this thesis is to understand the impact that autocrine IL-2 signaling has on antigen-specific CD8 T cell responses.

References

1. Poole, J. C. & Holladay, A. J. *Thucydides and the plague of Athens. Classical quarterly* **29,** 282–300 (1979).
2. Riedel, S. Edward Jenner and the history of smallpox and vaccination. *Proc (Bayl Univ Med Cent)* **18,** 21–25 (2005).
3. Andre, F. E. *et al.* Vaccination greatly reduces disease, disability, death and inequity worldwide. *Bull. World Health Organ.* **86,** 140–146 (2008).
4. Arya, S. C. Human immunization in developing countries: practical and theoretical problems and prospects. *Vaccine* **12,** 1423–1435 (1994).
5. Plotkin, S. A. Correlates of protection induced by vaccination. *Clin. Vaccine Immunol.* **17,** 1055–1065 (2010).
6. Zhang, N. & Bevan, M. J. CD8(+) T cells: foot soldiers of the immune system. *Immunity* **35,** 161–168 (2011).
7. Ahmed, R. & Gray, D. Immunological memory and protective immunity: understanding their relation. *Science* **272,** 54–60 (1996).
8. Koopmann, J. O., Hämmerling, G. J. & Momburg, F. Generation, intracellular transport and loading of peptides associated with MHC class I molecules. *Current Opinion in Immunology* **9,** 80–88 (1997).
9. Wong, P. & Pamer, E. G. CD8 T cell responses to infectious pathogens. *Annu. Rev. Immunol.* **21,** 29–70 (2003).
10. Qi, Q. *et al.* Diversity and clonal selection in the human T-cell repertoire. *Proc. Natl. Acad. Sci. U.S.A.* **111,** 13139–13144 (2014).
11. Lythe, G., Callard, R. E., Hoare, R. L. & Molina-París, C. How many TCR clonotypes does a body maintain? *J. Theor. Biol.* **389,** 214–224 (2016).
12. Goldrath, A. W. & Bevan, M. J. Selecting and maintaining a diverse T-cell repertoire. *Nature* **402,** 255–262 (1999).
13. Byrne, J. A., Butler, J. L. & Cooper, M. D. Differential activation requirements for virgin and memory T cells. *The Journal of Immunology* (1988).
14. Wherry, E. J. & Ahmed, R. Memory CD8 T-cell differentiation during viral infection.

Journal of Virology **78,** 5535–5545 (2004).
15. Veiga-Fernandes, H., Walter, U., Bourgeois, C., McLean, A. & Rocha, B. Response of naïve and memory CD8+ T cells to antigen stimulation in vivo. *Nat Immunol* **1,** 47–53 (2000).
16. van der Most, R. G. *et al.* Identification of Db- and Kb-restricted subdominant cytotoxic T-cell responses in lymphocytic choriomeningitis virus-infected mice. *Virology* **240,** 158–167 (1998).
17. van der Most, R. G. *et al.* Analysis of cytotoxic T cell responses to dominant and subdominant epitopes during acute and chronic lymphocytic choriomeningitis virus infection. *J. Immunol.* **157,** 5543–5554 (1996).
18. Kotturi, M. F. *et al.* Naive precursor frequencies and MHC binding rather than the degree of epitope diversity shape CD8+ T cell immunodominance. *The Journal of Immunology* **181,** 2124–2133 (2008).
19. Pircher, H., Bürki, K., Lang, R., Hengartner, H. & Zinkernagel, R. M. Tolerance induction in double specific T-cell receptor transgenic mice varies with antigen. *Nature* **342,** 559–561 (1989).
20. Kalia, V. *et al.* Prolonged interleukin-2Ralpha expression on virus-specific CD8+ T cells favors terminal-effector differentiation in vivo. *Immunity* **32,** 91–103 (2010).
21. Sarkar, S. *et al.* Functional and genomic profiling of effector CD8 T cell subsets with distinct memory fates. *The Journal of* (2008).
22. Oliaro, J. *et al.* Asymmetric cell division of T cells upon antigen presentation uses multiple conserved mechanisms. *The Journal of Immunology* **185,** 367–375 (2010).
23. Yuzefpolskiy, Y. *et al.* Vitamin D Receptor Signals Regulate Effector and Memory CD8 T Cell Responses to Infections in Mice. *J. Nutr.* **144,** 2073–2082 (2014).
24. Khan, A. A., Penny, L. A., Yuzefpolskiy, Y., Sarkar, S. & Kalia, V. MicroRNA-17∼92 regulates effector and memory CD8 T-cell fates by modulating proliferation in response to infections. **121,** 4473–4483 (2013).
25. Sprent, C. D. S. J. Homeostasis of Naive and Memory T Cells. *Immunity* **29,** 848–862 (2008).
26. Takada, K. & Jameson, S. C. Naive T cell homeostasis: from awareness of space to a sense of place. *Nature Publishing Group* **9,** 823–832 (2009).
27. Lenschow, D. J., Walunas, T. L. & Bluestone, J. A. CD28/B7 system of T cell costimulation. *Annu. Rev. Immunol.* **14,** 233–258 (1996).
28. van Stipdonk, M. J., Lemmens, E. E. & Schoenberger, S. P. Naïve CTLs require a single brief period of antigenic stimulation for clonal expansion and differentiation. *Nat Immunol* **2,** 423–429 (2001).
29. Michalek, R. D. & Rathmell, J. C. The metabolic life and times of a T-cell. *Immunological Reviews* **236,** 190–202 (2010).
30. Curtsinger, J. M. & Mescher, M. F. Inflammatory cytokines as a third signal for T cell activation. *Current Opinion in Immunology* **22,** 333–340 (2010).
31. Fitzpatrick, D. R., Shirley, K. M. & Kelso, A. Cutting edge: stable epigenetic inheritance of regional IFN-gamma promoter demethylation in CD44highCD8+ T lymphocytes. *J. Immunol.* **162,** 5053–5057 (1999).
32. Yuzefpolskiy, Y., Baumann, F. M., Kalia, V. & Sarkar, S. Early CD8 T-cell memory precursors and terminal effectors exhibit equipotent in vivo degranulation. *Cell. Mol. Immunol.* (2014). doi:10.1038/cmi.2014.48

33. Pearce, E. L. Metabolism in T cell activation and differentiation. *Current Opinion in Immunology* (2010).
34. Fox, C. J., Hammerman, P. S. & Thompson, C. B. Fuel feeds function: energy metabolism and the T-cell response. *Nat Rev Immunol* **5,** 844–852 (2005).
35. Buchholz, V. R. *et al.* Disparate individual fates compose robust CD8+ T cell immunity. *Science* **340,** 630–635 (2013).
36. Sarkar, S. *et al.* Strength of Stimulus and Clonal Competition Impact the Rate of Memory CD8 T Cell Differentiation. *The Journal of Immunology* **179,** 6704–6714 (2007).
37. O'Sullivan, D. *et al.* Memory CD8+ T Cells Use Cell-Intrinsic Lipolysis to Support the Metabolic Programming Necessary for Development. *Immunity* **41,** 75–88 (2014).
38. de Ara xfa *et al.* Epigenetic Control of Interferon-Gamma Expression in CD8 T Cells. *Journal of Immunology Research* **2015,** 1–7 (2015).
39. Schluns, K. S., Kieper, W. C., Jameson, S. C. & Lefrançois, L. Interleukin-7 mediates the homeostasis of naïve and memory CD8 T cells in vivo. *Nat Immunol* **1,** 426–432 (2000).
40. Kaech, S. M. *et al.* Selective expression of the interleukin 7 receptor identifies effector CD8 T cells that give rise to long-lived memory cells. *Nat Immunol* **4,** 1191–1198 (2003).
41. Taub, D. D. *et al.* Immunity from smallpox vaccine persists for decades: a longitudinal study. *Am. J. Med.* **121,** 1058–1064 (2008).
42. Wherry, E. J., Blattman, J. N., Murali-Krishna, K., van der Most, R. & Ahmed, R. Viral persistence alters CD8 T-cell immunodominance and tissue distribution and results in distinct stages of functional impairment. *Journal of Virology* **77,** 4911–4927 (2003).
43. Wherry, E. J. & Kurachi, M. Molecular and cellular insights into T cell exhaustion. *Nat Rev Immunol* **15,** 486–499 (2015).
44. Wherry, E. J. *et al.* Molecular Signature of CD8+ T Cell Exhaustion during Chronic Viral Infection. *Immunity* **27,** 670–684 (2007).
45. Bengsch, B. *et al.* Bioenergetic Insufficiencies Due to Metabolic Alterations Regulated by the Inhibitory Receptor PD-1 Are an Early Driver of CD8+ T Cell Exhaustion. *Immunity* **45,** 358–373 (2016).
46. Shin, H. *et al.* A Role for the Transcriptional Repressor Blimp-1 in CD8+ T Cell Exhaustion during Chronic Viral Infection. *Immunity* **31,** 309–320 (2009).
47. Kao, C., Oestreich, K. J., Paley, M. A. & Crawford, A. Transcription factor T-bet represses expression of the inhibitory receptor PD-1 and sustains virus-specific CD8+ T cell responses during chronic infection. *Nature* (2011).
48. Im, S. J. *et al.* Defining CD8+ T cells that provide the proliferative burst after PD-1 therapy. *Nature* **537,** 417–421 (2016).
49. He, R. *et al.* Follicular CXCR5-expressing CD8(+) T cells curtail chronic viral infection. *Nature* **537,** 412–428 (2016).
50. Utzschneider, D. T. *et al.* T Cell Factor 1-Expressing Memory-like CD8(+) T Cells Sustain the Immune Response to Chronic Viral Infections. *Immunity* **45,** 415–427 (2016).
51. Barber, D. L. *et al.* Restoring function in exhausted CD8 T cells during chronic viral infection. *Nature* **439,** 682–687 (2006).

52. Curran, M. A., Montalvo, W., Yagita, H. & Allison, J. P. PD-1 and CTLA-4 combination blockade expands infiltrating T cells and reduces regulatory T and myeloid cells within B16 melanoma tumors. *Proc. Natl. Acad. Sci. U.S.A.* **107,** 4275–4280 (2010).
53. Baker, P. E., Gillis, S., Ferm, M. M. & Smith, K. A. The effect of T cell growth factor on the generation of cytolytic T cells. *J. Immunol.* **121,** 2168–2173 (1978).
54. Cheng, L. E., Ohlén, C., Nelson, B. H. & Greenberg, P. D. Enhanced signaling through the IL-2 receptor in CD8+ T cells regulated by antigen recognition results in preferential proliferation and expansion of responding CD8+ T cells rather than promotion of cell death. *Proc. Natl. Acad. Sci. U.S.A.* **99,** 3001–3006 (2002).
55. Smith, K. A. Conditional IL-2 gene deletion: consequences for T cell proliferation. 1–12 (2012). doi:10.3389/fimmu.2012.00102/abstract
56. Liao, W., Lin, J.-X. & Leonard, W. J. Interleukin-2 at the Crossroads of Effector Responses, Tolerance, and Immunotherapy. *Immunity* **38,** 13–25 (2013).
57. West, E. E. *et al.* PD-L1 blockade synergizes with IL-2 therapy in reinvigorating exhausted T cells. *J. Clin. Invest.* **123,** 2604–2615 (2013).

Utilizing CRISPR to Discover Targets Critical for CD8 T cell Mediated Tumor Clearance

Yevgeniy Yuzefpolskiy[1,2], , Surojit Sarkar[1,2,3,4], and Vandana Kalia[1,3,4] ✦

[1] Ben Towne Center for Childhood Cancer Research, Seattle Children's Research Institute, Seattle WA 98101.
[2] M3D Graduate Program, University of Washington School of Medicine, Seattle, WA 98195
[3] Department of Pathology, University of Washington School of Medicine, Seattle, WA 98195
[4] Department of Pediatrics, Division of Hematology and Oncology, University of Washington

★Corresponding authors: Surojit Sarkar and Vandana Kalia, sarkarkalia@gmail.com
1100 Olive Lab, Suite 100
Ben Towne Center for Childhood Cancer Research
University of Washington School of Medicine
Seattle, WA 98101

Footnote: This work was supported by research funding from the Seattle Children's Research Institute to SS and VK.

Running Title:
Word Count (Abstract): 248
Word Count (Text): 5127
Figure/Table Count: 5 Main Figures, 5 Supplemental Figures
Reference Count: 26

Abstract

Cytotoxic CD8 T cells are critical in the clearance of pathogenic cells via antigen mediated cell lysis, providing protection against infectious diseases and cancers. As so, they have become one of the primary targets of immunotherapies and vaccine design. Microarray and single-cell RNA sequencing of effector and memory CD8 T cells has yielded innumerable gene targets that modulate CD8 T cell responses, however, generating CD8 T cell specific knockout mice for each target is both fiscally infeasible as well as exceedingly time consuming. Here we have demonstrated a protocol that allows the deletion of genes from activated effector, as well as resting naïve and memory murine CD8 T cells. This CRISPR modification of CD8 T cells was then adapted to study the effects of gene deletion in the context of acute memory differentiation as well as chronic exhaustion of CD8 T cells. To this end, we have titrated the necessary dose of antigen-specific CD8 T cells to study their differentiation in acute and chronic infections and confirmed the model by demonstrating the rapid expansion of CRISPR mediated PD-1 ablated CD8 T cells in a chronic viral infection. Finally, by combining this methodology with a murine model of subcutaneous tumor challenge, we have developed a unique screening system for genes critical in mediating cytotoxic CD8 T cells clearance of malignant tumor cells. Our model protocol allows for the quick screening of any gene deleted at any stage of CD8 T cell differentiation and determining its effects on tumor clearance.

Introduction

T cells continuously circulate the body protecting their host from invasive intracellular infections and cancers[1]. Understanding the signals that drive CD8 T cell differentiation to terminal effector and central memory fates[2-6] and how chronic antigen stimulation drives T cell exhaustion[7-9] has enriched our methodology in designing potent long-lasting vaccines and is driving the revolutionary field of personalized medicine with tumor-specific CAR therapy, at the forefront of the industry. Through the advent of population and single cell sequencing of antigen-specific T cells, the field is moving towards a better understanding of the factors driving effector T cell differentiation[2,8,10]. To probe these genes the field has generated an extensive library of germline knockout mice. However, studying T cells isolated from knockout mice can have a myriad of compounding errors as CD8 T cells maturing in a knockout environment could be different due to extrinsic or intrinsic genetic effects. This was partially answered with the development of mice with flox genes bred to cell-subset specific Cre expressing mice[11-13], which allow for a more eloquent approach to studying gene ablation. While these powerful techniques have generated the foundation of our understanding in T cell differentiation, the process is expensive and extremely time consuming.

The advent of utilizing retroviral delivery of for gene knock-down has become a staple in immunology for accessing the function of genes and how they directly control T cell differentiation *in vitro* and *in vivo*[14-16]. Furthermore, CRISPR Genome editing has revolutionized the biological sciences by creating a simple method of targeted gene ablation. In this study we have aimed to develop workflow in which we can study the role of relevant genes in naïve, effector, and memory CD8 T cells and combine these knockout modalities with the existing *in vivo* models of T cell memory differentiation and exhaustion. The synthesis of these tools provides a dynamic range of CD8 T cell manipulation that has not been demonstrated.

We have utilized the IDT CRIPSR-Cas9 platform combined with the Neon transfection system to knockout genes in naïve, primed effector, and memory CD8 T cells. We have demonstrated that the genes can be knockout in effector CD8 T cells following optimal CD8 T cell priming, as well as in naïve and memory CD8 T cells following cytokine incubation. We further standardized the voltage conditions, cell-yield approximations, adoptive cell dose

transfer, and time of transfer to properly study these antigen-specific responses under conditions of acute memory differentiation, chronic viral exhaustion, as well as in the context of solid tumor clearance. To confirm the fidelity of the CRISPR knockout model, we repeated a study that demonstrated that germline PD-$1^{-/-}$ CD8 T cells undergo unchecked expansion in a chronic antigen milieu[17]. Our repeat compared WT, PD-1 CRISPR knockout and the same germline PD-1 knockouts that were used for the initial study to show that CRIPSR knockout CD8 T cells were able to phenocopy the germline knockouts. Finally, we were able to generate a high-throughput model that delineates genes critical in T cell mediated tumor clearance. As a proof of concept we utilized the MC38 solid tumor model and adoptively transferred WT and CRISPR PD-1 knockout tumor-specific CD8 T cells and observed a significant increase in tumor regression upon PD-1 ablation.

Materials and Methods:

CRISPR-CAS9

Protocol for preparation of CRISPR-Cas9 reagents was followed closely to that provided by IDT Alt-R CRISPR-Cas9 System (www.idtdna.com/pages/support/guides-and-protocols). In short, crRNA and ATTO550-tracrRNA (keep protected from light) were resuspended in nuclease free IDTE buffer at 200μM and stored at -20°C until day of electroporation. crRNA and ATTO550 tracrRNA were melted together at a 1:1 mixture with a final concentration of both RNA at 44μM at 95°C for 5 min in a thermocycler. Products were then allowed to cool at room temperature for 15 minutes. Alt-R Cas9 enzyme was also stored at -20°C at 61 μM until day of experiment. Cas9 enzyme was diluted to 36μM in T buffer when using voltages greater than 1600 V and R buffer when using voltages less than 1600 V on the Neon System. Once the 44μM crRNA-tracrRNA mixture cooled to room temperature, it was combined 1:1 with the 36μM Cas9 solution, and incubated at room temperature for 15 minutes. The CAS9-tracr-crRNA were then combined with Electroporation enhancer at a 1:2 ratio (Complex:EPE). Electroporation enhancer was stored at 10.8μM at -20°C until the day of electroporation. Antigen-specific CD8 T cells were resuspended in R or T buffer, depending on necessary voltage, at $35x10^6$ cells/mL and combined at a 3:1 ratio of cells:Complex-EPE. Mixture was stored at room temperature prior to Neon electroporation.

crRNA

crRNA was designed using the Broad Institute Genetic Perturbation Platform (portals.broadinstitute.org/gpp/public/analysis-tools/sgrna-design). The PD-1 crRNA used was as follows crRNA#1 CAATACAGGGATACCCACTA, #2 GACACACGGCGCAATGACAG, #3 CAGCTTGTCCAACTGGTCGG, #4 TTGGCTCAAACCATTACAGA, #5 GCACCCCAAGGCAAAAATCG. The CD25 crRNA used was GTGTCTGTATGACCCACCCG. The SATB1 crRNA used was as follows #1 GTACGTGCTGTTCACAATGG, #2 GCATCTGTCACATACGACAG. The CXCR3 crRNA used was as follows TCTGCGTGTACTGCAGCTAG. crRNA was resuspended at 200μM in nuclease free IDTE buffer and stored at -20°C.

Neon Electroporation system

The Neon 10μL and 100μL kits (Invitrogen MPK1096) were used depending on cell numbers. When fewer than $6x10^6$ cells, 10μL kit was used with 3 mL of room temperature E buffer in the Neon chamber. For greater than $6x10^6$ cells the 100μL kit with 3mL of room temperature E2 buffer in the Neon chamber was used. Naïve and memory CD8 T cells were resuspended in T buffer and electroporated using 2200V, 10ms, 3 pulses. CD8 T cells activated for 24-60hrs were resuspended in R buffer and electroporated using 1600V, 10ms, 3 pulses. Regardless of buffer, cells were resuspended at $35x10^6$ cells/mL before being mixed with their respective CRISPR-CAS9 reagents. Electroporated cells were pipetted into room temperature RPMI media (Thermo), made with 10% FBS (Gibco), 1% Penn-Strep/L-Glu (ThermoFisher), 0.4% BME (Sigma). Following electroporation cells were rested at 37°C, 5% CO_2 for 30 minutes.

CD8 T cell preparation:

Direct *ex vivo* Neon Transfection of naïve and memory CD8 T cell results in large cell loss, and low transfection efficacy. To increase survival and frequency of transfection: first naïve and memory CD8 T cells were purified from spleen using a CD8 negative purification MojoSort kit (Biolegend); CD8 T cells were purified from naïve P14 mouse splenocytes, and memory CD8 T cells were obtained from B6 mouse splenocytes after day 60 post-$LCMV_{Arm}$ infection. Following purification, naïve and memory CD8 T cells were plated in 6 well plates at $6x10^6$ cells/well in RPMI 10% FBS, 1% Penn-Strep/L-Glu, 0.4% BME and 10ng/mL mIL-7 (PeproTech)[18]. Cells were incubated at 37°C, 5% CO_2 for 24 hours. As described previously, incubation with IL-7 increased T cell survival, as well as Neon transfection[18].

To generate activated CD8 T cells, CD8 T cells were purified using CD8 negative purification Mojo Kit from naïve P14 mouse spleens and activated *in vitro* with antigen presenting beads, or plates coated with αCD3/αCD28. Cells were plated at $2\text{-}3x10^6$ cells/well in 6 well plates in RPMI supplemented with 10% FBS, 1% Penn-Strep/L-Glu, 0.4% BME. Antigen-presenting beads were generated by incubating SA-Magnetic Beads (Sigma) with αCD3/αCD28-Biotin (Biolegend), or MHCI-GP33/αCD28-Biotin. Where indicated, αCD3(4μg/mL)/αCD28(4μg/mL) was also coated on F-Bottom plates for 2hrs prior to T cell activation at 37°C, 5% CO_2, or O/N at 4°C. Prior to

neon transfection, if APBs were used, magnetic beads were removed from T cells using Stem Cell/MojoSort magnet incubation for 2 min at room temperature.

Following Neon transfection antigen specific CD8 T cells were transferred into warm RPMI supplemented with 10% FBS, 1% Penn-Strep/L-Glu, 0.4% BME. Cells were rested at 37°C, 5% CO_2 for 20-30min as post-electroporation efficiency was checked. Naïve and effector CD8 T cells were then plated with APB or on αCD3/αCD28 coated plates for activation. Effector cells were restimulated in the presence of mIL-2 (10ng/mL). Memory cells were cultured with mIL-7/-15 (10ng/mL).

Antibody Staining

All antibodies for FACS staining were purchased from Biolegend (San Diego, CA, USA) with the exception of SATB1 (Abcam). Cells were stained for surface markers in 1% PBS, 1%FBS, 0.2% Sodium Azide. Intracellular staining was performed using the BD intracellular staining kit. Intranuclear staining for SATB1 was performed using the FOXP3 staining kit (Invitrogen). Flow cytometry was performed on an LSRII Fortessa (BD Biosciences, San Jose, CA). FlowJo (TreeStar, Inc) was used to analyze and plot FACS data. For direct *ex vivo* analysis of T cells from spleens (SPL) and inguinal lymph nodes (iLN), SPL and iLN were first mechanically disturbed using frosted slides, and 0.83% ammonium chloride was used to remove RBC contamination in SPL. Following Lung perfusion with cold 1xdPBS, TILs and lungs (LNG) were isolated and cut into pieces. Tumors and lungs were processed in Collagenase A, and then TILs, LNG and liver (LVR) were pushed through a 70 micron cell strainer, followed by Percoll centrifugation to isolate the T cell containing buffy coat.

Mice

C57BL/6J mice (Thy1.2/1.2) were purchased from Jackson Laboratory and maintained in house. Thy1.1+ P14 mice expressing the H-2D^{b}GP33 TCR specific to the GP_{33-41} epitope of LCMV were fully backcrossed to C57BL/6 mice and were maintained in our animal colony. Mice were infected with $2x10^5$ PFU $LCMV_{Arm}$ IP for acute challenge, and $2x10^6$ PFU $LCMV_{Cl-13}$ IV for chronic

challenge. To generate memory mice, 10^5 antigen-specific P14 CD8 T cells were adoptively transferred into naïve B6 mice, which were subsequently infected IP with $2x10^5$ PFU $LCMV_{Arm}$. To standardize dose of electroporated donors in chronic infections, Neon transduced effector CD8 T cells were adoptively transferred IV at varying doses into day 2 chronic $LCMV_{CL-13}$ infection matched recipient mice. To study effector T cells in the tumor setting, 10^6 MC38 cells expressing GP_{33-41} peptide of LCMV were grown *in vitro* and transferred subcutaneously into the flank of naïve B6 mice. Once tumors were palpable at day 8 post-tumor challenge, Neon transfected CD8 T cells were adoptively transferred at 10^6 cells per mouse IV. Tumors were measured every third day for three weeks. Tumor measurements were based on the formula $[(\text{larger length})x(\text{smaller length})^2]x(1/2)$.

Statistical analysis

Paired or unpaired Student's t-test was used as indicated to evaluate differences between two group means. One-way ANOVA analysis with a Tukey post-test was used when comparing more than two groups. All statistical analyses were performed using Prism 5 and P values of statistical significance are depicted by asterisk per the Michelin guide scale: * ($P \leq 0.05$), ** ($P \leq 0.01$), *** ($P \leq 0.001$) and ($P > 0.05$) was considered not significant (ns).

Results

Protocol for screening genes critical for cytotoxic T cell function

The goal of this protocol was to genetically modify antigen-specific CD8 T cells regardless of their state of differentiation using the Neon CRISPR platform. To achieve this, we first standardized proper preincubation conditions to make the T cells amenable to Neon mediated CRISPR uptake to optimize gene deletion. The gene ablation was confirmed by following Neon transfected cells *in vitro* under conditions relevant to the gene being deleted (eg. genes upregulated upon activation were stimulated with antigen, while ablation of memory markers was confirmed with culture of cells in IL-7, IL-15 media). Following Neon CRISPR transfection, the transfected CD8 T cells will were transferred *in vivo* into the antigen milieu of choice to observe the effect of the gene knockout on the CD8 T cell kinetics and function (Figure 1A).

Standardizing Activation Conditions

We first optimized the *in vitro* activation conditions necessary for optimum uptake of CRISPR-Cas9 by CD8 T cells. As activated cells are fragile and amenable to death, it was important to develop a method of stimulation that required the least amount of handling. Thus, we magnetically purified CD8 T cells from naïve P14 spleens to prevent the need for purification at any later point in the protocol. To determine optimal CD8 T cells activation we applied two separate modalities, the first was stimulating with αCD3/αCD28 coated F-bottom plates which provides a mono-interface for T cell activation and is widely used in the field. This plate coated stimulation for 48 hours provided efficient stimulation increasing cell size (FSC), and driving upregulation of activation markers CD69, PD-1, CD25 and effector molecule Granzyme B (Figure S1C). However, to attempt a more physiologically relevant stimulation, we used SA-coated magnetic beads, which were bound with MHC-GP33 and αCD28 in equimolar concentrations. This provided a cell-cell approximate interface for activation, which is increasingly used in the field of CAR immunotherapy for T cell expansion. Titration of these antigen-presenting beads (APB-GP33) demonstrated that a ratio of 1 APB for every two T cell yielded the optimum activation in terms of activation marker expression, blast size as measured by FSC (Figure 1B, S1A), and yielded similar cell numbers compared to the other ratios tested (Figure S1B). Thus,

for the future experiments where T cells are activated we utilized antigen-presenting beads at a 2-1 cell-bead ratio (Figure 1C).

Optimizing voltage for CRISPR-CAS9 Uptake

The CRISPR-Neon protocol relies on the uptake of the CRISPR-CAS9 complex into cells via micropores opening upon the application of a voltage pulse through the cell solution. By utilizing the fluorescently labeled ATTO550-tracrRNA from IDT we were able to use flowcytometry to compare the uptake of CRISPR-CAS9 by the P14 T cells. Standardization of different voltages revealed that activated effector CD8 T cells required a pulse of 1600V to uptake the majority of the CAS9 complex (Figure 2A). However this uptake was paired with the loss of about 50% of the T cells directly after electroporation (Figure 2B). While this is a large cell loss it is important to have a high percent uptake as cell loss from sorting electroporated cells will be significantly higher (data not shown). Following electroporation, antigen-specific CD8 T cells were then maintained *in vitro* with antigen presenting beads for 48 hours, however, no additional toxicity was observed as the cells were still at about 50% survival compared to the 0V control (Figure 2C). Furthermore, we confirmed the uptake of ATTO550 was not due to surface binding, as the fluorescence was maintained long after electroporation, and exhibited a gradual decrease in fluorescence overtime as the cells proliferated (Figure 2D). However, 48hrs following Neon transfection the majority of the Cas9 complex has been diluted from the system or broken down (Figure 2D).

In stark contrast to the activated T cells, direct *ex vivo* purified naive T cells were not as amenable to Neon transfection. Using the highest recommended voltage on the Neon resulted in only an 80% uptake in ATTO550 (Figure S2A). This electroporation resulted in a significant decline in CD8 T cells numbers directly after transfection (Figure S2B). The cells were then activated with GP33-APB and analyzed 48 hours later, where significant cell death was still observed (Figure S2C). The decreased uptake of Cas9 in naïve CD8 T cells was also paired with a dramatic decline in the observed CAS9 protein even just 24 hours after electroporation, with no observable CAS9 present 48 hours after (Figure S2D). This suggests that the majority of the ATTO550 expression observed is a superficial coating on the cell surface of protein that was

unable to enter the cell. To mitigate the issue of CAS9 uptake, we drew from previous studies using CD8 T cells that showed preincubation of resting CD8 T cells in IL-7 helped increase the fold-uptake of Cas9 product[18]. Thus we utilized a similar preconditioning method on purified naïve CD8 T cells for 24 hours in IL-7, and while we did not see a deviation from their resting phenotype (data not shown) we observed a dramatic increase in the uptake of CAS9 (Figure S2D).

Choosing the appropriate crRNA target for protein knockout and validation

We next wanted to test if the increased ATTO550 fluorescence, which is our readout for CAS9 protein uptake, correlated with a functional CAS9 mediated gene deletion. To test the CAS9 mediated gene-knockout, we targeted a protein that becomes rapidly upregulated following T cell activation, PD-1. We demonstrated that within the first 24-48 hours of activation PD-1 becomes rapidly upregulated by effector CD8 T cells (Figure 1C, S1A, S1C). Furthermore, the wealth of data on PD-1 expression in chronic infections and tumors made it a perfect candidate for system validation[19,20]. Thus we electroporated these activated T cells with ATTO-CAS9 with a PD-1 crRNA and then cultured them for 2 days *in vitro* to asses PD-1 knockout efficiency. We observed that PD-1 MFI and % positivity was drastically decreased with increasing voltage (Figure 3A) and directly correlated with the ATTO550 Cas9 uptake observed (Figure 2A). To determine which sgRNA to utilize we used the Broad Institute Genetic Perturbation Platform and generated the top 5 best candidates. We demonstrated that all 5 candidates caused a significant decrease in PD-1 expression following Neon Transfection causing a decrease in PD-1 as early as 24 hours after Neon transfection, with nearly complete deletion by 48 hours following electroporation (Figure 3B). We confirmed that it was not a toxicity mediated effect of Cas9-ATTO addition that caused the decrease in PD-1 expression, as both –ve (no neon) and ATTO+Cas9 (neon control) sans PD-1 sgRNA had similar PD-1 expression (Figure 3C). Finally, to show that this method can target a wide variety of not only surface proteins but also transcription factors we targeted SATB1, shown to be relevant in antitumor function[21], with the top two candidate sgRNAs. We observed that both targets showed pronounced decrease in

SATB1 expression by 48 hours after electroporation compared to the electroporated control. (Figure 3D).

To test the PD-1 knockout efficacy on naive CD8 T cells, we stimulated the T cells with antigen presenting beads for 48 hours following Neon transfection. As expected, naïve CD8 T cells electroporated with CAS9 and PD-1 crRNA only showed deletion in the highest voltage tested, however, even at this voltage we observed the majority of cells still expressing PD-1 (Figure S3A). On the other hand, naïve T cells incubated in mIL-7 for 24 hours prior to electroporation had a dramatically decreased PD-1 expression by 48 hours after activation (Figure S3C). As CD25 also becomes drastically upregulated following CD8 T cell priming we used it as a knockout candidate to study the efficiency in CRISPR knock out of naïve IL-7 pretreated CD8 T cells. We observed that like with PD-1, although it still requires a higher voltage of 2200 V, the majority of the cells are knocked out when pretreated with IL-7 (Figure S3B).

Finally, memory CD8 T cells are a hallmark of an optimum immune response, however their resting state makes it impossible to probe gene functions by knockout, without a conditional knockout Cre-lox system. However, naïve and memory CD8 T cells share a large overlap in critical survival cytokines with long-lasting memory cells upregulating their expression of IL-7Rα (CD127). Thus, we wanted to test if we could use this naïve Neon CRISPR modality to knockout genes from memory CD8 T cells. To this end, we used LCMV memory mouse spleens and purified them for CD8 T cells utilizing CD44 as a marker of antigen experience[22], and CXCR3 as a protein known to be upregulated in memory T cells[23]. We incubated the memory cells in IL-7 for 24 hours prior to transfection, and then performed Neon electroporation with Cas9 loaded with CXCR3 crRNA. We observed a significant decrease in CXCR3 expression in the CD44+ memory T cells (Figure S3D). We hypothesize that the remaining CXCR3 expression at day 3 post-Neon is due to the slow turnover in protein in resting memory cells as we observed a slow but steady decline from day 1 to day 3 post electroporation (Figure S3D).

Collectively, we have demonstrated that this Neon CRIPSR protocol selectively knocks out surface and intracellular proteins from antigen-specific T cells prior to infection, during

effector differentiation, and in resting memory cells. This provides a powerful toolset to study CD8 T cells at all points of their immune responses.

Comparison of established knockout model with CRISPR mediated knockout.

Having standardized a efficient CRISPR-CAS knockout system, we next wanted to confirm that the CRISPR mediated protein knockout led to physiologically relevant outcomes compared to established somatic murine P14 knockouts. Recent studies utilizing PD-$1^{-/-}$ P14 in chronic infections demonstrated that in the absence of PD-1, CD8 T cells undergo a vigorous expansion compared to their WT counterparts[17]. Thus, to understand how well our CRISPR model aligns with the somatic knockout, we first needed to standardize how many CRISPR modified T cells must be transferred into an infected mouse to obtain a measurable T cell response without causing supraphysiological levels of donors. To standardize the appropriate T cell dose, we cotransferred *in vitro* activated non-electroporated (control) cells with varying amounts of electroporated but non-CRISPR containing (Neon) T cells into infection matched $LCMV_{CL-13}$ infected mice. Mice were followed to the peak of effector expansion (day 8) and spleens were stained to compare survival of the donor cells compared to the endogenous GP33 response. We observed that an adoptive transfer of $2x10^5$, *in vitro* 48hr activated, antigen-specific CD8 T cells into day 2 infected mice was able to match the endogenous frequency of GP33-specific CD8 T cells (Figure S4A-B). However, as we showed previously, the electroporation process causes a significant amount of cell death and we observed this *in vivo* as well, as it required 400-500k Neon antigen-specific CD8 T cells to match the number of control donors (Figure S4A-B). The transfer of these cells did not impact the exhaustion of the endogenous or donor CD8 T cells as evidenced by their day 8 post-infection expression of high levels of PD-1, consistent with a chronic viral infection (Figure S4C).

Utilizing these standardizations, we performed a PD-1 CRISPR knockout on WT (Thy1.1/1.1) *in vitro* activated CD8 T cells, and cotransferred them with WT electroporated control (Thy1.1/1.2) cells into day 2 $LCMV_{CL-13}$ infected B6 mice (Figure 4A). A parallel experimental branch was setup to recapitulate the previous findings; containing *in vitro* activated germline PD-$1^{-/-}$ P14 T cells (Thy1.1/1.1) cotransferred with WT electroporated control

(Thy1.1/1.2) cells into day 2 $LCMV_{CL-13}$ infected B6 mice. Utilizing the Neon conditions established in Figure 2, we confirmed that all cells effectively took up the ATTO550-Cas9 protein (Figure 4B). Furthermore, we demonstrated that prior to CRISPR mediated deletion of PD-1 both WT groups expressed similar levels, and only the somatic PD-$1^{-/-}$ expressed basal levels of PD-1 (Figure 4B). We confirmed the knockout of PD-1 *in vitro* 48hrs post-Neon transfection and demonstrated that the knocked out cells had expression similar to PD-$1^{-/-}$ CD8 T cells that were electroporated with just ATTO-Cas9 (Figure 4B). WT and PD-1 knockout CD8 T cells had similar starting ratios (Figure 4D), and were still comparable by day 8 post-infection. Following day 8 post-LCMV infection we observed a dramatic expansion in PD-1 knockout CD8 T cells in both the CRISPR knockout, and somatic knockout CD8 T cells, resulting in increased number of cells detected in PBMC of infected animals (Figure 4D). We confirmed that PD-1 was knocked out even *in vivo* with PD-1 CRISPR knockout cells showing baseline levels of PD-1 in spleen, but still expressing effector molecule Granzyme B showing CRISPR didn't affect their effector function (Figure 4E). We next compared the expansion in secondary lymphoid tissues as well as peripheral sites of infection and observed a significant expansion of PD-1 CRISPR knockout donor cells in all tissues (Figure 4F). This recapitulates the previously published role of PD-1 mediated suppression of exhausted CD8 T cells[17].

Effect of CRISPR transfection protocol on memory differentiation.

We next wanted to confirm that we could also recapitulate normal memory differentiation following Neon electroporation. Thus, we electroporated *in vitro* activated CD8 T cells and adoptively transferred them into infection matched mice infected with acute $LCMV_{Arm}$ strain. Donor cells underwent vigorous effector expansion forming MPEC and SLEC ratios at all doses measured consistent with previously published data (Figure S4D)[2,6]. We then followed these cells to memory differentiation and observed the formation of long-lived memory cells by day 30 post-infection (Figure S4E). Furthermore, we observed that Neon electroporated naïve CD8 T cells preconditioned with IL-7 for 24 hours, could be transferred at numbers identical to their direct *ex vivo* naïve transferred counterparts, resulting in similar effector expansion and memory differentiation kinetics (data not shown). This data demonstrates the robust

application of the CRISPR-CAS9 knockout system to acute effector expansion and memory differentiation.

Utilizing the CRISPR transfection to predict gene function in tumor environment.

Being able to recapitulate CD8 T cells dynamics under acute and chronic conditions following CRISPR editing, led us to test whether it could be utilized to study T cell dynamics in a localized exhausted environment of solid tumors. Between the advent of checkpoint blockade therapy, and the new development of CAR T cell therapy, there is a growing impetus for discovering targets critical in maintaining CD8 T cells in an activated state to prevent tumor mediated exhaustion and promote the clearance of the malignant tissue. PD-1 checkpoint blockade therapy was demonstrated to drive powerful T cell rescue in both chronic viral infections, as well as certain solid tumors[19,24]. MC38 is one such tumor that is highly amenable to PD-1/PDL1 checkpoint blockade therapy[24]. Thus, to create a model for testing protein function in a tumor environment, we started by knocking out the best candidate, PD-1, from activated effector cells to compare how ablation of this inhibitory signal for the antigen-specific T cells will impact tumor growth. We generated an MC38 cell line expressing GP33-41 peptide of LCMV and demonstrated that on its own it is capable of establishing extensive tumor burden (Figure 5A). We then compared the impact of transferring activated effector CD8 T cells that were electroporated with ATTO (control) or ATTO with PD-1-CAS9 (knockout). We separately transferred both sets of cells into mice with established tumor burden to compare the ability of the T cells to drive tumor recession (Figure S5A). We observed that donor ATTO CD8 T cells were able to stabilize the tumor and prevent further tumor growth, demonstrating the benefit of transferring activated effector CD8 T cells (Figure 5A). However, the adoptive transfer of PD-1 CRISPR knockout CD8 T cells was able to suppress tumor growth and drive tumor recession (Figure 5A). We observed that these effects were not due to differential survival between WT and CRISPR KO during transfer, as both populations were able to maintain similar frequencies in PBMC (Figure 5B). These peripheral cells had similar resting levels of activation markers and cells size in the spleen at day 24 post-tumor transplant (Figure S5B). This resting phenotype in the donors was consistent with their high polyfunctionality, demonstrating that the cells in the

periphery are not being exposed to the tumor antigen (Figure S5D). However, when comparing donor cells isolated from tumors, we observed that CRISPR knockout CD8 T cells were unable to upregulate PD-1 in the tumor environment, however, they still expressed similar levels of activation marker CD69, exhaustion marker TIM3, as well as similar cell size (Figure S5B). When comparing the function of the PD-1 KO T cells, we observed that in the absence of PD-1 signaling, donor TILs had slightly higher polyfunctionality expressing higher levels of IFN-γ, TNF-α and IL-2 (Figure 5D), consistent with the known effect of PDL1 blockade in chronic infections. However, despite the differences in function and tumor clearance we did not see differences in total cell number accumulation in spleen or TIL, nor an increase in the density of donor PD-1KO CD8 T cells in the tumors (Figure 5C, S5C). This suggests that while knocking out PD-1 increases their effectiveness in tumor clearance, it does not prevent the exhaustion of CD8 T cells, but merely delays it, which is consistent with its function during chronic infection[17]. This data demonstrates a useful model of CRISPR Cas9 editing in a tumor setting that can be used to screen a variety of gene function in T cells in a solid tumor with multiple readouts including tumor cell growth, phenotypic analysis of donor cells, and functional cytokine profile of exhausted TILs and peripheral circulating T cells.

Discussion.

In this paper we have laid out the groundwork for studying effects of gene knockout in antigen-specific CD8 T cells during distinct phases of differentiation, without significantly perturbing them from their naïve, effector or memory states. We were able to demonstrate that this model works during acute infections, with CRISPR control cells undergoing standard effector expansion and memory differentiation. Furthermore, using PD-1 CRISPR KO CD8 T cells we were able to recapitulate the exaggerated T cell expansion during chronic infection, phenocopying the corresponding germline PD-$1^{-/-}$ phenotype. To increase the utility of this process we also titrated the number of donor CD8 T cells necessary to match endogenous frequencies following chronic infection, as well as the donors transferred during acute infection to match specific T cell benchmarks for day 8 effector expansion and memory formation.

The murine model of solid tumors is rich with a wide array of tumor specific T cell mouse lines, as well as a multitude of different types of tumors such as glioma, melanoma, colorectal, and breast cancer lines, to name a few. In each scenario antigen-specific CD8 T cells respond uniquely and have different requirements to undergo sufficient rescue and tumor growth suppression. Using this Neon CRISPR protocol, we have demonstrated that we can target the genetic ablation of any target protein, and evaluate its effect on CD8 T cell mediated tumor growth kinetics. The difference between untransferred tumor growth, and the delayed tumor growth observed upon transfer of activated CD8 T cells demonstrates that there is flexibility in this model to show negative and positive gene regulators of antitumor responses. In fact, we have shown for the first time the effect of transferring PD-$1^{-/-}$ effector CD8 T cells into MC38 tumor bearing mice, and the increased clearance that these cells were able to impose. Furthermore, we observed that despite lacking the PD-1 inhibitory receptor, these cells were still significantly exhausted compared to their peripheral circulating T cell counterparts. This experimental model system creates an exciting environment for deconvoluting signals necessary for understanding CD8 T cell immunosuppression in chronic environments.

Recent studies have demonstrated that Tox1/2-NR4A signaling axis is a critical mediator in the differentiation of exhausted CD8 T cells, and that a knockout of Tox1/2 could be beneficial in the clearance of tumor specific T cells[25,26]. Utilizing the Neon CRIPSR model laid out here could help test multiple potential targets in parallel to compare localization, effector

function, and polyfunctionality following genetic perturbation of the antigen-specific CD8 T cells. We believe the tools we have standardized will be broadly applicable in T cell immunology, and can accelerate the field in determining genes critical for potent CD8 T cell responses.

Authorship and Conflict of Interest Statements

Contribution: YY carried out experiments, analyzed data, prepared figures and wrote manuscript. VK and SS conceptualized the project, designed the experiments, carried out experiments, supervised the work, analyzed data, interpreted the results and helped prepare the manuscript.

Conflict-of-interest disclosure: The authors declare no competing financial interests.

References

1. Zhang, N. & Bevan, M. J. CD8(+) T cells: foot soldiers of the immune system. *Immunity* **35,** 161–168 (2011).
2. Sarkar, S. *et al.* Functional and genomic profiling of effector CD8 T cell subsets with distinct memory fates. *The Journal of …* (2008).
3. Kalia, V. *et al.* Prolonged interleukin-2Ralpha expression on virus-specific CD8+ T cells favors terminal-effector differentiation in vivo. *Immunity* **32,** 91–103 (2010).
4. Sarkar, S. *et al.* Programming of CD8 T Cell Quantity and Polyfunctionality by Direct IL-1 Signals. *The Journal of Immunology* **201,** 3641–3650 (2018).
5. Kaech, S. M., Hemby, S., Kersh, E. & Ahmed, R. Molecular and functional profiling of memory CD8 T cell differentiation. *Cell* **111,** 837–851 (2002).
6. Kaech, S. M. *et al.* Selective expression of the interleukin 7 receptor identifies effector CD8 T cells that give rise to long-lived memory cells. *Nat Immunol* **4,** 1191–1198 (2003).
7. Wherry, E. J. & Kurachi, M. Molecular and cellular insights into T cell exhaustion. *Nat Rev Immunol* **15,** 486–499 (2015).
8. Wherry, E. J. *et al.* Molecular Signature of CD8+ T Cell Exhaustion during Chronic Viral Infection. *Immunity* **27,** 670–684 (2007).
9. Wherry, E. J., Blattman, J. N., Murali-Krishna, K., van der Most, R. & Ahmed, R. Viral persistence alters CD8 T-cell immunodominance and tissue distribution and results in distinct stages of functional impairment. *Journal of Virology* **77,** 4911–4927 (2003).
10. Arsenio, J. *et al.* Early specification of CD8+ T lymphocyte fates during adaptive immunity revealed by single-cell gene-expression analyses. *Nat Immunol* **15,** 365–372 (2014).
11. Smith, K. A. Conditional IL-2 gene deletion: consequences for T cell proliferation. 1–12 (2012). doi:10.3389/fimmu.2012.00102/abstract
12. Khan, A. A., Penny, L. A., Yuzefpolskiy, Y., Sarkar, S. & Kalia, V. MicroRNA-17~92 regulates effector and memory CD8 T-cell fates by modulating proliferation in response to infections. **121,** 4473–4483 (2013).
13. Baumann, F. M., Yuzefpolskiy, Y., Sarkar, S. & Kalia, V. Dicer Regulates the Balance of Short-Lived Effector and Long-Lived Memory CD8 T Cell Lineages. *PLoS ONE* **11,** e0162674 (2016).
14. Kurachi, M. *et al.* Optimized retroviral transduction of mouse T cells for in vivo assessment of gene function. *Nat Protoc* **12,** 1980–1998 (2017).
15. Yeo, C. J. J. & Fearon, D. T. T-bet-mediated differentiation of the activated CD8+ T cell. *Eur. J. Immunol.* **41,** 60–66 (2011).
16. Araki, K. *et al.* mTOR regulates memory CD8 T-cell differentiation. *Nature* **460,** 108–112 (2009).
17. Odorizzi, P. M., Pauken, K. E., Paley, M. A., Sharpe, A. & Wherry, E. J. Genetic absence of PD-1 promotes accumulation of terminally differentiated exhausted CD8+ T cells. *J. Exp. Med.* **212,** 1125–1137 (2015).
18. Seki, A. & Rutz, S. Optimized RNP transfection for highly efficient CRISPR/Cas9-mediated gene knockout in primary T cells. *Journal of Experimental Medicine* **215,** 985–997 (2018).
19. Barber, D. L. *et al.* Restoring function in exhausted CD8 T cells during chronic viral infection. *Nature* **439,** 682–687 (2006).
20. Curran, M. A., Montalvo, W., Yagita, H. & Allison, J. P. PD-1 and CTLA-4 combination

blockade expands infiltrating T cells and reduces regulatory T and myeloid cells within B16 melanoma tumors. *Proc. Natl. Acad. Sci. U.S.A.* **107,** 4275–4280 (2010).
21. Stephen, T. L. *et al.* SATB1 Expression Governs Epigenetic Repression of PD-1 in Tumor-Reactive T Cells. *Immunity* **46,** 51–64 (2017).
22. Budd, R. C. *et al.* Distinction of virgin and memory T lymphocytes. Stable acquisition of the Pgp-1 glycoprotein concomitant with antigenic stimulation. *J. Immunol.* **138,** 3120–3129 (1987).
23. Hu, J. K., Kagari, T., Clingan, J. M. & Matloubian, M. Expression of chemokine receptor CXCR3 on T cells affects the balance between effector and memory CD8 T-cell generation. *Proc. Natl. Acad. Sci. U.S.A.* **108,** E118–27 (2011).
24. Juneja, V. R. *et al.* PD-L1 on tumor cells is sufficient for immune evasion in immunogenic tumors and inhibits CD8 T cell cytotoxicity. *Journal of Experimental Medicine* **214,** 895–904 (2017).
25. Seo, H. *et al.* TOX and TOX2 transcription factors cooperate with NR4A transcription factors to impose CD8+ T cell exhaustion. *Proc. Natl. Acad. Sci. U.S.A.* **116,** 12410–12415 (2019).
26. Khan, O. *et al.* TOX transcriptionally and epigenetically programs CD8+ T cell exhaustion. *Nature* **571,** 211–218 (2019).

Figures

Figure 1

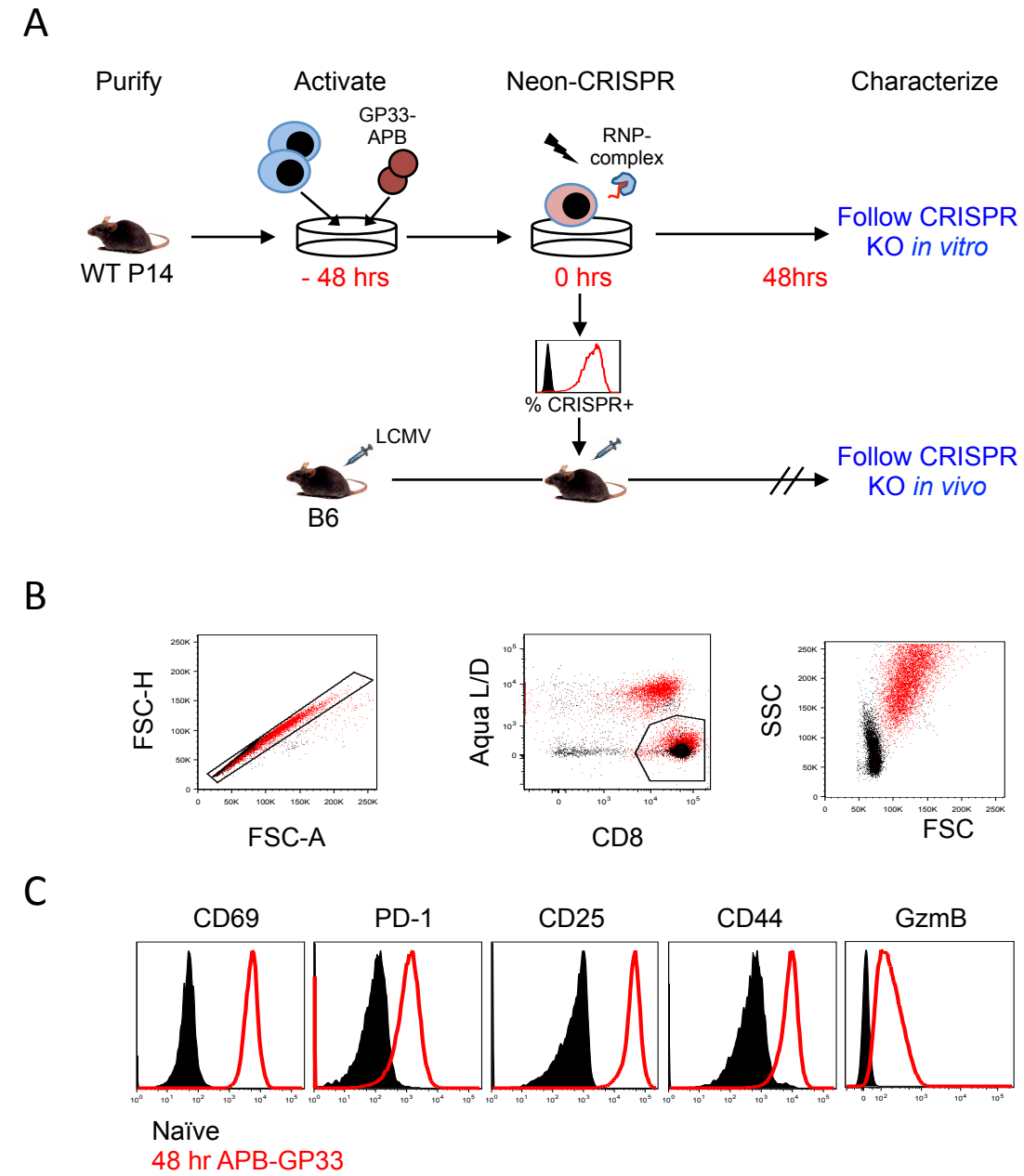

Supplemental Figure 1

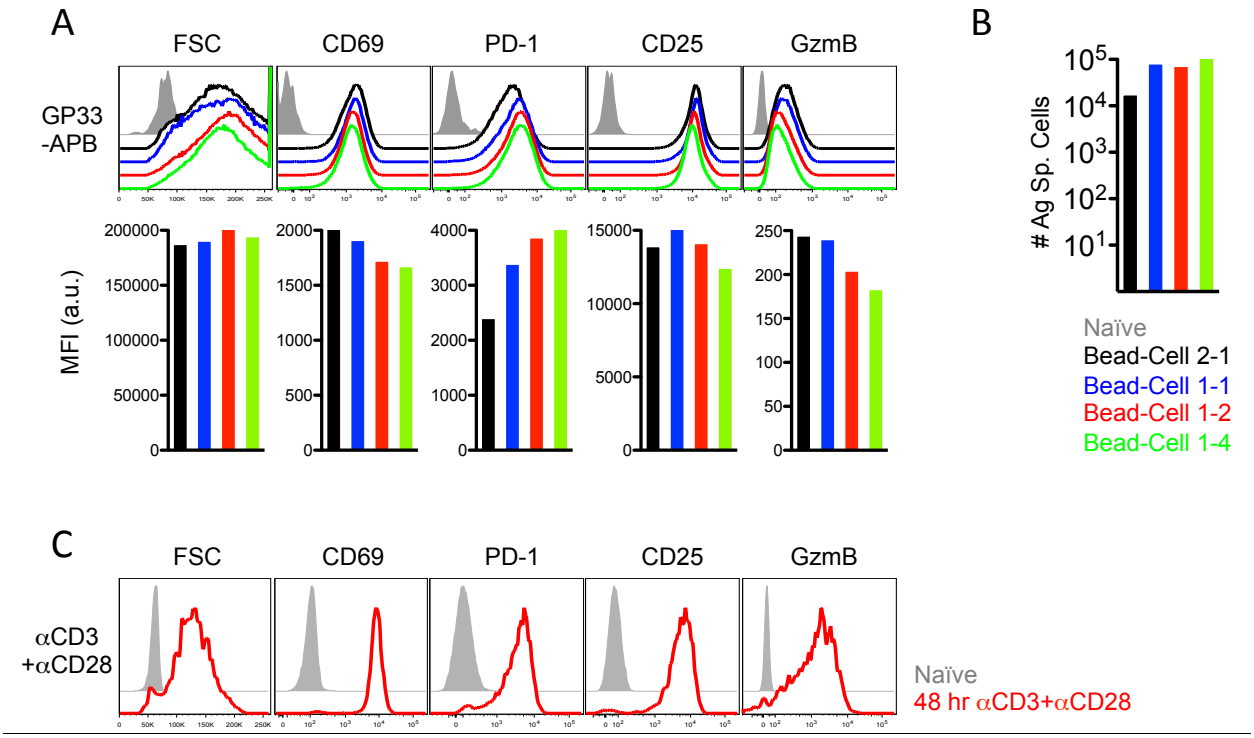

Figure 2

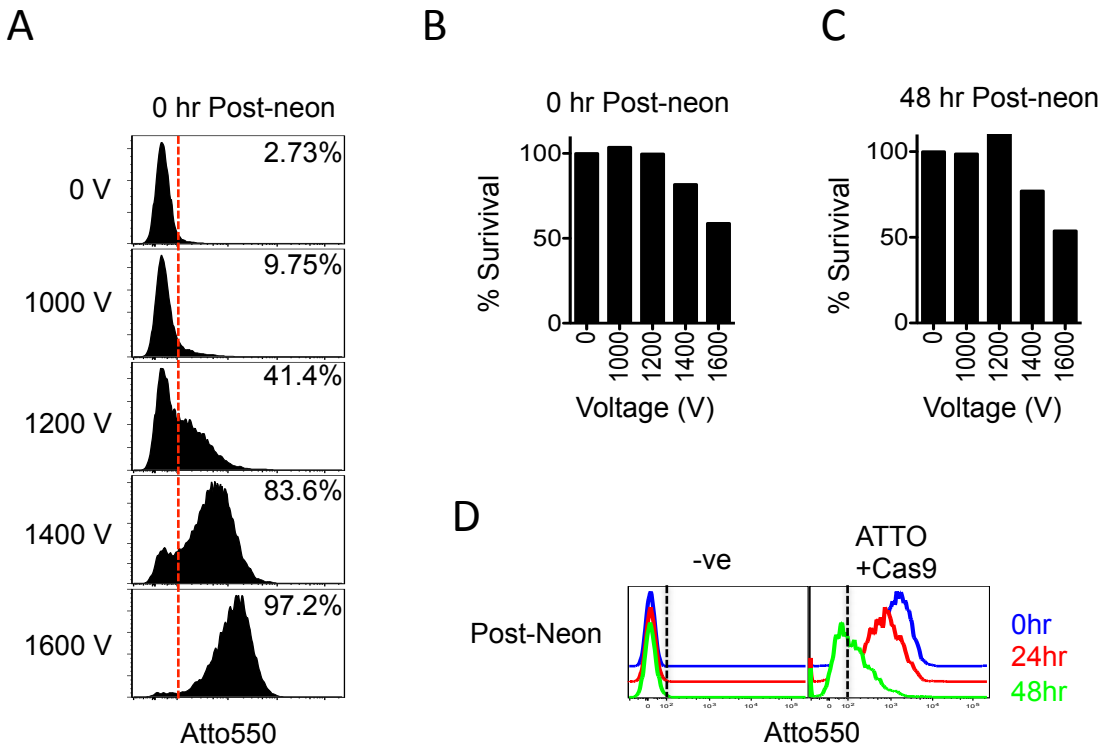
A
0 hr Post-neon
0 V
1000 V
1200 V
1400 V
1600 V
2.73%
9.75%
41.4%
83.6%
97.2%
Atto550
B
0 hr Post-neon
% Survival
100
50
0
0
1000
1200
1400
1600
Voltage (V)
C
48 hr Post-neon
% Survival
100
50
0
0
1000
1200
1400
1600
Voltage (V)
D
-ve
ATTO
+Cas9
Post-Neon
0hr
24hr
48hr
Atto550

Supplemental Figure 2

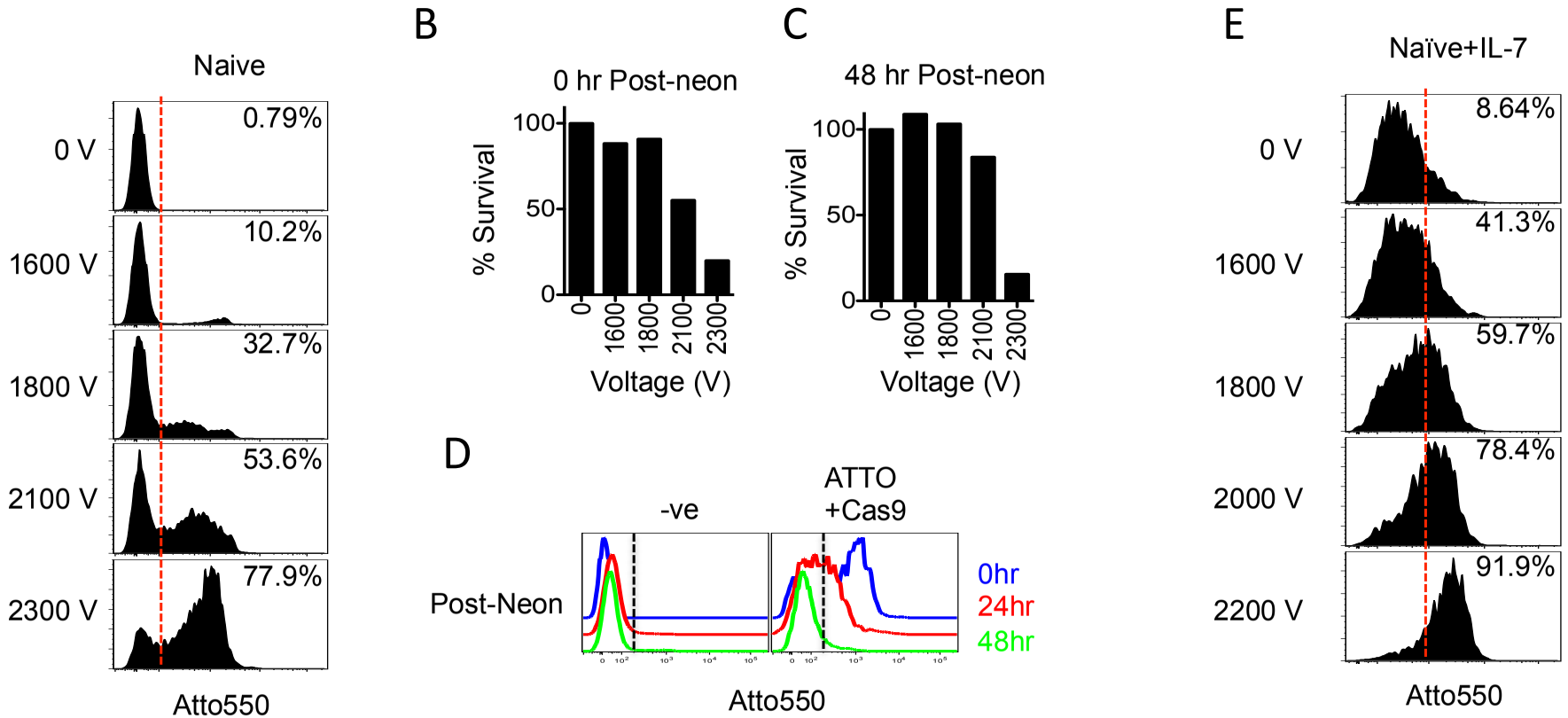

Figure 3

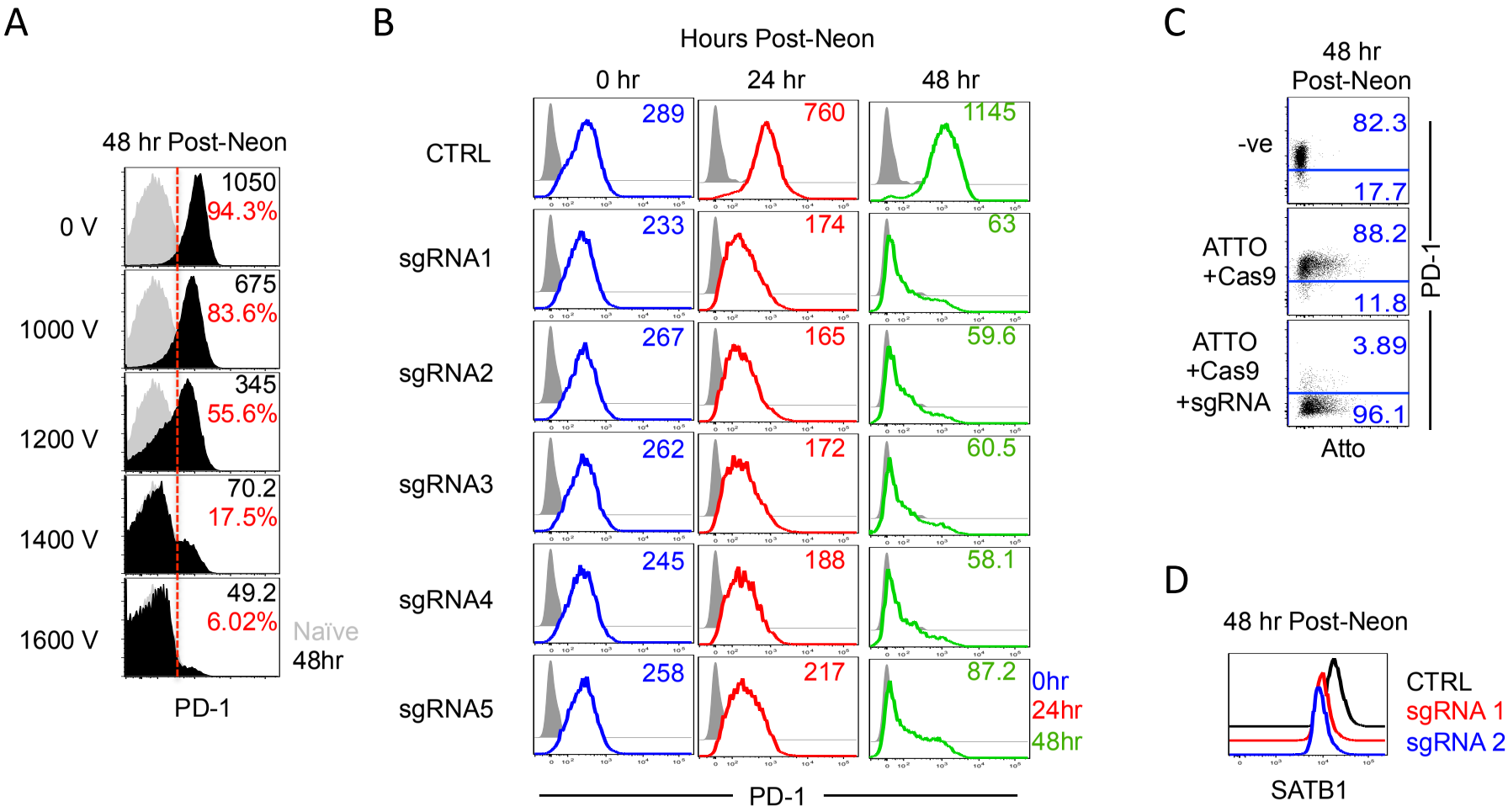
A
48 hr Post-Neon
0 V
1000 V
1200 V
1400 V
1600 V
1050
94.3%
675
83.6%
345
55.6%
70.2
17.5%
49.2
6.02%
Naïve
48hr
PD-1
B
Hours Post-Neon
0 hr
24 hr
48 hr
CTRL
sgRNA1
sgRNA2
sgRNA3
sgRNA4
sgRNA5
289
760
1145
233
174
63
267
165
59.6
262
172
60.5
245
188
58.1
258
217
87.2
0hr
24hr
48hr
PD-1
C
48 hr
Post-Neon
-ve
ATTO
+Cas9
ATTO
+Cas9
+sgRNA
82.3
17.7
88.2
11.8
3.89
96.1
PD-1
Atto
D
48 hr Post-Neon
CTRL
sgRNA 1
sgRNA 2
SATB1

Supplemental Figure 3

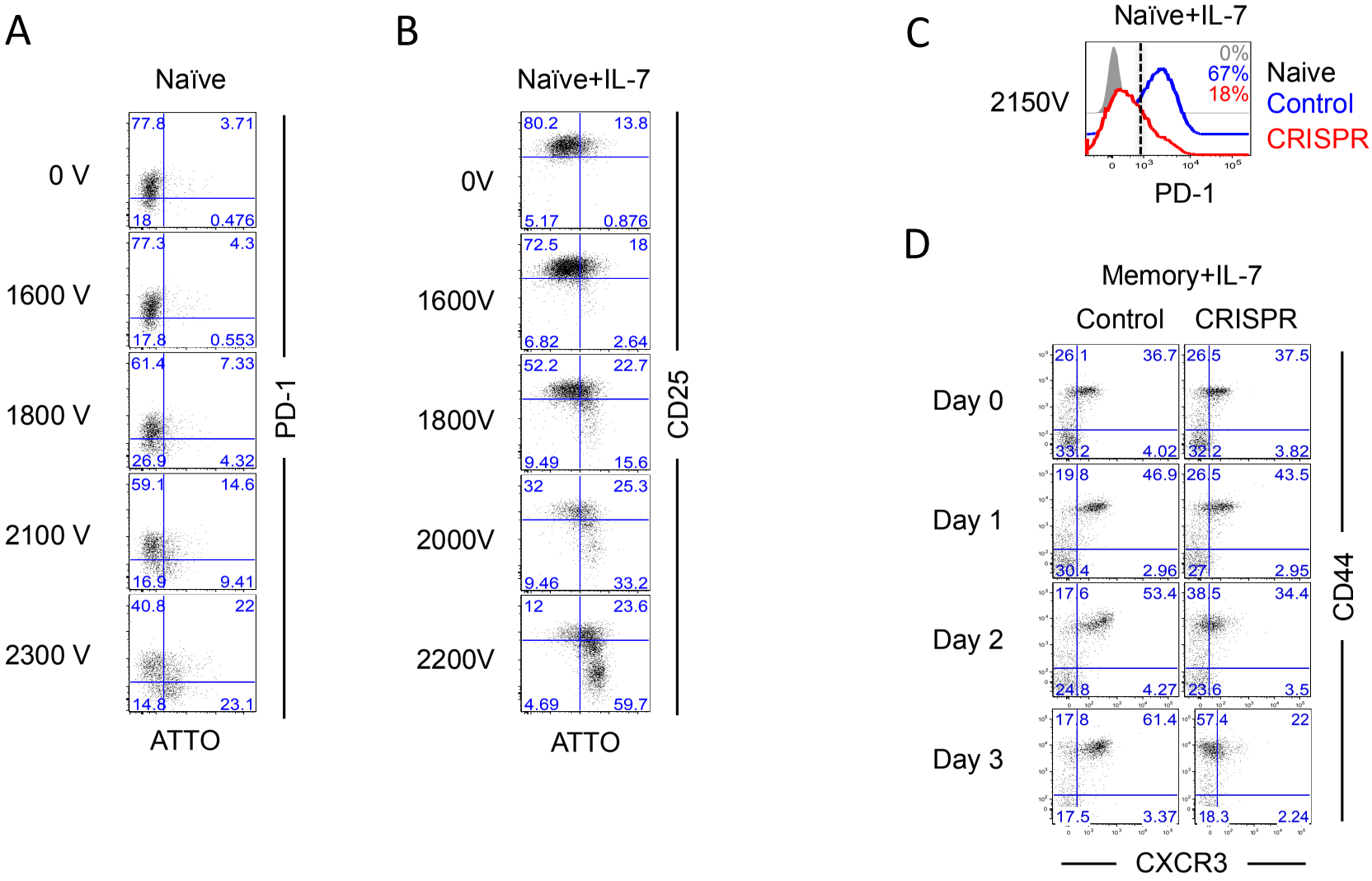

Figure 4

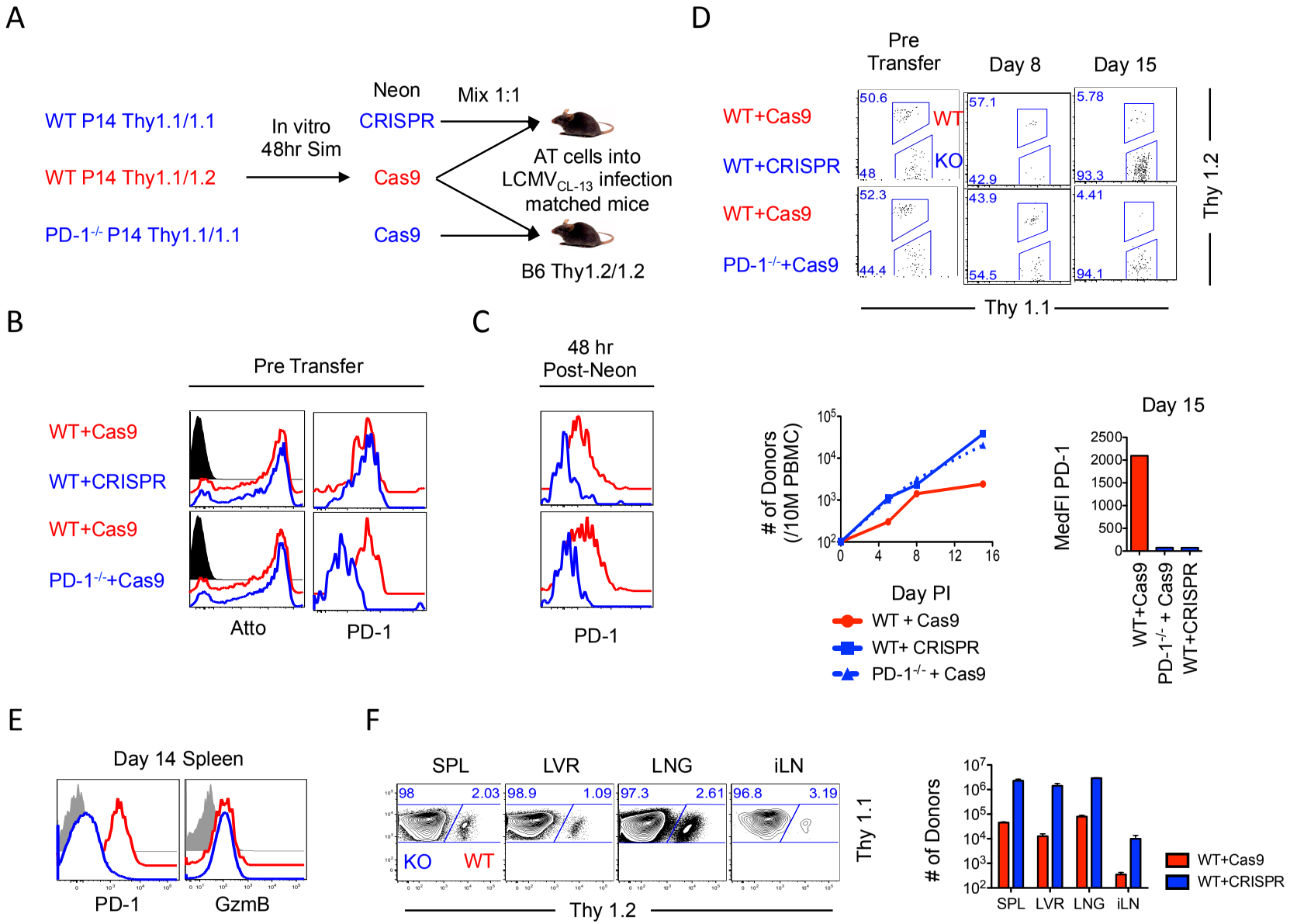
A
WT P14 Thy1.1/1.1
WT P14 Thy1.1/1.2
PD-1-/- P14 Thy1.1/1.1
In vitro 48hr Sim
Neon
CRISPR
Cas9
Cas9
Mix 1:1
AT cells into LCMVCL-13 infection matched mice
B6 Thy1.2/1.2
B
Pre Transfer
WT+Cas9
WT+CRISPR
WT+Cas9
PD-1-/-+Cas9
Atto
PD-1
C
48 hr Post-Neon
PD-1
D
Pre Transfer
Day 8
Day 15
WT+Cas9
WT+CRISPR
WT+Cas9
PD-1-/-+Cas9
50.6
WT
48
KO
57.1
42.9
5.78
93.3
52.3
44.4
43.9
54.5
4.41
94.1
Thy 1.2
Thy 1.1
# of Donors (/10M PBMC)
Day PI
WT + Cas9
WT+ CRISPR
PD-1-/- + Cas9
Day 15
MedFI PD-1
WT+Cas9
PD-1-/- + Cas9
WT+CRISPR
E
Day 14 Spleen
PD-1
GzmB
F
SPL
LVR
LNG
iLN
98
2.03
98.9
1.09
97.3
2.61
96.8
3.19
KO
WT
Thy 1.1
Thy 1.2
# of Donors
SPL
LVR
LNG
iLN
WT+Cas9
WT+CRISPR

Supplemental Figure 4

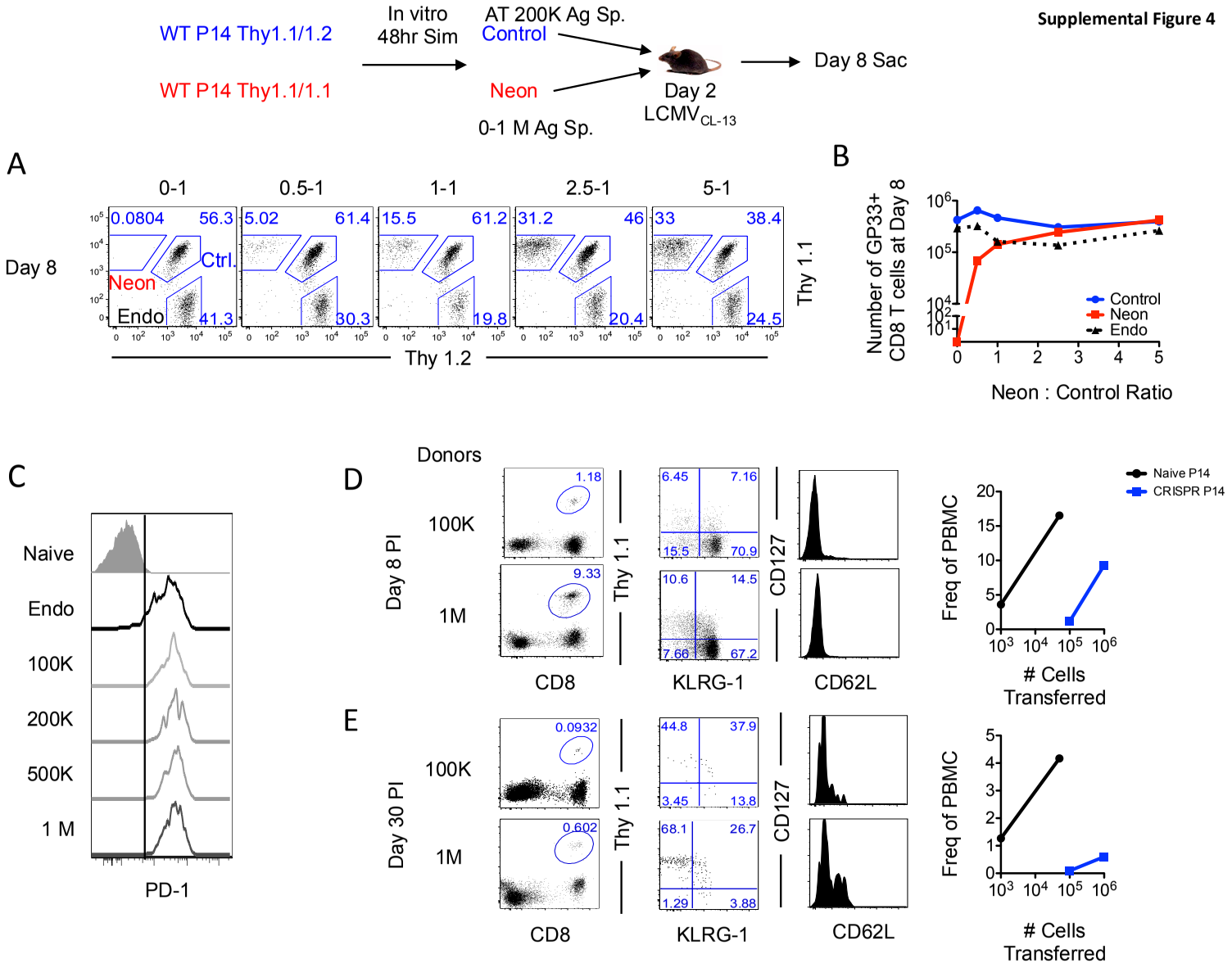

Figure 5

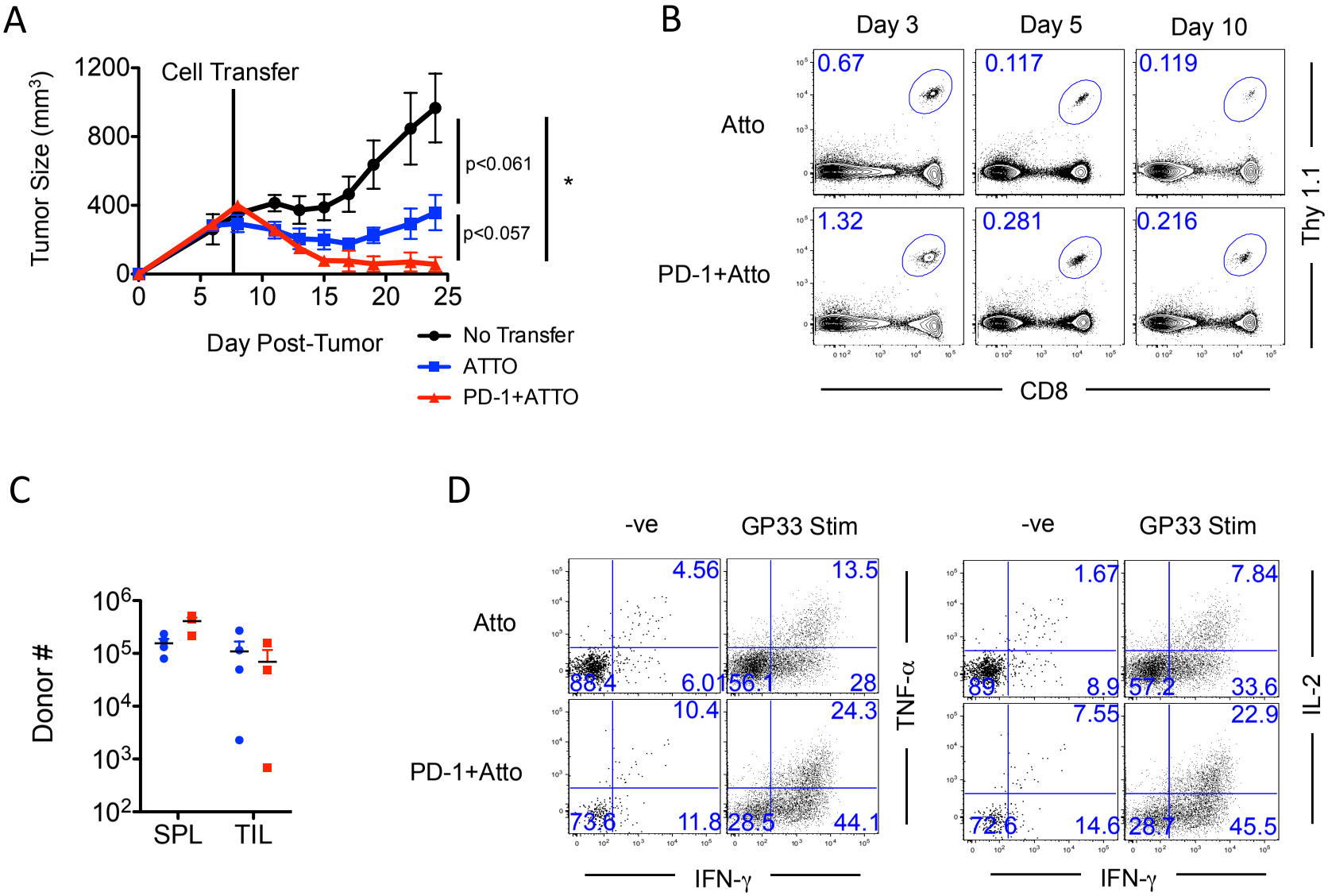
A
Tumor Size (mm3)
1200
800
400
0
Cell Transfer
0
5
10
15
20
25
Day Post-Tumor
p<0.061
p<0.057
*
No Transfer
ATTO
PD-1+ATTO
B
Day 3
Day 5
Day 10
Atto
PD-1+Atto
0.67
0.117
0.119
1.32
0.281
0.216
Thy 1.1
CD8
C
Donor #
10^6
10^5
10^4
10^3
10^2
SPL
TIL
D
-ve
GP33 Stim
-ve
GP33 Stim
Atto
PD-1+Atto
4.56
13.5
88.4
6.01
56.1
28
1.67
7.84
89
8.9
57.2
33.6
10.4
24.3
73.6
11.8
28.5
44.1
7.55
22.9
72.6
14.6
28.7
45.5
TNF-α
IL-2
IFN-γ
IFN-γ

Supplemental Figure 5

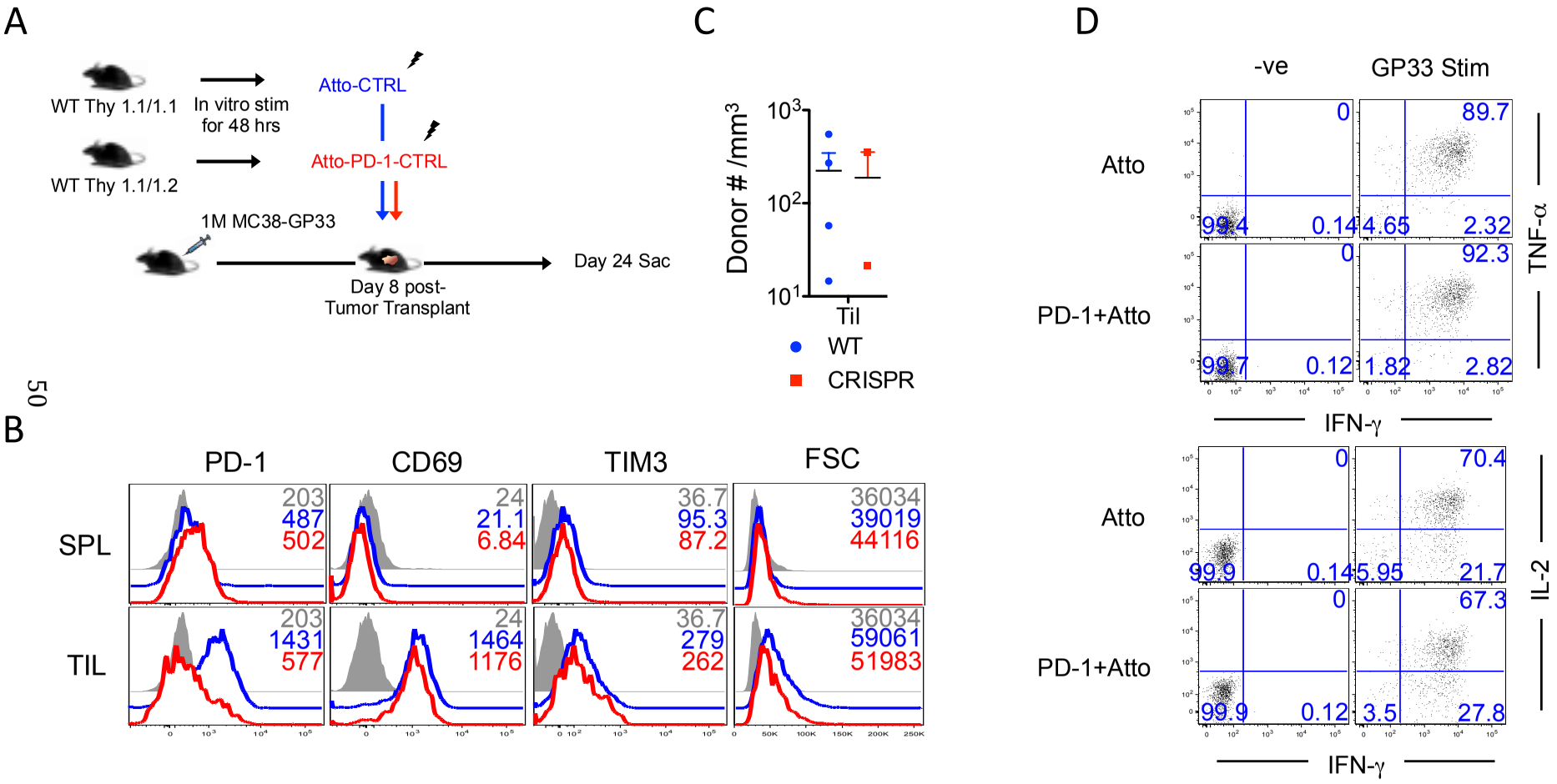

Figure Legends:

Figure 1. Optimal activation of antigen-specific CD8 T cells for CRISPR transfection. **A.** Experimental design. WT antigen-specific CD8 T cells are isolated from P14 mice and activated *in vitro* with antigen presenting beads coated with MHC-GP33 and αCD28. Cells are cultured for 36-48 hrs and magnetic beads are removed. Cells are resuspended in electroporation buffer together with CAS9 complex and electroporated using the Neon instrument. Cells are transferred into infection-matched mice and followed *in vitro* for knockout confirmation. B-C. Antigen-specific CD8 T cells are cultured *in vitro* with antigen presenting beads for 48 hrs. **B.** FACS plots show representative cell gating of naïve (black) and 48hr post-stimulation (red) antigen-specific CD8 T cells. **C.** Histograms depict activation markers of CD8 T cells 48 hrs post activation.

Supplemental Figure 1. Titration of antigen presenting beads for *in vitro* priming of antigen-specific CD8 T cells. A. Antigen-specific CD8 T cells activated with different APB-CD8 T cell ratios. FACS plots depict markers after 48hrs *in vitro* stimulation. Bar graphs show MFI of respective markers. **B**. Bar graph shows number of antigen-specific CD8 T cells following 48 hr stimulation. **C**. Histograms depict activation markers following 48 hours of activation (red histogram) using αCD3/αCD28 coated plates. Gray histograms show expression in naïve T cells.

Figure 2. Activated CD8 T cells take up and retain CAS9 complex following electroporation. A-B. Antigen-specific CD8 T cells are electroporated following 48 hr stimulation. **A**. Histograms depict uptake CAS9 complex by fluorescence of tracrRNA-ATTO550. FACS plots depict survival of antigen-specific CD8 T cells following electroporation. **B**. Bar graph shows survival of antigen-specific CD8 T cells directly after electroporation. **C**. Following electroporation using 1600V antigen-specific CD8 T cells were cultured *in vitro* with APB-33+IL-2. Histograms depict ATTO550 at indicated times post electroporation.

Supplemental Figure 2. Naïve CD8 T cells need IL-7 stimulation to take up CAS9 complex following electroporation. A. Antigen-specific CD8 T cells were purified from naïve spleens and electroporated with ATTO550-tagged Cas9. Histograms depict uptake CAS9 complex by

fluorescence of tracrRNA-ATTO550. B-C. Bar graph shows survival of antigen-specific CD8 T cells **B**. directly after electroporation or **C**. following electroporation and 48 hours of *in vitro* stimulation with APB-GP33+IL-2 for 48 hrs. **D**. Histograms depict amount of ATTO550 retained 0-48 hours post-electroporation. **E**. Antigen-specific CD8 T cells were purified from naïve spleens and cultured for 24hrs with IL-7. Cells were then electroporated with ATTO550-tagged Cas9 and indicated voltages. Percent in histogram represents amount of cells beyond the red dotted line.

Figure 3. Incorporation of CRISPR following electroporation results in robust gene deletion. **A-D**. Antigen-specific CD8 T cells were stimulated for 48 hours using GP33-APB followed by Neon mediated electroporation with CAS9-crRNA. Cells were then transferred back *in vitro* and stimulated for 48 hours with APB-GP33. **A**. FACS plots depict PD-1 MFI following electroporation of CAS9-PD-1 crRNA (Black) compared to naive controls (grey) 48hours after Neon Transfection. **B**. FACS plots depict PD-1 MFI following electroporation using 1600V of top 5 PD-1 sgRNA candidates at given time post-electroporation. **C**. FACS plots show PD-1 expression as a function of CAS9 incorporation using 1600V for electroporation. **D.** FACS plots depict expression of SATB1 48hrs following electroporation of control (black) or two top candidate sgRNAs (Red and Blue) for SATB1.

Supplemental Figure 3. Incubation with IL-7 leads to optimal CRISPR mediated knockout in resting CD8 T cells. A. Naïve CD8 T cells were purified from spleens and electroporated with Cas9-PD1. Cells were then cultured *in vitro* with GP33-APB for 48 hours. B-C. Naïve CD8 T cells were purified from spleens and cultured for 24hrs with IL-7 *in vitro*. Cells were then electroporated with **B**. Cas9-CD25 or **C.** Cas9-PD-1. Cells were then stimulated *in vitro* with GP33-APB and target protein expression was measured 48hours following *in vitro* activation. **D**. Naïve B6 mice were infected with LCMV Arm. Spleens were collected from infected mice at day >60 post infection when memory has formed. CD8 T cells were purified from spleens and cultured for 24hrs in IL-7. Cells were then electroporated with Control or Cas9-CXCR3(CRISPR)

at 2200V. Cells were transferred back *in vitro* and stimulated with IL-7 and IL-15. FACS plots depict CXCR3 expression as a function of CD44 at given times post neon transfection.

Figure 4. CAS9 gene deletion of PD-1 phenocopies a somatic PD-1$^{-/-}$ CD8 T cells during a chronic infection. A. WT or PD-1$^{-/-}$ antigen-specific CD8 T cells were activated using APB-GP33 for 48hrs. Antigen-specific CD8 T cells were electroporated with CAS9 (control) or CAS9-PD-1 (CRISPR PD-1 knockout). WT control and WT CRISPR cells or WT control and PD-1KO control cells were cotransferred into infection matched LCMVCl-13 B6 mice. **B**. Histograms depict electroporation success and PD-1 expression prior to transfer into infection matched mice. **C**. Following eletroporation cells that were not transferred in vivo, were cultured *in vitro* with APB-GP33+IL-2. Histograms depict expression of PD-1 48 hrs after electroporation. **D.** FACS plot shows relative ratio of WT Cas9 and WT CRISPR cells or WT Cas9 and PD-1KO Cas9 cells prior to transfer into infection matched B6 mice. FACS plots show relative ratio of donors at day 8 and 15 post infection. Line graph shows number of respective donor cells in blood of infected animals. Bar graph shows MFI of PD-1 in respective donor CD8 T cells at day 15 post-infection. **E**. Infected mice were analyzed at day 14 post-infection and spleen, iLN, LVR, and LNG were collected. Histograms show marker expression of PD-1 and GzmB at day 14 post-infection gated on donor WT-CAS9 (Red) and WT-CRISPR (Blue) cells, and naïve endogenous CD8 T cells (gray). **F.** FACS plots depict relative ratio of WT-Cas9 (WT) or WT-CRISPR (KO) in respective tissues. Bar graphs enumerate donor CD8 T cells numbers.

Supplemental Figure 4. Titration of Donor CD8 T cells into infection matched mice to match endogenous CD8 T cell responses. Thy mismatched P14 CD8 T cells were purified from naïve mice and activated *in vitro* using GP33-APB for 48 hours. Cells were then electroporated using 1600V (Neon) or left unelectroporated (Control). Control and Neon cells were mixed together at given ratios and transferred into LCMVCL-13 infection matched mice. **A.** Mice were followed to peak of effector expansion at day 8 post-infection and spleens were collected. FACS plots are gated on GP33+CD44+ antigen-specific CD8 T cells. **B.** Line graph shows number of cells isolated from spleens of infected animals. **C.** Histograms are gated on Endogenous GP33 specific (Endo),

or Neon Donor cells at day 8 post-infection. **D-E**. Antigen-specific CD8 T cells were activated for 48hrs *in vitro* and electroporated using the Neon instrument. Cells were immediately transferred into LCMV Arm infection matched mice at given amounts and followed to day 8 and 30 post infection. FACS plots depict frequency of donors in PBMC as well as the phenotype of donors. Line plot shows the relationship between transferred antigen-specific CD8 T cells and the observed frequency in PBMCs for Naïve cells transferred prior to LCMV infection (Black) or day 2 transferred CRISPR electroporated cells (Blue).

Figure 5. CRISPR model for determining genes critical in mediating CD8 T cell antitumor function. Naïve CD8 T cells were purified from spleens and stimulated for 48 hours using GP33-APB. Cells were electroporated with ATTO alone (control) or CAS9-PD-1-ATTO (PD-1 knockout) and transferred into tumor-burdened mice. **A**. Line graph depicts tumor size in mice, which received no donors (No transfer), WT effectors (ATTO), or PD-1 KO effectors (PD-1+ATTO). **B.** FACS plots show frequency of donor CD8 T cells in blood of recipient mice at given times post T cell transfer. **C**. Mice were carries to day 24 post-infection and tumors and spleens were collected. Graph depicts number of donor cells in spleen and TIL. **D**. TILs were stimulated for 5 hours in the presence of GP33 and BFA to measure cytokine functionality. FACS plots are gated on donor CD8 T cells in TILs.

Supplemental Figure 5. Distinct phenotypes of antigen-specific CD8 T cells in antigen free and tumor burdened environments. **A.** Naïve CD8 T cells were purified from spleens and stimulated *in vitro* for 48 hours using GP33-APB. Cells were electroporated with ATTO alone (control) or CAS9-PD-1-ATTO (PD-1 knockout) and transferred into tumor-burdened mice. **B.** Histograms are gated on donor antigen-specific CD8 T cells in spleen and TILs at day 24-post tumor transfer. Gray histogram is gated on endogenous $CD44^{lo}$ splenocytes. **C.** Graph shows number of donor CD8 T cells in TIL by volume of tumor. **D.** Splenocytes were stimulated for 5 hours in the presence of GP33 and BFA to measure cytokine functionality of donor cells. FACS plots are gated on donor CD8 T cells in spleen.

Distinct Roles of Autocrine and Paracrine IL-2 Signals in Primary and Secondary Cytotoxic T cell Responses

Yevgeniy Yuzefpolskiy[1,2], Laura A. Penny[3], Kendall A. Smith[4], Surojit Sarkar[1,2,5,6]✦, and Vandana Kalia[1,,6]✦

[1] Ben Towne Center for Childhood Cancer Research, Seattle Children's Research Institute, Seattle WA 98101.

[2] M3D Graduate Program, University of Washington School of Medicine, Seattle, WA 98195

[3] The Huck Institutes of Life Sciences, The Pennsylvania State University, University Park, PA 16802

[4] Division of Immunology, Joan and Sanford I. Weill Department of Medicine, Weill Cornell Medicine, Cornell University, New York, NY, USA

[5]Department of Pathology, University of Washington School of Medicine, Seattle, WA 98195

[6] Department of Pediatrics, Division of Hematology and Oncology, University of Washington

*Corresponding authors: Surojit Sarkar and Vandana Kalia, sarkarkalia@gmail.com
1100 Olive Lab, Suite 100
Ben Towne Center for Childhood Cancer Research
University of Washington School of Medicine
Seattle, WA 98101

Footnote: This work was supported by research funding from the NIH (IL-2 R03#) and the Seattle Children's Research Institute to SS and VK.

Running Title: Roles of Autocrine and Paracrine IL-2 Signals in Antigen Mediated CTL Responses

Word Count (Abstract): 242

Word Count (Text): 4,309

Figure/Table Count: 6 Main Figures, 6 Supplemental Figures

Reference Count: 33

Abstract

Cytotoxic CD8 T cell priming drives potent effector responses following infection, however, improper antigen and cytokine signaling can cause defects in memory T cell differentiation and survival following antigen clearance. The heightened ability of memory CD8 T cells to recognize, expand and expunge intracellular pathogens upon reinfection is vital for the protection of the host, and represents the driving stimulus for development long-lasting vaccines. In this study we query the unique roles of paracrine and autocrine IL-2 signals in the development of effector and memory CD8 T cell responses using murine model of acute viral infection. We demonstrate that paracrine IL-2 is sufficient to drive CD8 T cell aerobic glycolysis, expansion and effector differentiation and memory formation. As antigen-specific cells were capable of robust T cell expansion, production of effector cytokines, and formation of stable homeostatic maintenance of memory cells in the absence of autocrine IL-2. A heterologous rechallenge of these memory CD8 T cells demonstrated a sever defect in the maintenance but not proliferation of memory CD8 T cells lacking autocrine IL-2, resulting in a dramatically smaller pool of secondary memory cells. Using a model of temporal autocrine IL-2 ablation, we were able to show for the first time, that these autocrine IL-2 signals are critical during the early priming of CD8 T cells against the primary acute infection.

Introduction

IL-2 was first discovered and characterized as a T cell growth factor by its ability to drastically boost T cell proliferation *in vitro*(1, 2). In fact, IL-2 is a keystone cytokine in immune system modulation, not only boosting T cell proliferation(3-5), but also driving thymocyte development, T helper cell polarization (6-8), and is deemed critical for the maintenance of the regulatory T cell population(9, 10). T_{H1} CD4 T cells were determined as the main producers of IL-2, and upregulate its production in response to antigen-driven activation(11-13). This potent cytokine maintains T cell expansion against intracellular pathogens, keeping CD8 T cells in a glycolytic and proteolytic state necessary to drive proliferation, cytokine production, and cytotoxic function(14-17). IL-2 signals are potent modulators of the effector state where early heterogeneity in the expression of IL-2Rα causes a decrease in the sensitivity to IL-2 signals and the bifurcation of the effector CD8 T cell lineage into less sensitive memory precursors, and vigorously proliferating terminal effector cells(18-20). This early impact of IL-2 sensitivity echoes through the CD8 T cell response resulting in vastly different fates, with long-lived memory cells maintained for up to the lifetime of the individual, while terminal effectors rapidly die following antigen clearance(21, 22).

In addition to paracrine IL-2 signals received from CD4 T cells, cytotoxic CD8 T cells also exhibit the ability to produce their own IL-2, referred to as autocrine IL-2. Recent studies in CD4 T cells demonstrate that autocrine IL-2 production drives heterogeneity and the formation of T_{FH} cells from activated CD4 T cells that produce autocrine IL-2(23). While it has been shown that autocrine and paracrine IL-2 signals are critical in the secondary expansion of memory CD8 T cells(24, 25), here we aim to deconvolute the effects of paracrine IL-2 from autocrine, and the timing during which autocrine IL-2 is necessary to facilitate ideal memory programming.

Using an *in vitro* model of CD8 T cell activation combining WT antigen-specific T cells with blocking IL-2 antibodies, or IL-$2^{-/-}$ CD8 T cells with IL-2 supplementation, we demonstrate that paracrine IL-2 signals sufficiently drive the activation, metabolic conversion, and proliferation of antigen-specific CD8 T cells. *In vivo* cotransfer of WT and IL-$2^{-/-}$ antigen-specific CD8 T cells further confirmed that early paracrine IL-2 signals during infection were sufficient to drive activation and expansion of T cells. As we followed these cells through effector differentiation, we observed similar numbers accumulating at the peak of infection as well as similar expression of effector molecule Granzyme B and cytokine polyfunctionality. In the absence of autocrine IL-2, we did observe a modest increase in early T cell contraction; however, the result was a stable long-lived memory pool. As reported previously, we observed that memory cells lacking autocrine IL-2 displayed a defect in their secondary rechallenge expansion when challenged with a heterologous Listeria *monocytogenes* infection. However, we were able to show that this expansion defect was due to decreased survival and not proliferation. Finally, using a unique model of temporal IL-2 deletion with Tamoxifen inducible Cre-ERT IL-$2^{fl/fl}$ donor CD8 T cells, we were able to narrow down the CD8 T cell intrinsic window of autocrine IL-2 signaling and show that it is critical during the initial activation and expansion of CD8 T cells during the primary immune response. Deleting IL-2 following expansion, or during memory, prior to rechallenge, had no effect on secondary T cell kinetics.

Materials and Methods

Mice and infection

C57BL/6 mice (Thy1.2/1.2+ and Ly5.1/5.1+) were purchased from the Jackson Laboratory (Sacramento, CA, USA) and maintained in house. Thy1.1+ P14 mice bearing the H-2D^{b}GP$_{33-41}$ LCMV epitope-specific TCR were fully backcrossed to C57BL/6 mice and maintained in our animal colony. IL-2$^{-/-}$ mice were purchased from the Jackson Laboratory and crossed to P14 mice. IL-2$^{flox/flox}$ ERT2-Cre mice were generated in Kendall A. Smith's laboratory(17) and also crossed to P14 mice. To generate P14 chimeric mice, indicated numbers of antigen-specific CD8 T cells were adoptively transferred intravenously into naïve mice, about 12 hours prior to infection. Armstrong strain of LCMV was propagated, titered, and used as previously described (26). For primary infections, mice were injected intraperitoneally with 2×10^{5} PFU LCMV. Heterologous secondary challenge was performed by transferring memory CD8 T cells from LCMV memory mice into naïve C57BL/6 mice, which were then infected with 3x10^{4} CFU Listeria *monocytogenes* expressing GP33 peptide of LCMV (LM-GP33).

Flow cytometry

All antibodies were purchased from Biolegend (San Diego, CA, USA). MHC class I tetramers were made as described previously (22). Cells were stained for surface or intracellular proteins and cytokines as previously described(22). For analysis of intracellular cytokines, 2x10^{6} lymphocytes were stimulated with 0.2μg/mL GP$_{33-41}$ peptide in the presence of Brefeldin A for 5h, followed by surface staining for CD8, Ly5.1, Thy1.1, and Thy1.2, and intracellular staining for IFN-γ, TNF-α, or IL-2. Flow cytometric analysis was performed on LSRII Fortessa (BD Biosciences,

San Jose, CA). Single cell suspensions of spleen cells, lymph nodes, lungs, livers or PBMCs from mice were prepared and direct *ex vivo* staining was carried out as described previously(18).

Seahorse Assay

Oxygen consumption and extracellular acidification were measured using the XFe96 well Seahorse Analyzer (Agilent). Cells were purified and based on Thy1.1 expression from mice at indicated days post infection and adhered to plates using poly-L-lysine at 100K (*in vitro* activated) or 120K (direct *ex vivo* acquired) cells per well. Where indicated, a Mitostress test was performed in the presence of 10mM glucose (Agilent) with an addition of 2-Deoxyglucose (20mM) to obtain the zero point value of extracellular acidification.

***In vitro* Experiments**

Antigen-specific CD8 T cells were purified from naïve spleens using CD8 T cell negative selection Mojo Sort kit (Biolegend). WT or IL-$2^{-/-}$ CD8 T cells were stimulated *in vitro* using GP33 loaded splenocytes or GP33-antigen presenting beads (SA-Beads coated with GP33-MHC and αCD28 antibody) for 48hrs at 37°C. Where indicated, cells were given paracrine mIL-2 at 10ng/mL, or cells were deprived of IL-2 signals by using a combination of JES61A12 and S4B6 αIL-2 antibodies at 0.1μg/mL (Bio X Cell).

Statistical analysis

Paired or unpaired Student's t-test was used as indicated to evaluate differences between two group means. One-way ANOVA analysis with a Tukey post-test was used when comparing more than two groups. All statistical analyses were performed using Prism 5 and P values of statistical significance are depicted by asterisk per the Michelin guide scale: * ($P \leq 0.05$), ** ($P \leq 0.01$), *** ($P \leq 0.001$) and ($P > 0.05$) was considered not significant (ns).

Results

IL-2 signals are critical for CD8 T cell priming and memory differentiation.

Aside from activation with TCR and co-stimulation with CD28, CD8 T cells require a third signal like IL-2 to drive their effector expansion and differentiation into cytotoxic killer cells(27). While it has been demonstrated that CD8 T cells are capable of producing IL-2, we first wanted to see if this autocrine IL-2 was sufficient to affect CD8 T cell activation. Thus, we activated D^bGP33 specific CD8 T cells *in vitro* using antigen presenting beads (expressing GP33-MHC as well as αCD28 antibody) in the presence (UnTx) or absence (αIL-2 Tx) of autocrine IL-2 for 2 days. Regardless of IL-2 signaling, cells stimulated with APB were activated as indicated by upregulated CD44, and increased cell size (Figure 1A, Figure S1A data not shown). To demonstrate that autocrine IL-2 was produced at levels capable of signaling, we looked at the expression of IL-2Rα (CD25), which follows a positive feedback loop upon receiving IL-2 stimulation. IL-2 sufficient cells upregulated CD25, demonstrating that IL-2 signals were present, and also upregulated IL-2 dependent effector molecule Granzyme B (Figure 1A, Figure S1A). Antibody blockade of autocrine IL-2 signals caused a significant decrease in CD25 expression, as well as Granzyme B (Figure 1A, Figure S1A). Furthermore, we observed that reduced IL-2 signals significantly reduced glycolysis, the main source of energy production for cells during effector expansion (Figure S1B). To see if modulating energy production affected the T cell expansion, we looked at the uptake of BrdU at 48 post-stimulation. In line with the reduced energy production, we observed a significant decrease in cell cycling when blocking IL-2 signals (Figure 1B). Thus, we are able to demonstrate that CD8 T cell produce sufficient levels of IL-2 to recapitulate the classic function of IL-2 during T cell priming.

We next looked at the kinetics of autocrine IL-2 production *in vivo* to see how it parallels CD8 T cell effector expansion. We adoptively transferred naïve WT P14 CD8 T cells into naïve C57BL6 mice, and infected them with $LCMV_{Arm}$, we collected spleens from the mice prior to infection (naïve), following priming (day 2.75), during the effector response (days 5-8) and through memory differentiation (day 15-30). Following the activation of naïve CD8 T cells, IL-2 production is rapidly upregulated, preceding the production of IFN-γ (Figure 1C). The ability of the CD8 T cells to produce autocrine IL-2 maintains throughout the priming phase, however this functionality is rapidly lost during the effector expansion of the cytotoxic T cell responses (Figure 1C). However, following antigen clearance we observed an increase in IL-2 production in the antigen-specific CD8 T cells, which is the hallmark polyfunctionality of memory CD8 T cells. To demonstrate the enrichment of IL-2 production in memory fated T cells, we used CD127 and KLRG-1 to distinguish between memory precursor (CD127+KLRG-1-) and terminal effector cells (KLRG-1+CD127-). We observed that autocrine IL-2 production was contained strictly within the memory precursor CD8 T cells, and short-lived effector cells were barely able to make any autocrine IL-2 (Figure 1D). This held true for both immuno-dominant and recessive epitopes of LCMV (Figure S1C). This suggests that autocrine IL-2 is intrinsically tied to the formation or function of long-lived memory T cells.

IL-$2^{-/-}$ CD8 T cells demonstrate that paracrine IL-2 is sufficient for T cell priming.

To better understand the role of autocrine IL-2 without hindering paracrine signals, we utilized a model of WT and IL-$2^{-/-}$ P14 CD8 T cells, cotransferred into C57BL6 mice at low frequency, to match endogenous levels of GP33 specific CD8 T cells. We first wanted to verify that P14 CD8 T cells isolated from IL-$2^{-/-}$ mice were not defective due to their thymic maturation in the absence

of IL-2 (Figure 1A-B, Figure S1A-B). To this end, we purified WT and IL-$2^{-/-}$ P14 T cells from naïve mice and activated them *in vitro* using GP33-APC for 48 hrs. Genomic ablation of IL-2 caused a decrease in CD25 expression, and reduction in the production of effector molecule GzmB, similar to αIL-2 blockade of WT T cells (Figure S2A). We used BrdU to quantify cell cycling, and observed a significant decrease in IL-$2^{-/-}$ CD8 T cell division (Figure S2A). This decreased activation and proliferation caused by autocrine IL-2 deletion paralleled a decrease in glycolysis, quantified by the ECAR of the cells at day 2 post-activation (Figure S2B). To verify that this was a defect of IL-2 production, and not intrinsic defect of CD8 T cells isolated from an IL-$2^{-/-}$ mouse, we added paracrine IL-2 and observed a complete rescue of activation and proliferation to WT levels (Figure S2A). These results exactly match the data obtained from activated T cells with blocking IL-2 antibody (Figure 1A-B, S1A-B), thus demonstrating that IL-$2^{-/-}$ CD8 T cells are not intrinsically defective and furthermore suggests that many of the observed differences were driven by paracrine IL-2 signaling between activated CD8 T cells.

As others and we have shown that autocrine IL-2 is made early on following T cell priming (Figure 1 C). Thus, to study the effects of these autocrine signals we transferred CFSE labeled WT and IL-$2^{-/-}$ CD8 T cells into naïve C57BL6 mice and infected them with $LCMV_{Arm}$. We analyzed the T cell responses following CD8 T cell priming at day 2.75 post-infection. We characterized the donor cells for activation markers CD69, PD-1, and CD25 and observed no differences between WT and IL-$2^{-/-}$ CD8 T cells (Figure 2A). Quantification of CD8 T cell numbers showed similar accumulation of WT and IL-$2^{-/-}$ CD8 T cells, which mirrored their nearly identical CFSE dilution profiles (Figure 2A-B). To compare the donors' functional differences, we performed a direct *ex vivo* peptide stimulation. We observed that in the absence of autocrine

IL-2 the polyfunctionality is very similar to WT with the exception of IL-2 production (Figure 2C-D, Figure S2C). In fact, IL-$2^{-/-}$ CD8 T cells produced similar proportions of TNF-α+ and IFN-γ+ cells, and MFI of markers showed only a slight negative trend in the absence of IL-2. Pairing this data with the *in vitro* data shows that paracrine signals received during priming are sufficient to drive the effector differentiation and expansion programming that CD8 T cells require (Figure 1A-B, S1A-B, S2A).

Ablation of autocrine IL-2 does not hinder CD8 T cell effector differentiation programming.
Following T cell priming, antigen and cytokines drive an exponential increase in the effector T cell pool(28). We next explored whether ablation of autocrine IL-2 would affect effector expansion of antigen-specific CD8 T cells. We cotransferred WT and IL-$2^{-/-}$ CD8 T cells into naïve C57BL6 mice, and infected them with $LCMV_{Arm}$. Donor cells were isolated from peripheral (LNG, LVR) and secondary lymphoid (SPL, iLN) tissues at day 8 post-infection. (Figure S3A) In line with their similar numbers at day 2.75 (Figure 2B), by day 8 post-infection IL-$2^{-/-}$ T cells had accumulated to similar numbers compared to WT T cells in both secondary lymphoid tissue (SPL and iLN) as well as peripheral sites of infection (LNG and LVR) (Figure 3A). Mice were treated with BrdU prior to analysis at day 8 post-infection to compare proliferation rates at the peak of the immune response but there were no observed difference in BrdU incorporation in the absence of autocrine IL-2 (Figure S3B). Furthermore, paracrine IL-2 signals were sufficient to drive normal terminal effector differentiation shown by similar accumulation of KLRG-1+CD127- SLECs as well as expression of effector molecule Granzyme B (Figure 3B-C). TCR signals drive expression of PD-1 and during chronic infections is one of the primary markers of exhaustion in antigen-specific CD8 T cells(29). However, during acute infection where antigen is cleared, it

can be used as a measure of TCR signaling. We observe that IL-2$^{-/-}$ CD8 T cells expressed slightly higher PD-1, suggesting they are more sensitive to antigen signals (Figure 3C). We performed direct *ex vivo* peptide stimulation on splenocytes to check whether the polyfunctionality of the donors was affected by the ablation of IL-2, but despite the consistent trend of decreased IFN-γ and TNF-α MFI, there seemed to be no significant differences in cytokine production (Figure 3D, S3C).

Increased contraction but stable homeostatic maintenance in the absence of autocrine IL-2.

Following viral clearance antigen-specific effector CD8 T cells undergo contraction as memory precursor effector cells (MPECs) differentiate into long-lived memory CD8 T cells and terminal effector cells die following antigen clearance. In the absence of autocrine IL-2 donor antigen-specific CD8 T cells died more rapidly compared to their WT counterparts (Figure 4A-B). This increased contraction only resulted in minimal differences in the final memory T cell numbers in secondary lymphoid tissues, and peripheral tissues (Figure 4C). In line with this, we observed that cell survival marker BCL-2 was similarly expressed in WT and IL-2$^{-/-}$ memory CD8 T cells suggesting the remaining memory cells were not defective (Figure 4D). As memory T cells rely on slow continuous turnover to maintain numbers, we gave continuous BrdU injections over the course of 10 days to memory mice to compare homeostatic proliferation of the donor cells. We confirmed that IL-2$^{-/-}$ memory T cells were able to undergo stable homeostatic turnover as they incorporated similar levels of BrdU (Figure 4E). When comparing the quality of the memory cells we observed that WT and IL-2$^{-/-}$ CD8 T cells form similar MPEC proportions when comparing CD127+KLRG-1-CD62L+ cell proportions at day 50 post-infection (Figure 4F). Finally, similar to observations during priming and peak expansion, we observed no differences in

polyfunctionality of the memory CD8 T cells (Figure 4G). All together, these data show that paracrine IL-2 signals are sufficient to form long-lived memory, but autocrine IL-2 signals do seem to play a role in the early survival of effector cells following antigen clearance.

Following antigen clearance effector CD8 T cells must convert from a highly energetic and glycolytic energy state, to a resting oxidative phosphorylation state to transition to homeostatic maintenance(30, 31). Thus we looked to metabolism to try and understand the increased early contraction of IL-$2^{-/-}$ effector cells. We purified antigen-specific CD8 T cells from effector and memory time points and compared their glucose metabolism. While we observed that day 8 effectors were significantly higher for extracellular acidification compared to the memory T cells, however, we observed no differences between WT and IL-$2^{-/-}$ CD8 T cells (Figure S4C). Also, both WT and IL-$2^{-/-}$ CD8 T cells were able to differentiate into memory cells with a high spare respiratory capacity predicting robust secondary T cell expansion (Figure S4D).

IL-$2^{-/-}$ T cells display a significant defect in secondary CD8 T cell expansion.

The distinct property of memory cells to respond quickly and overwhelm secondary infections is the hallmark of memory T cell quality. We purified WT and IL-$2^{-/-}$ memory CD8 T cells from $LCMV_{Arm}$ mice and transferred them into naïve C57BL6 mice, which were subsequently infected with Listeria *monocytogenes,* expressing GP33-41 fragment of $LCMV_{Arm,}$ to study secondary T cell responses (Figure S5A). WT and IL-$2^{-/-}$ memory T cells started at similar numbers early during infection, however, IL-$2^{-/-}$ CD8 T cells were drastically hindered in their ability to expand during the heterologous challenge (Figure 5A-B). Decreased expansion of IL-$2^{-/-}$ memory T cells upon rechallenge resulted in significantly decreased accumulation of secondary memory T cells in spleen and liver (Figure 5C). Expansion of effector T cell responses is the cumulative sum of

both proliferation and survival. Hence we next analyzed BrdU uptake, as well as survival marker expression, to understand whether the defect was from decreased proliferation or increased cell death. Analysis of BrdU uptake during the peak of T cell expansion showed very similar cell cycling between WT and IL-$2^{-/-}$ CD8 T cells (Figure 5D) similar to primary expansion and homeostatic proliferation. Conversely, IL-$2^{-/-}$ CD8 T cells had a significant reduction in the expression of pro-survival marker BCL-2, suggesting they are more predisposed to the mitochondrial death pathway (Figure 5E). Indeed, when we look at cleaved Caspase 3/7 activities, they were significantly higher in the IL-$2^{-/-}$ CD8 T cells (Figure 5F). Thus, despite the formation of highly functional memory T cells capable of long homeostatic maintenance and robust spare respiratory capacity (Figure 4, S4), we observed that autocrine IL-2 has a paramount role in programming survival of secondary memory CD8 T cell responses.

Autocrine IL-2 is critical for programming CD8 T cells during the initial priming of antigen-specific responses.

Given that IL-$2^{-/-}$ CD8 T cells differentiated into phenotypically similar memory cells and with no defect in their polyfunctionality, or metabolic fitness, it is possible autocrine IL-2 is strictly necessary during secondary rechallenge to help drive T cell survival (Figure 4F-G, S4B-D). To address this question, we used a conditional knockout of IL-2 using IL-$2^{fl/fl}$ Cre-ERT2 P14 mice. Treating these mice with a Tamoxifen causes the Cre-ERT to change confirmation and transition from the cytoplasm to the nucleus, where the Cre can drive the deletion of the floxed IL-2. To confirm that these mice function as IL-$2^{-/-}$ mice we pretreated P14 mice with Tamoxifen and transferred them into naïve C57BL6 mice, and infected them with $LCMV_{Arm}$ (Figure S6A). By day 8 post-infection we observed a small but not significant reduction in T cell accumulation in secondary lymphoid tissue, as well as peripheral sites of infection (Figure 6A). Furthermore,

similar to the IL-2$^{-/-}$ CD8 T cells we observed a trend of PD-1 upregulation at peak of expansion in the absence of autocrine IL-2 compared to the UnTx IL-2$^{fl/fl}$ control (Figure 6F). Following antigen clearance, donor PreTx (IL-2$^{-/-}$) CD8 T cells also underwent increased contraction like their germline knockout counterparts (Figure 4B, 6C). To assess memory T cell polyfunctionality we performed a direct *ex vivo* restimulation of the donor memory cells. We observed that while IL-2 was knocked out as expected, UnTx (WT) and PreTx (IL-2$^{-/-}$) mice had similar production of TNF-α and IFN-γ (Figure S6B-C). All together these data suggest that following Tamoxifen treatment the IL-2$^{fl/fl}$ P14 are acting like the traditional IL-2$^{-/-}$ mice. Using this model we were able to setup a unique experiment that gauges the window during which CD8 T cell intrinsic autocrine IL-2 signals are necessary to program memory T cell survival. To this end, we deleted IL-2 in the naïve cells prior to infection (PreTx), directly following antigen priming (Day 2 Tx), or following memory formation prior to secondary rechallenge (Memory Tx). We followed these mice to memory, and purified out the donor cells to assess their secondary expansion kinetics. We observed that the ablation of IL-2 following priming, or directly prior to recall did not affect CD8 T cell expansion (Figure 6E-F, S6E). In fact, only ablation of IL-2 prior to infection was able to recapitulate the secondary expansion defect observed in germline IL-2$^{-/-}$ CD8 T cells (Figure 6E-F, S6E). These data show that during early CD8 T cell activation autocrine IL-2 signals program critical aspects of CD8 T cell survival necessary to maintain T cell expansion during secondary recall.

Discussion

TCR stimulation together with CD28 co-stimulation drives the activation and recruitment of primary CD8 T cells responses. However, it is now well appreciated that these cells heavily rely on a third signal delivered via cytokine mediators to the cell to achieve proper expansion, differentiation, and to elicit their full effector function. IL-2 is one of the most crucial cytokines as evidenced by the strong upregulation of the IL-2Rα upon activation of CD8 T cells(18). These IL-2 signals are critical for maintaining the CD8 T cells in the catabolic state necessary for the expansion and production of cytokine and effector molecule mediators. Our data demonstrate that paracrine IL-2 signals are not sufficient to satisfy the programming of these cells during primary T cell expansion, and that only together with autocrine IL-2 is it possible to generate fully functional memory CD8 T cells. This research expands on the previous report that IL-$2^{-/-}$ T cells have a defect in secondary expansion(24) by not only characterizing the timing during which these signals are necessary but also demonstrating that the defect we observe is in the survival and not proliferation of the IL-$2^{-/-}$ memory cells.

Using a unique combination of WT and IL-$2^{-/-}$ transgenic CD8 T cells as well as unique IL-$2^{fl/fl}$ Cre-ERT transgenic P14 mice we were able to characterize the distinct effects of paracrine and autocrine IL-2 during CD8 T cell priming. Our results are in line with the expected role of paracrine IL-2 in driving CD8 T cell proliferation and increased expression of effector molecules and putting CD8 T cells into glycolytic overdrive. However, we have shown for the first time that autocrine IL-2 signals are not necessary for driving glycolysis during the effector phase, nor do they affect the metabolic homeostasis during memory formation. This suggests that the increased ability to produce IL-2, ie. Polyfunctionality, observed in memory CD8 T cells is likely a correlative of increased function, and not a causative effect.

We observed very little effect of autocrine IL-2 ablation on the differentiation of effector CD8 T cells into long-lived memory. It's likely that paracrine IL-2 is sufficient to mediate the necessary signals for these processes. Our study deviates slightly from the previously published data showing that IL-$2^{-/-}$ CD8 T cells display lower polyfunctionality and accumulation. In those studies LM-ova was used in conjunction with OT-I IL-$2^{-/-}$ CD8 T cells, its possible LM causes a distinct inflammation response compared to the $LCMV_{Arm}$ virus that we have used(28, 32), it's possible the reliance on autocrine IL-2 was more severe in this system and thus displayed defects that were masked by the paracrine IL-2 in the LCMV model. However, the major phenotype of secondary expansion defect was present in both the LM and our LCMV system. The study by Schoenberger et al. did not address how autocrine IL-2 affected the secondary expansion, and when it was necessary. Using a unique model of temporal IL-2 ablation, we were able to demonstrate for the first time that IL-2 signals delivered during the priming phase of the primary infection were critical to the development of a robust secondary expansion. Previous observations from our lab and others' show that the window of systemic IL-2 production is constrained to the first 4 days following $LCMV_{Arm}$ infection(18). This observation is consistent with the timing that we see that autocrine signaling is also necessary. This largely mirrors the role that paracrine IL-2 has on the development on memory CD8 T cells when $CD25^{-/-}$ P14 cells were used to completely ablate IL-2 signals to antigen-specific CD8 T cells(25). It is likely that during effector T cell expansion, there are pockets of IL-2 depleted environments in which CD8 T cells rely strictly on autocrine IL-2 to program their effector phenotype. We demonstrate *in vitro*, that in the absence of these IL-2 signals CD8 T cells cannot maintain their proliferation, effector function, or metabolism, which likely provides defective programming.

The immunological landscape is quickly evolving as with the development of methods necessary to generating long-lasting vaccine induced memory T cells. Furthermore, Chimeric Antigen Receptor (CAR) therapies are at the forefront of anti-cancer therapy and recent clinical trials have demonstrated the power of these modalities. Furthermore, IL-2 therapy has not only shown to synergize with αPDL1 to rescue exhausted CD8 T cells(33). Thus it is increasingly important that we understand the priming and maintenance signals that CD8 T cells require to elicit cytotoxic function and create long-lived, highly functional CD8 T cells. In this study we have been able to show how paracrine and autocrine IL-2 signals work hand-in-hand to optimally prime cytotoxic T cell responses, and form potent long-lived memory CD8 T cells.

Acknowledgements

The authors would like to thank Dr. Kendall A. Smith for providing the conditional IL-2 knockout mice and for scientific discussions, and Ms. Laura Penny for excellent technical assistance.

Authorship and Conflict of Interest Statements

Contribution: YY carried out experiments, analyzed data, prepared figures and wrote manuscript. LAP conducted experiments and analyzed data. VK and SS conceptualized the project, designed the experiments, carried out experiments, supervised the work, analyzed data, interpreted the results and helped prepare the manuscript.

Conflict-of-interest disclosure: The authors declare no competing financial interests.

References

1. Smith, K. A., P. E. Baker, S. Gillis, and F. W. Ruscetti. 1980. Functional and molecular characteristics of T-cell growth factor. *Mol. Immunol.* 17: 579–589.
2. Gillis, S., M. M. Ferm, W. Ou, and K. A. Smith. 2016. Pillars Article: T Cell Growth Factor: Parameters of Production and a Quantitative Microassay for Activity. J. Immunol. 1978. 120: 2027-2032. *The Journal of Immunology* 197: 5–10.
3. Mostböck, S., M. E. C. Lutsiak, D. E. Milenic, K. Baidoo, J. Schlom, and H. Sabzevari. 2008. IL-2/anti-IL-2 antibody complex enhances vaccine-mediated antigen-specific CD8+ T cell responses and increases the ratio of effector/memory CD8+ T cells to regulatory T cells. *J. Immunol.* 180: 5118–5129.
4. Tomala, J., H. Chmelova, T. Mrkvan, B. Rihova, and M. Kovar. 2009. In Vivo Expansion of Activated Naive CD8+ T Cells and NK Cells Driven by Complexes of IL-2 and Anti-IL-2 Monoclonal Antibody As Novel Approach of Cancer Immunotherapy. *J. Immunol.* 183: 4904–4912.
5. Boyman, O., M. Kovar, M. P. Rubinstein, C. D. Surh, and J. Sprent. 2006. Selective stimulation of T cell subsets with antibody-cytokine immune complexes. *Science* 311: 1924–1927.
6. Liao, W., D. E. Schones, J. Oh, Y. Cui, K. Cui, T.-Y. Roh, K. Zhao, and W. J. Leonard. 2008. Priming for T helper type 2 differentiation by interleukin 2-mediated induction of interleukin 4 receptor alpha-chain expression. *Nat Immunol* 9: 1288–1296.
7. Cote-Sierra, J., G. Foucras, L. Guo, L. Chiodetti, H. A. Young, J. Hu-Li, J. Zhu, and W. E. Paul. 2004. Interleukin 2 plays a central role in Th2 differentiation. *Proc. Natl. Acad. Sci. U.S.A.* 101: 3880–3885.
8. Liao, W., J.-X. Lin, L. Wang, P. Li, and W. J. Leonard. 2011. Modulation of cytokine receptors by IL-2 broadly regulates differentiation into helper T cell lineages. *Nat Immunol* 12: 551–559.
9. Spangler, J. B., J. Tomala, V. C. Luca, K. M. Jude, S. Dong, A. M. Ring, P. Votavova, M. Pepper, M. Kovar, and K. C. Garcia. 2015. Antibodies to Interleukin-2 Elicit Selective T Cell Subset Potentiation through Distinct Conformational Mechanisms. *Immunity* 42: 815–825.
10. Zheng, S. G., J. Wang, P. Wang, J. D. Gray, and D. A. Horwitz. 2007. IL-2 is essential for TGF-beta to convert naive CD4+CD25- cells to CD25+Foxp3+ regulatory T cells and for expansion of these cells. *J. Immunol.* 178: 2018–2027.
11. Yamamoto, M., Y. Seki, K. Iwai, I. Ko, A. Martin, N. Tsuji, S. Miyagawa, R. B. Love, and M. Iwashima. 2013. Ontogeny and localization of the cells produce IL-2 in healthy animals. *Cytokine* 61: 831–841.
12. Owen, D. L., S. A. Mahmud, K. B. Vang, R. M. Kelly, B. R. Blazar, K. A. Smith, and M. A. Farrar. 2018. Identification of Cellular Sources of IL-2 Needed for Regulatory T Cell Development and Homeostasis. *The Journal of Immunology* 200: 3926–3933.
13. Sojka, D. K., D. Bruniquel, R. H. Schwartz, and N. J. Singh. 2004. IL-2 secretion by CD4+ T cells in vivo is rapid, transient, and influenced by TCR-specific competition. *J. Immunol.* 172: 6136–6143.
14. D'Souza, W. N., and L. Lefrançois. 2003. IL-2 is not required for the initiation of CD8 T cell cycling but sustains expansion. *J. Immunol.* 171: 5727–5735.
15. Janas, M. L., P. Groves, N. Kienzle, and A. Kelso. 2005. IL-2 regulates perforin and granzyme gene expression in CD8+ T cells independently of its effects on survival and proliferation. *J. Immunol.* 175: 8003–8010.
16. Rollings, C. M., L. V. Sinclair, H. J. M. Brady, D. A. Cantrell, and S. H. Ross. 2018. Interleukin-2

shapes the cytotoxic T cell proteome and immune environment-sensing programs. *Science Signaling* 11: eaap8112.
17. Smith, K. A. 2012. Conditional IL-2 gene deletion: consequences for T cell proliferation. 1–12.
18. Kalia, V., S. Sarkar, S. Subramaniam, W. N. Haining, K. A. Smith, and R. Ahmed. 2010. Prolonged interleukin-2Ralpha expression on virus-specific CD8+ T cells favors terminal-effector differentiation in vivo. *Immunity* 32: 91–103.
19. Hand, T. W., W. Cui, Y. W. Jung, E. Sefik, N. S. Joshi, A. Chandele, Y. Liu, and S. M. Kaech. 2010. Differential effects of STAT5 and PI3K/AKT signaling on effector and memory CD8 T-cell survival. *Proc. Natl. Acad. Sci. U.S.A.* 107: 16601–16606.
20. Pipkin, M. E., J. A. Sacks, F. Cruz-Guilloty, M. G. Lichtenheld, M. J. Bevan, and A. Rao. 2010. Interleukin-2 and Inflammation Induce Distinct Transcriptional Programs that Promote the Differentiation of Effector Cytolytic T Cells. *Immunity* 32: 79–90.
21. Kaech, S. M., J. T. Tan, E. J. Wherry, B. T. Konieczny, C. D. Surh, and R. Ahmed. 2003. Selective expression of the interleukin 7 receptor identifies effector CD8 T cells that give rise to long-lived memory cells. *Nat Immunol* 4: 1191–1198.
22. Sarkar, S., V. Kalia, W. N. Haining, B. T. Konieczny, S. Subramaniam, and R. Ahmed. 2008. Functional and genomic profiling of effector CD8 T cell subsets with distinct memory fates. *The Journal of …*.
23. Ditoro, D., C. J. Winstead, D. Pham, S. Witte, R. Andargachew, J. R. Singer, C. G. Wilson, C. L. Zindl, R. J. Luther, D. J. Silberger, B. T. Weaver, E. M. Kolawole, R. J. Martinez, H. Turner, R. D. Hatton, J. J. Moon, S. S. Way, B. D. Evavold, and C. T. Weaver. 2018. Differential IL-2 expression defines developmental fates of follicular versus nonfollicular helper T cells. *Science* 361: eaao2933.
24. Feau, S., R. Arens, S. Togher, and S. P. Schoenberger. 2011. Autocrine IL-2 is required for secondary population expansion of CD8(+) memory T cells. *Nat Immunol* 12: 908–913.
25. Williams, M. A., A. J. Tyznik, and M. J. Bevan. 2006. Interleukin-2 signals during priming are required for secondary expansion of CD8+ memory T cells. *Nature* 441: 890–893.
26. Kalia, V., L. A. Penny, Y. Yuzefpolskiy, F. M. Baumann, and S. Sarkar. 2015. Quiescence of Memory CD8+ T Cells Is Mediated by Regulatory T Cells through Inhibitory Receptor CTLA-4. *Immunity* 42: 1116–1129.
27. Curtsinger, J. M., and M. F. Mescher. 2010. Inflammatory cytokines as a third signal for T cell activation. *Current Opinion in Immunology* 22: 333–340.
28. Richer, M. J., J. C. Nolz, and J. T. Harty. 2013. Pathogen-specific inflammatory milieux tune the antigen sensitivity of CD8(+) T cells by enhancing T cell receptor signaling. *Immunity* 38: 140–152.
29. Wherry, E. J., S.-J. Ha, S. M. Kaech, W. N. Haining, S. Sarkar, V. Kalia, S. Subramaniam, J. N. Blattman, D. L. Barber, and R. Ahmed. 2007. Molecular Signature of CD8+ T Cell Exhaustion during Chronic Viral Infection. *Immunity* 27: 670–684.
30. O'Sullivan, D., G. J. W. van der Windt, S. C.-C. Huang, J. D. Curtis, C.-H. Chang, M. D. Buck, J. Qiu, A. M. Smith, W. Y. Lam, L. M. DiPlato, F.-F. Hsu, M. J. Birnbaum, E. J. Pearce, and E. L. Pearce. 2014. Memory CD8+ T Cells Use Cell-Intrinsic Lipolysis to Support the Metabolic Programming Necessary for Development. *Immunity* 41: 75–88.
31. van der Windt, G. J. W., B. Everts, C.-H. Chang, J. D. Curtis, T. C. Freitas, E. Amiel, E. J. Pearce,

and E. L. Pearce. 2012. Mitochondrial Respiratory Capacity Is a Critical Regulator of CD8+ T Cell Memory Development. *Immunity* 36: 68–78.
32. Welten, S. P. M., A. Redeker, K. L. M. C. Franken, J. D. Oduro, F. Ossendorp, L. Čičin-Šain, C. J. M. Melief, P. Aichele, and R. Arens. 2015. The viral context instructs the redundancy of costimulatory pathways in driving CD8(+) T cell expansion. *Elife* 4: 521.
33. West, E. E., H.-T. Jin, A.-U. Rasheed, P. Penaloza-MacMaster, S.-J. Ha, W. G. Tan, B. Youngblood, G. J. Freeman, K. A. Smith, and R. Ahmed. 2013. PD-L1 blockade synergizes with IL-2 therapy in reinvigorating exhausted T cells. *J. Clin. Invest.* 123: 2604–2615.

Figures

Figure 1

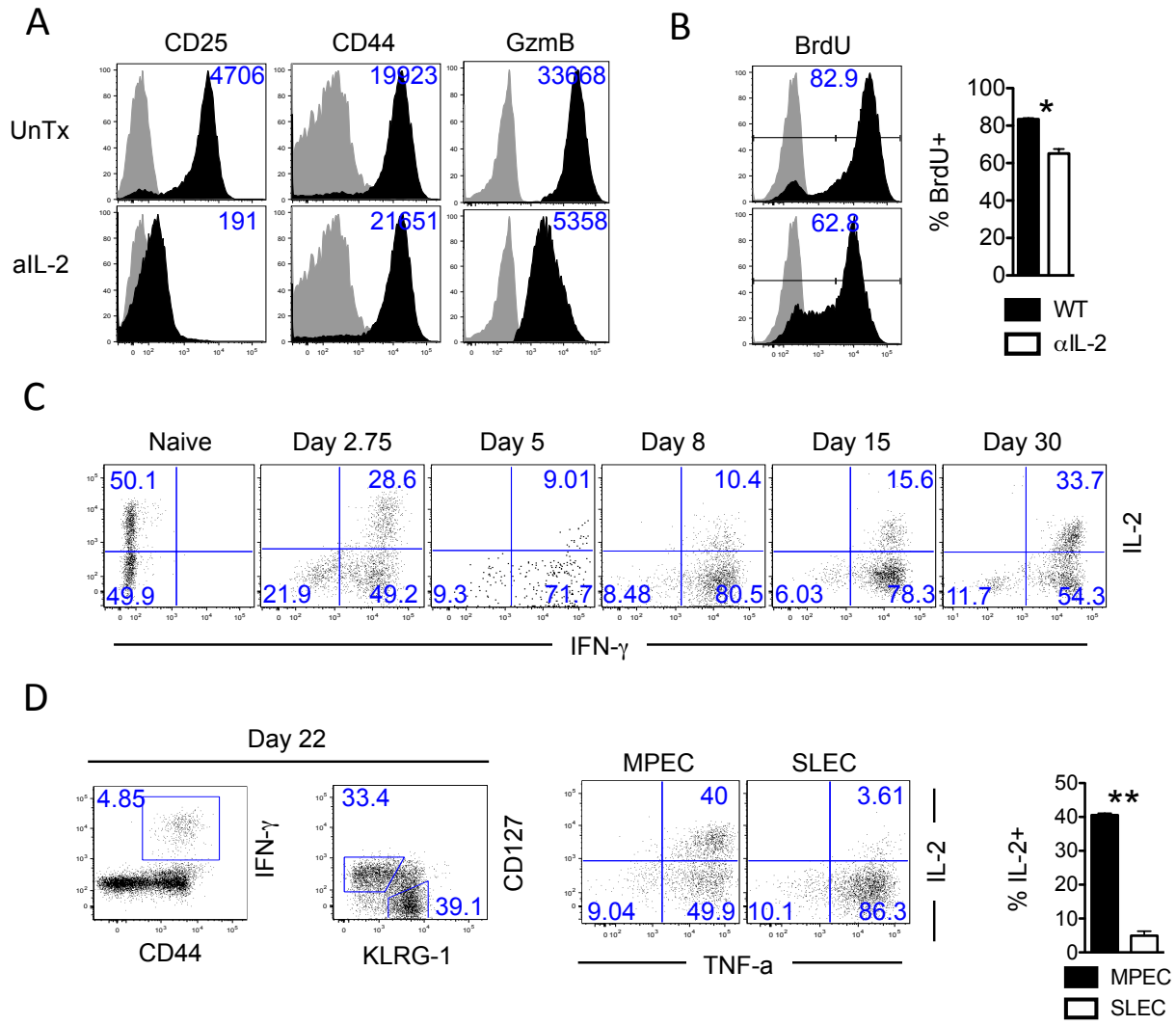

Supplemental Figure 1

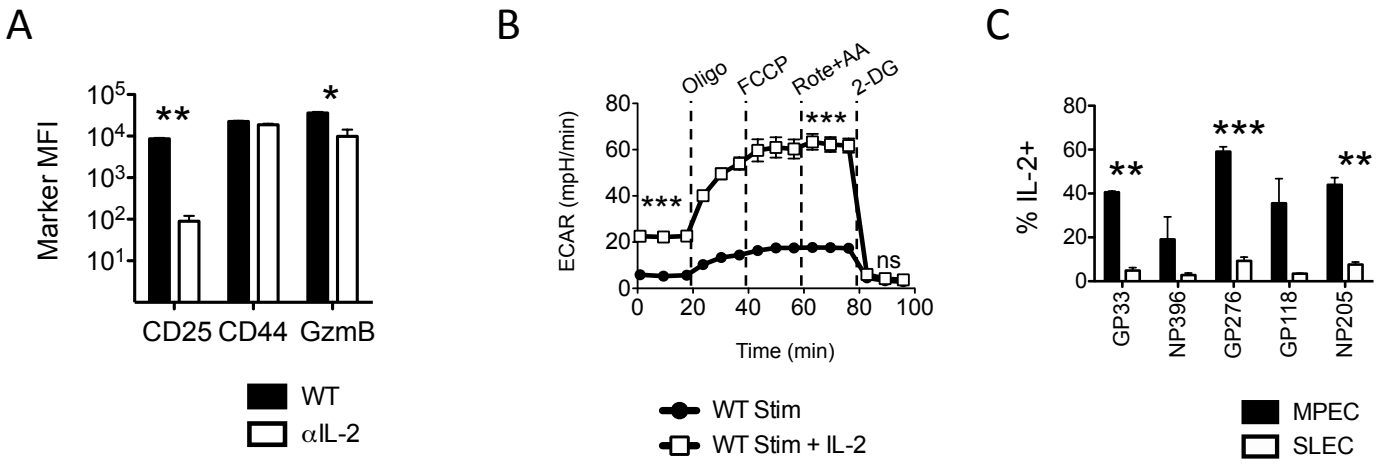

Figure 2

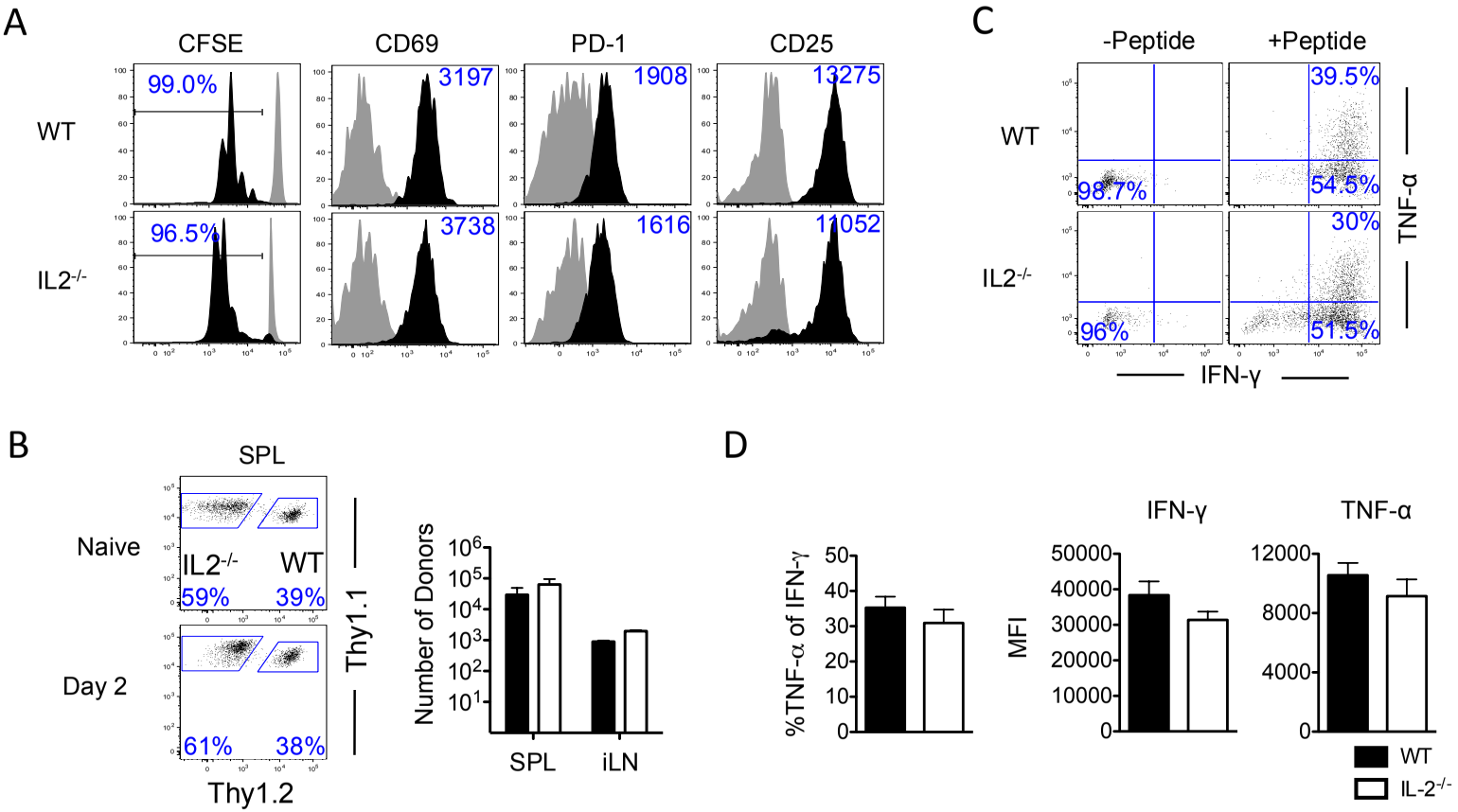
A
CFSE
CD69
PD-1
CD25
WT
IL2-/-
99.0%
96.5%
3197
3738
1908
1616
13275
11052
B
SPL
Naive
Day 2
IL2-/-
WT
59%
39%
61%
38%
Thy1.1
Thy1.2
Number of Donors
SPL
iLN
C
-Peptide
+Peptide
WT
IL2-/-
98.7%
54.5%
96%
51.5%
39.5%
30%
TNF-α
IFN-γ
D
%TNF-α of IFN-γ
IFN-γ
TNF-α
MFI
WT
IL-2-/-

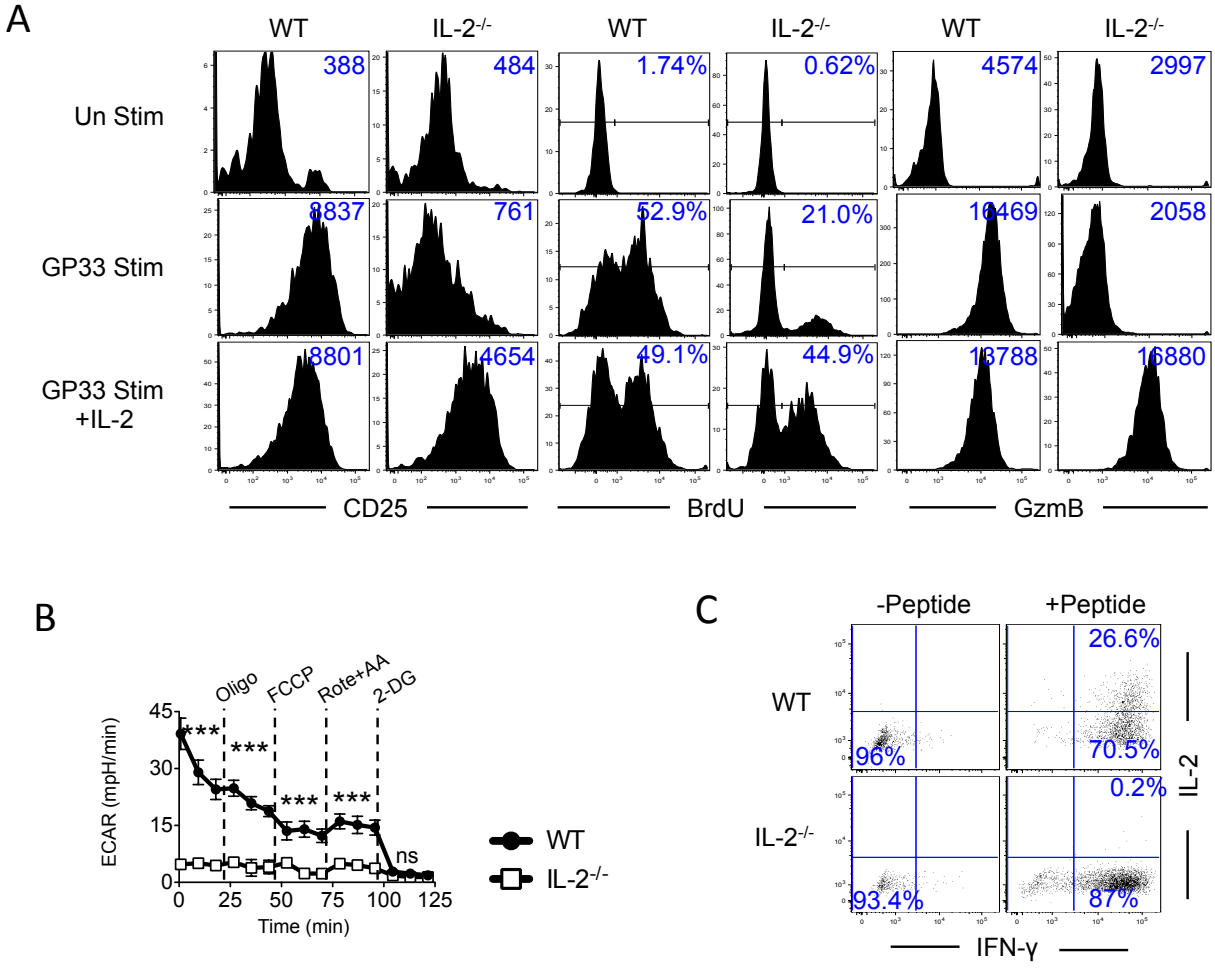
A
WT
IL-2-/-
WT
IL-2-/-
WT
IL-2-/-
Un Stim
GP33 Stim
GP33 Stim +IL-2
388
484
1.74%
0.62%
4574
2997
8837
761
52.9%
21.0%
10469
2058
8801
4654
49.1%
44.9%
13788
16880
CD25
BrdU
GzmB
B
Oligo
FCCP
Rote+AA
2-DG
ECAR (mpH/min)
Time (min)
***
ns
WT
IL-2-/-
C
-Peptide
+Peptide
WT
IL-2-/-
26.6%
96%
70.5%
0.2%
93.4%
87%
IL-2
IFN-γ

Figure 3

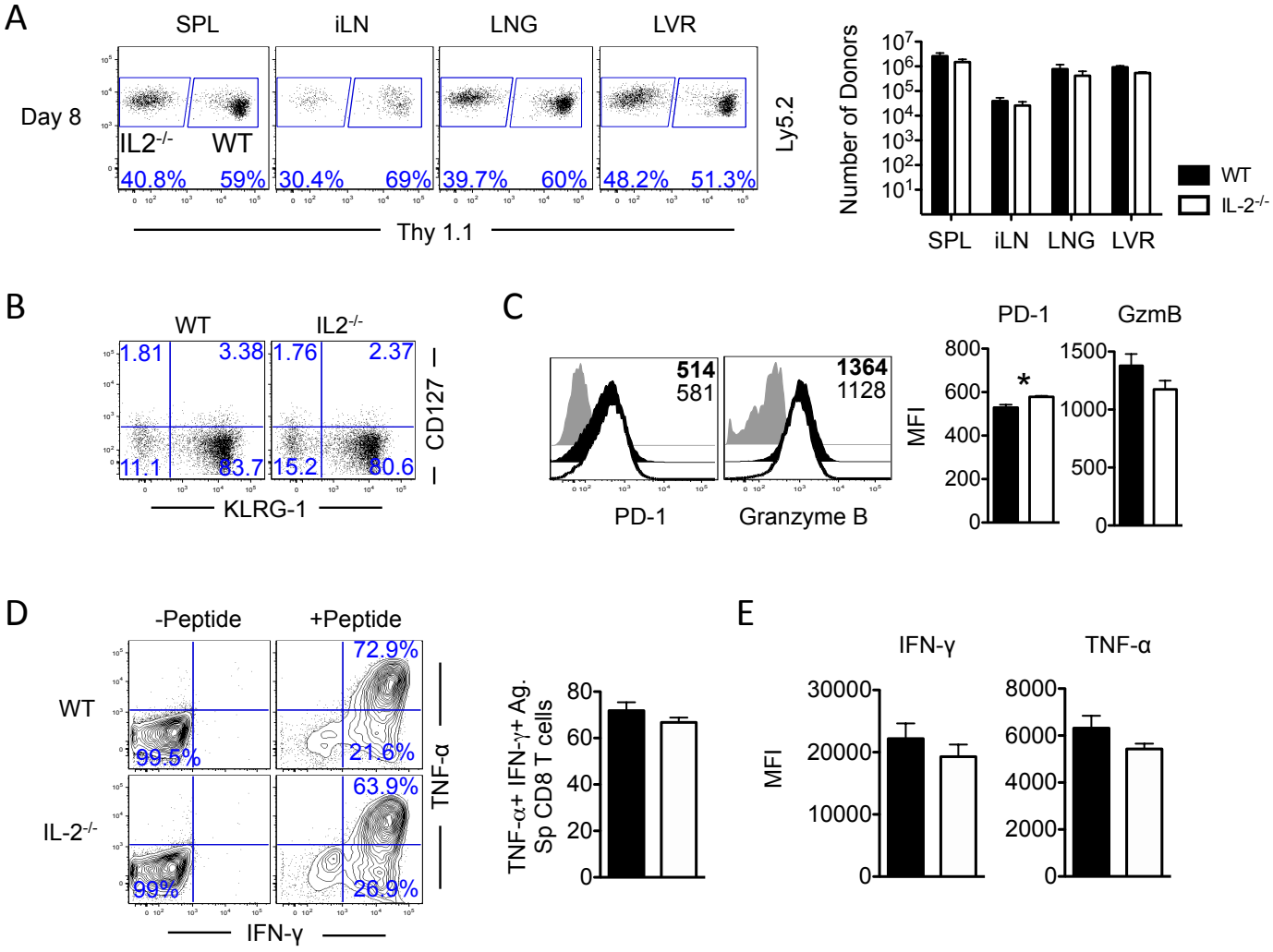
A
SPL
iLN
LNG
LVR
Day 8
IL2-/-
WT
40.8%
59%
30.4%
69%
39.7%
60%
48.2%
51.3%
Ly5.2
Thy 1.1
Number of Donors
WT
IL-2-/-
SPL
iLN
LNG
LVR
B
WT
IL2-/-
1.81
3.38
11.1
83.7
1.76
2.37
15.2
80.6
CD127
KLRG-1
C
514
581
1364
1128
PD-1
Granzyme B
MFI
PD-1
GzmB
D
-Peptide
+Peptide
WT
IL-2-/-
99.5%
72.9%
21.6%
99%
63.9%
26.9%
TNF-α
IFN-γ
TNF-α+ IFN-γ+ Ag. Sp CD8 T cells
E
IFN-γ
TNF-α
MFI

Supplemental Figure 3

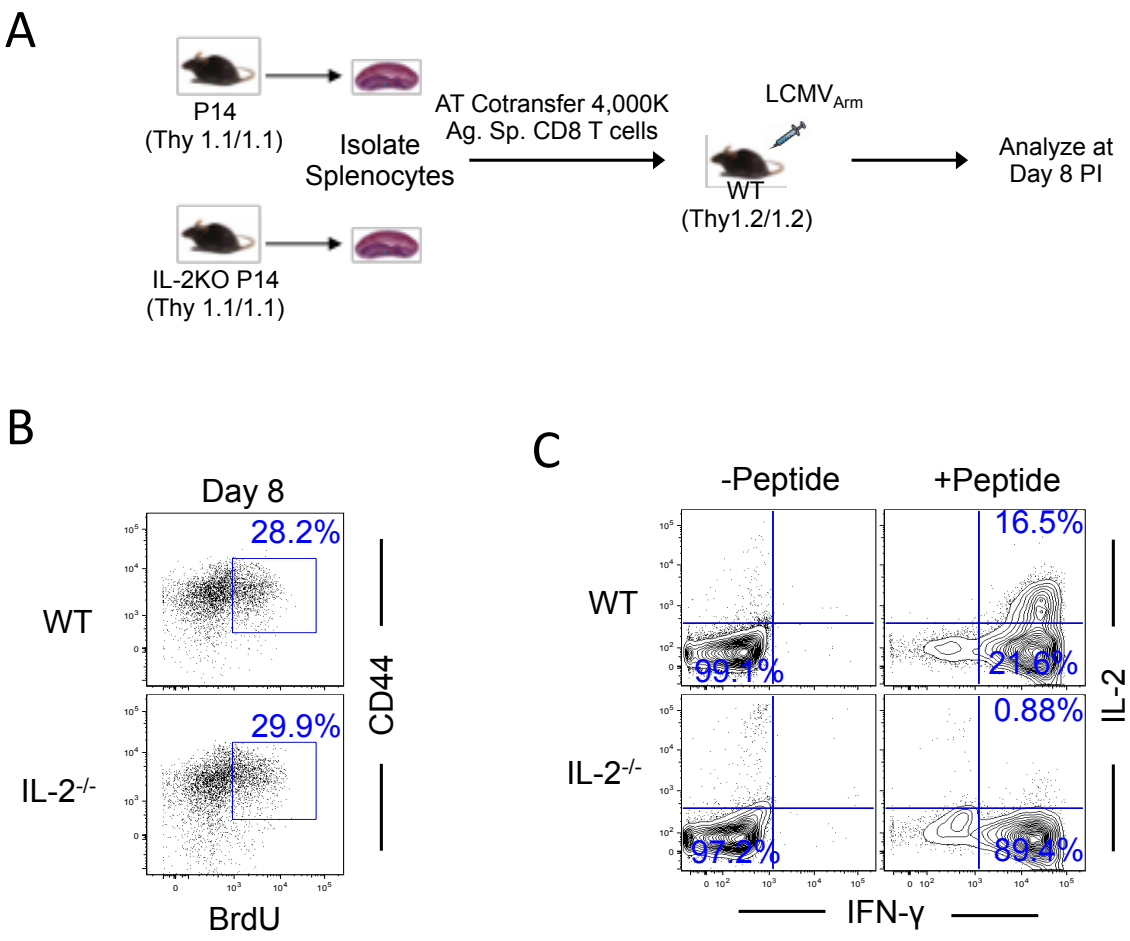

Figure 4

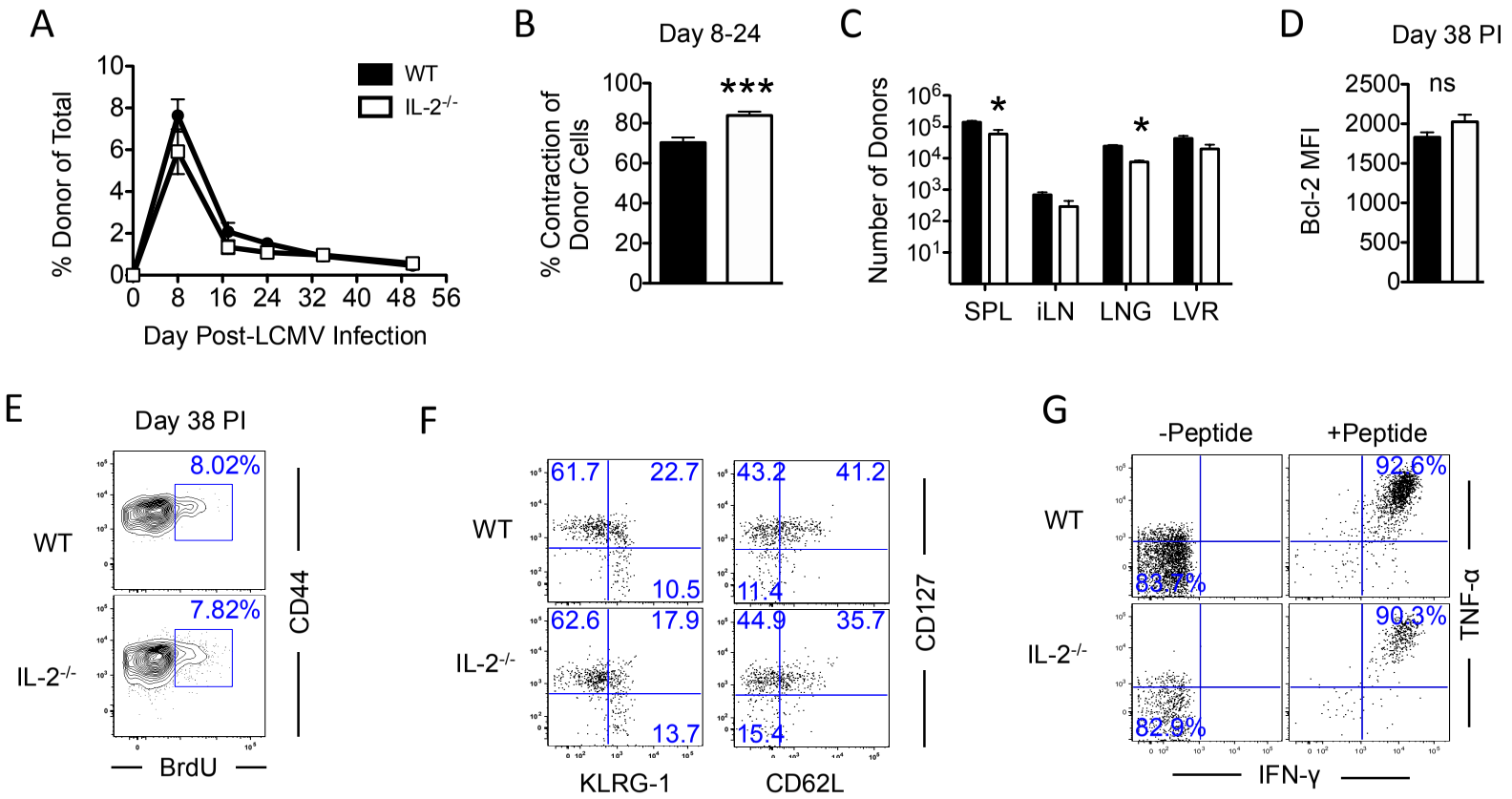
A
% Donor of Total
Day Post-LCMV Infection
WT
IL-2-/-
B
Day 8-24
% Contraction of Donor Cells
***
C
Number of Donors
SPL
iLN
LNG
LVR
D
Day 38 PI
Bcl-2 MFI
ns
E
Day 38 PI
8.02%
7.82%
WT
IL-2-/-
BrdU
CD44
F
61.7
22.7
10.5
43.2
41.2
11.4
62.6
17.9
13.7
44.9
35.7
15.4
KLRG-1
CD62L
CD127
G
-Peptide
+Peptide
92.6%
83.7%
90.3%
82.9%
IFN-γ
TNF-α

Supplemental Figure 4

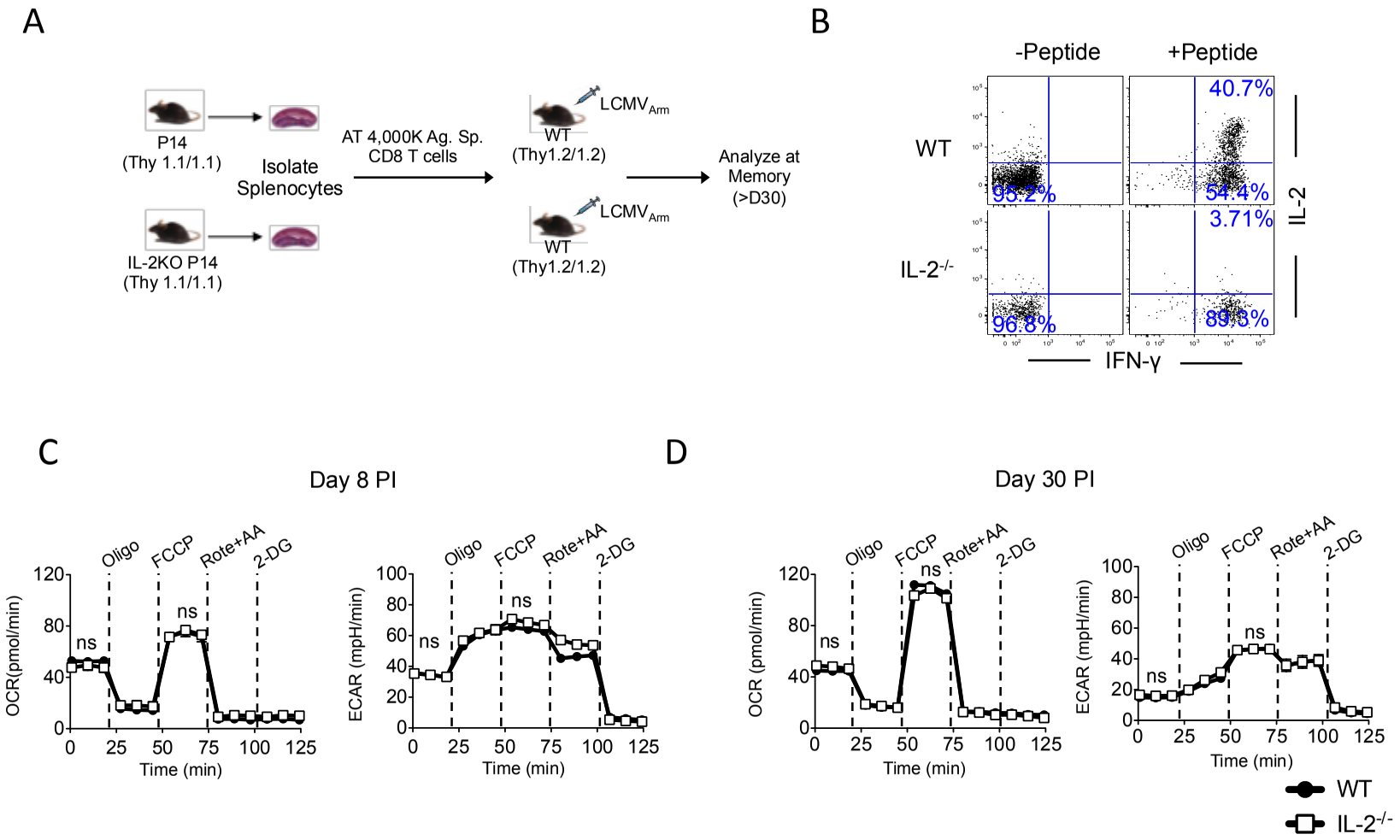

Figure 5

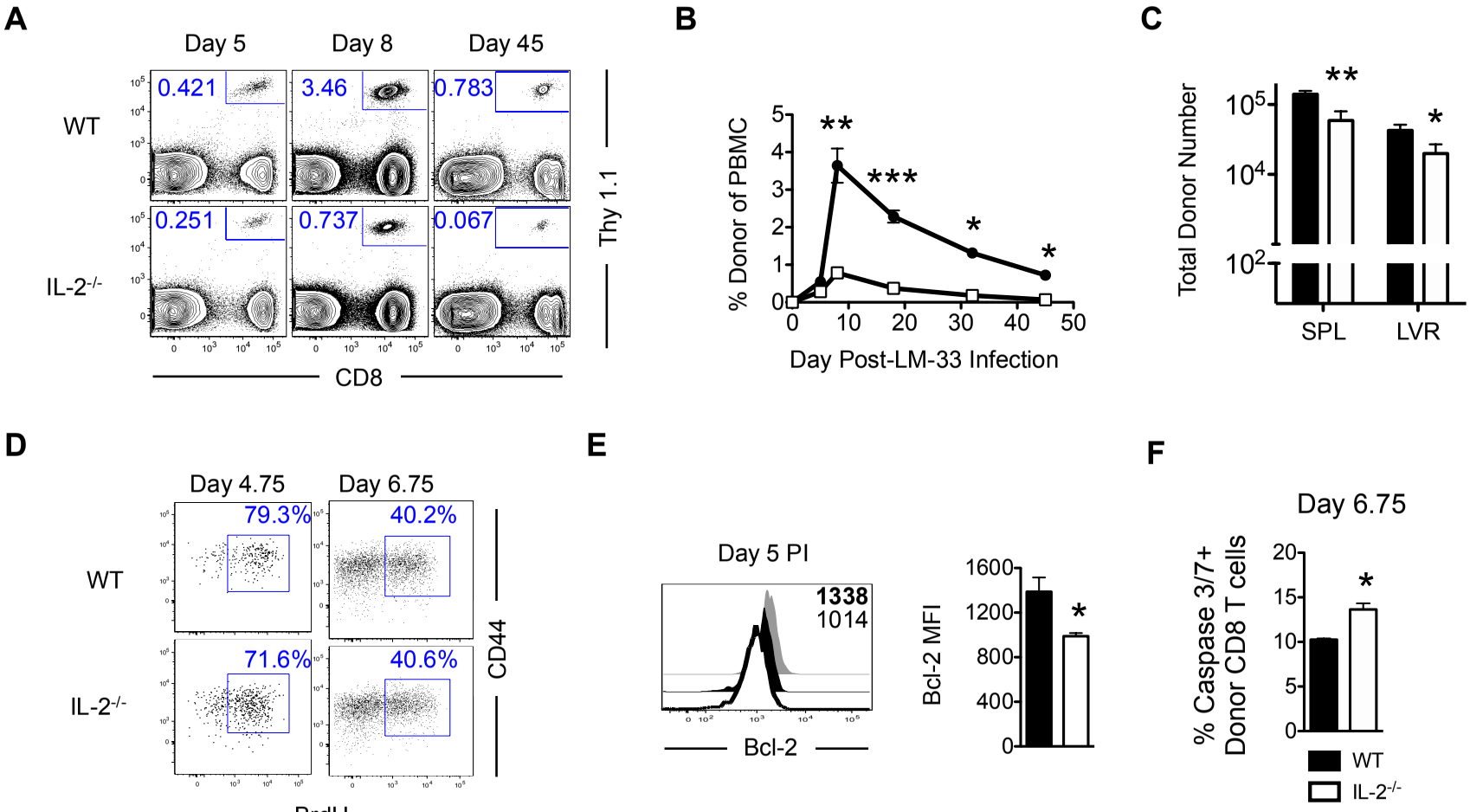
A
Day 5
Day 8
Day 45
WT
IL-2-/-
0.421
3.46
0.783
0.251
0.737
0.067
Thy 1.1
CD8
B
% Donor of PBMC
Day Post-LM-33 Infection
C
Total Donor Number
SPL
LVR
D
Day 4.75
Day 6.75
79.3%
40.2%
71.6%
40.6%
CD44
BrdU
E
Day 5 PI
1338
1014
Bcl-2
Bcl-2 MFI
F
Day 6.75
% Caspase 3/7+ Donor CD8 T cells
WT
IL-2-/-

Supplemental Figure 5

A

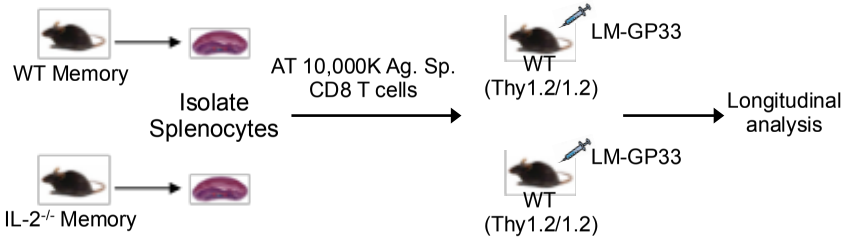

B

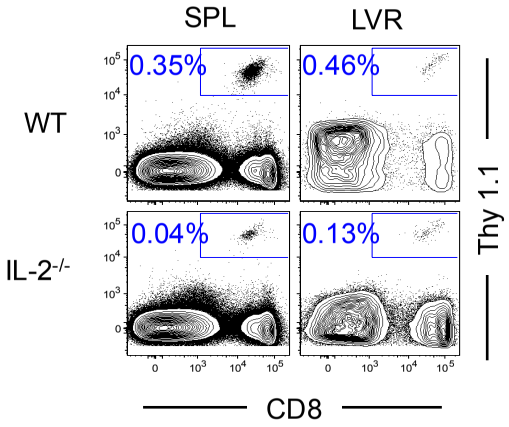

Figure 6

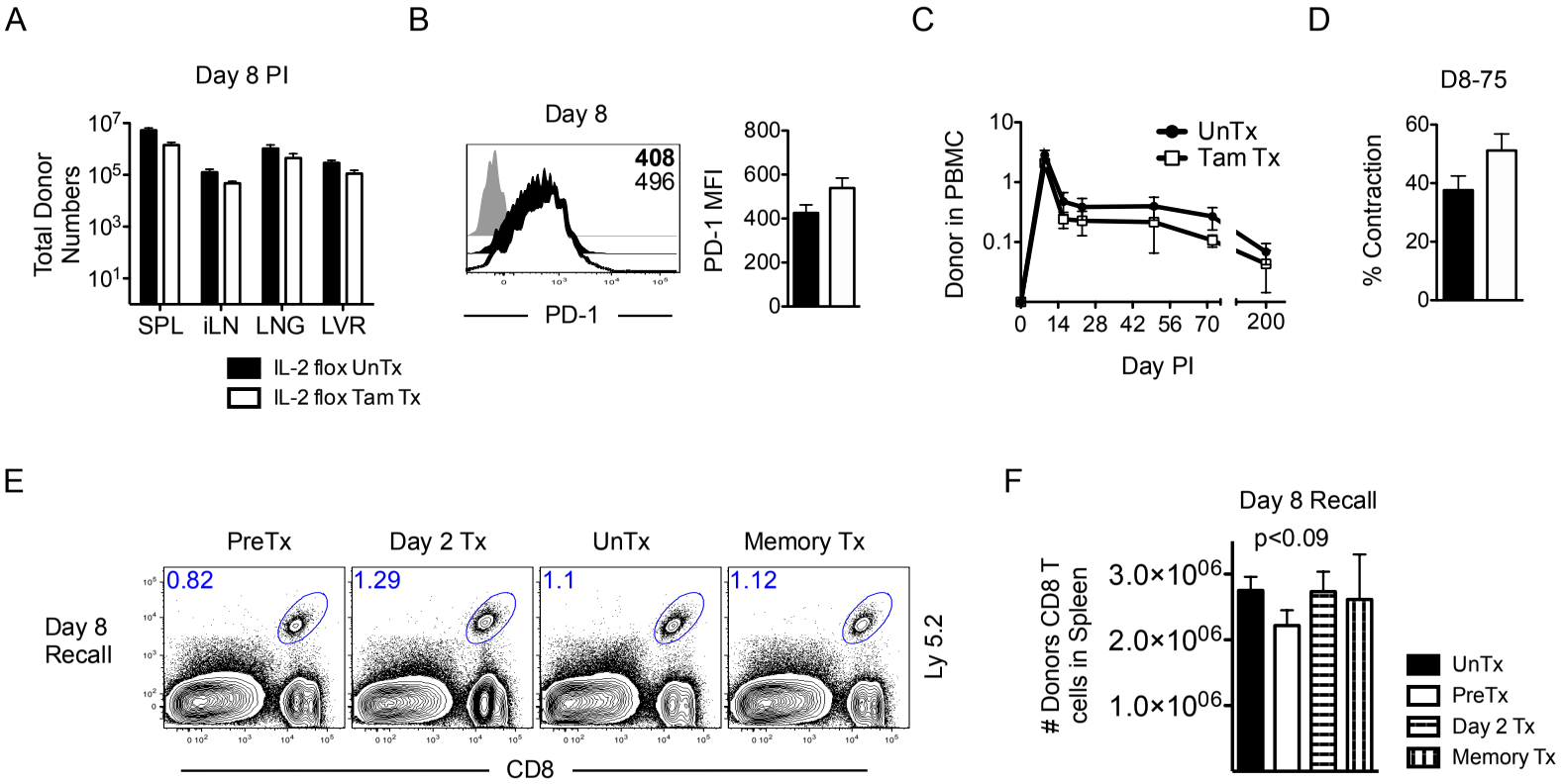
A
Day 8 PI
Total Donor Numbers
SPL
iLN
LNG
LVR
IL-2 flox UnTx
IL-2 flox Tam Tx
B
Day 8
408
496
PD-1
PD-1 MFI
C
Donor in PBMC
UnTx
Tam Tx
Day PI
D
D8-75
% Contraction
E
PreTx
Day 2 Tx
UnTx
Memory Tx
Day 8 Recall
0.82
1.29
1.1
1.12
CD8
Ly 5.2
F
Day 8 Recall
p<0.09
Donors CD8 T cells in Spleen
UnTx
PreTx
Day 2 Tx
Memory Tx

Supplemental Figure 6

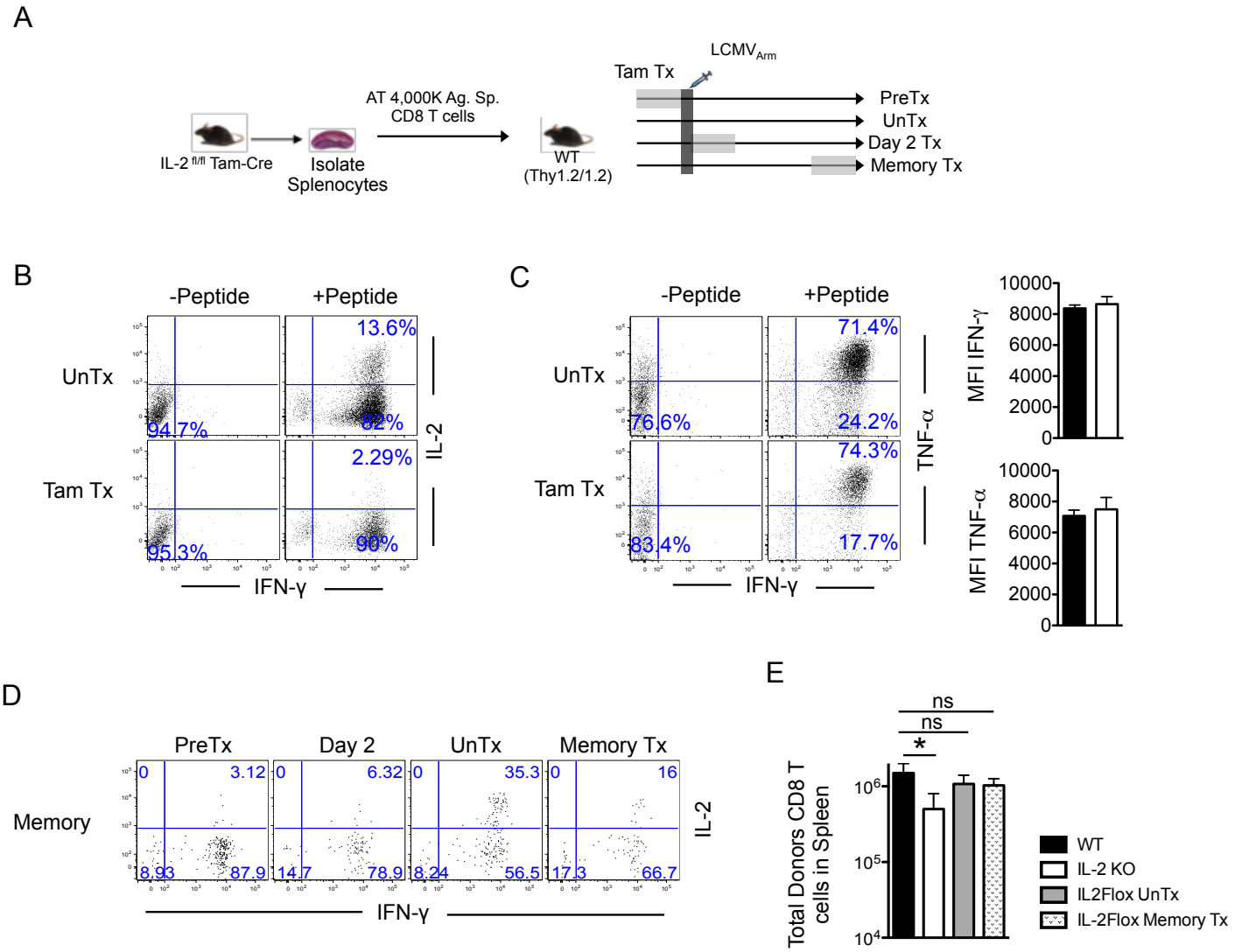

Figure Legends

Figure 1. IL-2 production is preferentially retained in memory precursor CD8 T cells.

A-B. Antigen-specific CD8 T cells were stimulated *in vitro* with GP33 loaded APCs for 2 days with (UnTx) or without (aIL-2 Tx) IL-2. A. Histograms are gated on antigen-specific CD8 T cells with activated (black) and naïve controls (gray). Numbers represent MFI of activated CD8 T cells. B. BrdU was added to the wells 6hrs prior to analysis, and uptake was compared. Activated CD8 T cells (black) and naïve controls (gray) are displayed in histograms. Numbers represent frequency of BrdU+ activated CD8 T cells. Bar graph depicts frequency of BrdU+ antigen-specific CD8 T cells with (Black) or without (White) IL-2 during priming. C. Antigen-specific CD8 T cells were transferred into naïve mice, which were then infected with $LCMV_{Arm}$. At indicated times post infection splenocytes were isolated and stimulated with GP33 peptide in the presence of BFA. FACS plots are gated on donor P14 CD8 T cells. D. Naïve mice were infected with $LCMV_{Arm}$ and splenocytes were collected at day 22 post-infection. Splenocytes were stimulated with GP33 in the presence of BFA to measure cytokine production. FACS plots are gated on CD8+ T cells and then subgated on IFN-γ+ T cells. IFN-γ+ T cells were gated on CD127+KLRG-1- (MPECs) and CD127-KLRG-1+(SLECs). FACS plots depict TNF-α and IL-2 production of MPECs and SLECs gated on IFN-g+ CD8 T cells. Bar graph depicts frequency of IL-2 producing of IFN-g+ antigen-specific CD8 T cells.

Figure 2. Early priming of cytotoxic T cells is mediated by paracrine IL-2 signals. Antigen-specific CD8 T cells were labeled with CFSE and adoptively transferred into naïve mice. Mice were infected with $LCMV_{Arm}$ and tissues were collected at day 2.75 post-infection. A. Histograms are gated on donor antigen-specific CD8 T cells. Frequency shows % of cells beyond

first cell division. Numbers depict MFI of given activation markers in naïve (gray) or day 2.75 post-infection (black) donor CD8 T cells. B. FACS plots are gated on donor CD8 T cells. Frequency shows ratio of WT and IL-2KO CD8 T cells. Bar graphs depict numbers of Donor CD8 T cells in spleen and iLN. C-D. Splenocytes were stimulated with GP33 peptide in the presence of BFA. C. FACS plots are gated on donor CD8 T cells. D. Bar graphs depict MFI of IFN-g and TNF-α and frequency of TNF-α+ of IFN-γ+ CD8 T cells.

Figure 3. Autocrine IL-2 signaling does not affect effector differentiation of antigen-specific CD8 T cells. A. Antigen-specific WT and IL-2 KO CD8 T cells were transferred into WT congenically mismatched mice which were then infected with $LCMV_{Arm}$. Mice were sacrificed at day 8 post infection and tissues were analyzed. FACS plots at day 8 post infection gated on donor antigen-specific CD8 T cells. Bar graphs depict number of donor CD8 T cells. B. FACS plots are gated on donor CD8 T cells in spleen. C. Histogram and bar graphs depicting mean fluorescence intensity of Granzyme B and PD-1. D. Spleens were stimulated for 5hrs *ex vivo* with GP33 peptide and cytokine production was measured. FACS plots gated on donor antigen-specific CD8 T cells show frequency of TNF-α+ and IFN-γ+ CD8 T cells. Bar graph shows % TNF-α+ of IFN-γ+ donor antigen-specific CD8 T cells. E. Bar graphs show MFI of IFN-γ and TNF-α in donor antigen-specific CD8 T cells.

Figure 4. IL-$2^{-/-}$ antigen-specific CD8 T cells show decreased maintenance properties upon memory differentiation. A-F. Antigen-specific WT and IL-2 KO CD8 T cells were transferred into WT congenically mismatched mice which were then infected with $LCMV_{Arm}$. Mice were bled longitudinally and sacrificed at day 50 post-infection. A. Line graph shows longitudinal plot of frequency of donor antigen-specific CD8 T cells of total PBMCs. B. Bar graph depicts percent

contraction between peak of effector response (Day 8 PI) and early memory (Day 24 PI). C. Bar graphs enumerate donor CD8 T cells in secondary lymphoid and peripheral tissues. D. Bar graphs show MFI of Bcl-2 at day 38 post infection. E. Mice were given BrdU for one week prior to analysis. FACS plots are gated on donor CD8 T cells in spleen. F. FACS plots are gated on donor CD8 T cells in spleen at day 50 post-infection. G. Spleens were stimulated for 5hrs *ex vivo* with GP33 peptide and cytokine production was measured. FACS plots gated on donor antigen-specific CD8 T cells show frequency of TNF-α+ and IFN-γ+ CD8 T cells.

Figure 5. Memory CD8 T cell recall expansion is defective in the absence of autocrine IL-2. IL-2 KO and WT memory cells were isolated from spleen and transferred into naïve, congenically mismatched mice, mice were challenged with rLM-GP33. A. FACS plots showing frequency of donor antigen-specific CD8 T cells in PBMC. B. Line graph shows kinetics of donor antigen-specific CD8 T cell responses in PBMC. C. Mice were sacrificed at day 45 post rechallenge and spleen and liver were enumerated for donor antigen-specific CD8 T cells. D. BrdU uptake was analyzed at day 4.75 and 6.75 post-infection. FACS plots are gated on donor CD8 T cells in spleens of infected mice. E. Histograms and bar graphs depict mean fluorescence intensity of Bcl-2 at day 5 post rechallenge. F. Bar graphs show percent Caspase 3 and 7+ donor antigen-specific CD8 T cells.

Figure 6. Autocrine IL-2 signals are critical during primary CD8 T cells expansion for memory recall. IL-2flox Cre-ERT P14 UnTx (Black) or Tam Tx (White) naive CD8 T cells were transferred into naïve B6 mice which were then infected with $LCMV_{Arm}$. A. Tissues were collected at day 8 post-infection and number of donor CD8 T cells was enumerated in spleen, iLN, lung and liver. B. Histograms are gated on donor UnTx(Black) or Tam Tx (white) or endogenous naïve (gray) in

spleen. Numbers represent MFI of PD-1. Bar graphs depict MFI of PD-1 at day 8 post-infection. C. Line graph shows frequency of donors in PBMC of infected mice. D. Bar graph enumerates percent contraction between day 8 and memory. E-F. Donor memory cells lacking IL-2 from prior to primary infection (PreTx), day 2 following primary infection, or during memory maintenance were isolated from splenocytes and adoptively transferred into naive B6 mice. Mice were infected with LM-GP33. E. FACS plots show frequency of donor cells in spleens of infected mice at day 8 post-infection. F. Bar graphs enumerate antigen-specific CD8 T cell numbers in spleens of infected mice.

Supplemental Figure 1. Paracrine IL-2 maintains activation and glycolysis of effector CD8 T cells. A. Antigen-specific CD8 T cells were stimulated in vitro with GP33 loaded APCs for 2 days with (UnTx) or without (aIL-2 Tx) IL-2. Bargraphs depict MFI of activation markers gated on antigen-specific CD8 T cells with (Black) or without (White) IL-2 during priming. **B.** Antigen-specific CD8 T cells were stimulated in vitro with gp33-APB supplemented with exogenous IL-2. Cells were collected at day 4 post-activation and mitostress test seahorse assay was performed. Line graph shows extracellular acidification rate of CD8 T cells. **C.** Naïve mice were infected with LCMVArm and splenocytes were collected at day 22 post-infection. Splenocytes were stimulated with respective LCMV peptide fragments in the presence of BFA to measure cytokine production. Bar graphs depict frequency of IL-2 producing of IFN-g+ antigen-specific CD8 T cells.

Supplemental Figure 2. Paracrine IL-2 is sufficient for the activation, proliferation, and glycolysis of effector CD8 T cells. A. WT and IL-2KO CD8 T cells were stimulated with GP33 loaded APCs with or without exogenous IL-2. Histograms were gated on antigen-specific CD8 T cells. Numbers depict MFI of activation markers. Frequencies depict number of BrdU+ CD8 T cells at day 2 post activation. **B.** WT and IL-2KO CD8 T cells were purified at day 2 post activation and a Mitostress test seahorse assay was performed. Line graph shows extracellular acidification rate of WT (black) or IL-2KO (white) CD8 T cells. **C**.

Antigen-specific CD8 T cells were adoptively transferred into naïve mice. Mice were infected with LCMVArm and tissues were collected at day 2.75 post-infection. Splenocytes were stimulated with GP33 peptide in the presence of BFA. FACS plots are gated on donor CD8 T cells.

Supplemental Figure 3. Similar proliferation in effector CD8 T cells in the absence of autocrine IL-2. A. Antigen-specific WT and IL-2 KO CD8 T cells were transferred into WT congenically mismatched mice which were then infected with LCMVArm. Mice were sacrificed at day 8 post infection and tissues were analyzed. **B**. Mice were injected IP with BrdU 12hrs prior to tissue collection. FACS plots are gated on donor CD8 T cells in spleen. **C**. Spleens were stimulated for 5hrs ex vivo with GP33 peptide and cytokine production was measured. FACS plots gated on donor antigen-specific CD8 T cells show frequency of IL-2+ and IFN-g+ CD8 T cells.

Supplemental Figure 4. Autocrine IL-2 does not impart effector and memory metabolic health. A. Antigen-specific WT and IL-2 KO CD8 T cells were transferred into WT congenically mismatched mice which were then infected with LCMVArm and followed through memory maintenance. **B**. Spleens were stimulated for 5hrs ex vivo with GP33 peptide and cytokine production was measured. FACS plots gated on donor antigen-specific CD8 T cells show frequency of IL-2+ and IFN-g+ CD8 T cells. **C**. Donor CD8 T cells were purified from effector (day 8 post-infection) and memory (day 30 post-infection) time points and analyzed using Seahorse Mitostress assay. Line graphs depict oxygen consumption rate and extracellular acidification rate.

Supplemental Figure 5. Decrease in accumulation of IL-2$^{-/-}$ memory cells following secondary challenge. A. IL-2 KO and WT memory cells were isolated from spleen and transferred into naïve, congenically mismatched mice, mice were challenged with rLM-GP33. **B**. FACS plots show frequency of donor CD8 T cells in spleen and liver.

Supplemental Figure 6. Effects of temporal ablation of autocrine IL-2 in antigen-specific CD8 T cells. A. IL-2fi/fl Cre-ERT P14 CD8 T cells were adoptively transferred into

naïve mice. Mice were treated with Tamoxifen to knock-out IL-2 gene in antigen-specific CD8 T cells at given times post infection; prior to infection (PreTx), day 2 post-infection (Day 2 Tx), or during memory (>Day 30 post-infection). **B-C**. IL-2fl/fl Cre-ERT donors were untx or IL-2 was knocked out prior to infection (PreTx). Mice were sacrificed at day 8 post-infection and spleens were stimulated for 5hrs ex vivo with GP33 peptide and cytokine production was measured. FACS plots gated on donor antigen-specific CD8 T cells show frequency of IL-2+ and TNF-a of IFN-g+ CD8 T cells. **D**. (Reference setup in A) Mice were sacrificed at memory and spleens were stimulated for 5hrs ex vivo with GP33 peptide and cytokine production was measured. FACS plots are gated on donor CD8 T cells. E. Memory WT, IL-$2^{-/-}$, IL-$2^{fl/fl}$ Tamoxifen untreated (UnTx), and IL-$2^{fl/fl}$ treated with tamoxifen prior to secondary rechallenge were adoptively transferred into naïve B6 mice. Mice were then infected with LM-GP33 and splenocytes were quantified following peak CD8 T cell expansion.

Early Autocrine IL-2 is Necessary for Maintenance of Exhausted CD8 T Cells

Yevgeniy Yuzefpolskiy[1,2], Laura A. Penny[3], Kendall A. Smith[4], Surojit Sarkar[1,2,5,6], and Vandana Kalia[1,5,6] ✦

[1] Ben Towne Center for Childhood Cancer Research, Seattle Children's Research Institute, Seattle WA 98101.

[2] M3D Graduate Program, University of Washington School of Medicine, Seattle, WA 98195

[3] The Huck Institutes of Life Sciences, The Pennsylvania State University, University Park, PA 16802

[4] Division of Immunology, Joan and Sanford I. Weill Department of Medicine, Weill Cornell Medicine, Cornell University, New York, NY, USA

[5]Department of Pathology, University of Washington School of Medicine, Seattle, WA 98195

[6] Department of Pediatrics, Division of Hematology and Oncology, University of Washington

*Corresponding authors: Surojit Sarkar and Vandana Kalia, sarkarkalia@gmail.com
1100 Olive Lab, Suite 100
Ben Towne Center for Childhood Cancer Research
University of Washington School of Medicine
Seattle, WA 98101

Footnote: This work was supported by research funding from the Seattle Children's Research Institute to SS and VK.

Running Title: Autocrine IL-2 Critical for Maintenance of Exhausted CD8 T Cells

Word Count (Abstract): 286

Word Count (Text): 4,082

Figure/Table Count: 5 Main Figures, 4 Supplemental Figures

Reference Count: 21

Abstract

As antigen persists during a chronic infection or in a tumor microenvironment, antigen-specific CD8 T cells begin a sequential process of exhaustion that depletes their ability to produce inflammatory cytokines, elicit cytotoxic effector function. Finally, the continuous TCR stimulation drives their antigen-mediated deletion. Current modalities in checkpoint blockade therapy aim to reduce the inhibitory signals placed on the exhausted CD8 T cells to rescue function in these cells and facilitate the clearance of the chronic pathogen. Studies in acute infection have demonstrated that antigen-specific CD8 T cells receive autocrine IL-2 programming early during priming, which instills survival benefits when rechallenged with antigen, following memory formation. As acute and chronic modes of infection have very similar priming events, we wanted to test whether similar autocrine IL-2 programming takes place during chronic infections. To this end, we have utilized a murine chronic LCMV model to study the effects of autocrine IL-2 ablation on antigen-specific CD8 T cell effector differentiation and exhaustion. We have demonstrated for the first time that in the absence of autocrine IL-2, CD8 T cells undergo decreased effector expansion, while maintaining regular T cell function. CD8 T cells lacking autocrine IL-2 signals also underwent accelerated contraction that was accompanied by overexpression of the inhibitory marker PD-1. This suggested that inhibitory signaling prevented normal maintenance of the exhausted cells. Indeed, we discovered that upon blockade with anti-PDL1 antigen-specific cells underwent robust expansion, accumulating to similar number as controls, despite starting at a significantly lower ratio. Thus, it is likely that antigen-specific CD8 T cell function can me modulated by decreasing IL-2 signals to increase responsiveness to future checkpoint blockade therapies.

Introduction

The process of antigen mediated exhaustion, seen during chronic infection or cancer microenvironments, converts potent effector T cells into dysfunctional cells lacking the ability to produce inflammatory cytokines or potentiate cytotoxic killing***(1-3)***. Understanding the mechanisms of T cell exhaustion has demonstrated that that these exhausted cells maintain a great deal of heterogeneity***(4-6)***. CXCR5 is one marker that differentiates between two major subsets of exhausted CD8 T cells. $CXCR5^{hi}$ $PD\text{-}1^{int}$ T cells exhibit a stem cell like quality in maintaining the chronic CD8 T cell responses by continuously proliferating and replenishing the pools of $CXCR5^{lo}$ $PD\text{-}1^{hi}$ terminally differentiated cells which will eventually be deleted from the infected host***(6, 7)***. These $CXCR5^{hi}$ exhausted T cells were demonstrated to be the main targets of checkpoint blockade therapy. In addition to CXCR5, many transcription factors have been confirmed to be critically involved in maintaining the exhausted T cell stem cells, such as the upregulation of Tbet, Eomes, and TCF-1 and downregulation of BLIMP-1***(4, 5, 8)***. Dissecting the necessary signals that drive the development and maintenance of these exhausted stem T cells is necessary for current and future anti-cancer therapies.

The rapid loss of IL-2 function during chronic CD8 T cell exhaustion has made it an unlikely target for study***(2)***. However, IL-2 is a potent mediator of CD8 T cell expansion(9, 10) and during acute infections autocrine IL-2 production is a hallmark feature of memory CD8 T cell differentiation(11, 12). Our laboratory and others have shown that autocrine IL-2 signals early during CD8 T cell priming are critical in programming survival of memory antigen-specific CD8 T cells following reintroduction to antigen***(13)***. Antigen-specific CD4 T cells are one of the primary producers of systemic IL-2; depletion of CD4 T cells during chronic infections has become a key model in studying exhausted CD8 T cells***(14)***. While

this CD4 depletion mediated exhaustion is likely mediated by more factors than IL-2, such as altered licensing of DCs and differentiation into more T_{FH}-like phenotypes(2), studies in checkpoint blockade therapy have demonstrated that transferring antigen specific CD4 T cells (15) results in a significant boost in the expansion of exhausted CD8 T cells when combined with PDL1 blockade(16). Together these data suggest that early during chronic infection there could be an important role for IL-2 signaling in programming the effector T cell response.

To study the role of autocrine IL-2, we have utilized wild-type (WT) and IL-$2^{-/-}$ P14 mice, which produce IL-2 autocrine sufficient or deficient LCMV specific CD8 T cells, respectively. By cotransferring these antigen-specific CD8 T cells into WT B6 recipients we were able to study the CD8 T cell intrinsic function of autocrine IL-2. We discovered that early priming and expansion of CD8 T cells is independent of autocrine IL-2 signaling, as IL-$2^{-/-}$ cells were able to undergo unperturbed proliferation, and acquired normal levels of cytokine production. However, following early expansion, we noticed a decrease in effector IL-$2^{-/-}$ CD8 T cell cycling, eventually resulting in decreased accumulation of peak effector numbers. While these effector cells displayed similar cytokine and effector molecule production they expressed significantly higher levels of the exhaustion marker PD-1. Following effector expansion, IL-$2^{-/-}$ CD8 T cells underwent a precipitous decline in cell numbers in peripheral sites of infection as well as secondary lymphoid tissues. Continued upregulation of PD-1 by IL-$2^{-/-}$ CD8 T cells suggested that these inhibitory signals prevented the slow turnover of exhausted CD8 T cells, supported by a slight increase in their proportion of $CXCR5^{hi}$ cells. We utilized PDL1 checkpoint blockade therapy to see if we could rescue the defect in the IL-$2^{-/-}$ CD8 T cells. Surprisingly, not only did PDL1

blockade rescue exhausted IL-2$^{-/-}$ CD8 T cells, we observed an increased capacity for T cell rescue in cells lacking autocrine IL-2 signals. We conclude that early autocrine IL-2 programming was responsible for decreasing the rate of conversion of the exhausted CD8 stem cells via PD-1 suppression driving the decline in accumulation of exhausted T cells. However this block created a population of exhausted CD8 T cells with an increased susceptibility to checkpoint blockade rescue.

Materials and Methods

Mice and infection

C57BL/6 mice were purchased from the Jackson Laboratory (Bar Harbor, ME, USA) and maintained in house. Thy1.1+ P14 mice bearing the H-2D^{b} GP33 epitope-specific TCR were fully backcrossed to C57BL/6 mice and were maintained in our animal colony. IL-2$^{-/-}$ mice were purchased from the Jackson Laboratory and crossed to P14 mice. IL-2$^{flox/flox}$ ERT2-Cre mice were generated in Kendall A. Smith's laboratory(9) and also crossed to P14 mice. Armstrong and CL-13 strains of LCMV was propagated, titered, and used as previously described(17). To establish chronic infection, mice were infected intravenously (IV) with 2x10^{6} pfu LCMV$_{CL\text{-}13}$. When indicated, prior to infection mice were depleted of CD4 T cells via intraperitoneal injection of aCD4 antibody GK1.5 (200mg/mouse; Day -1, 1 of infection). Acute infections were established by intraperitoneally injecting mice with 2x10^{5} pfu of LCMV$_{Arm}$. WT and IL-2$^{-/-}$ or WT and IL-2$^{flox/flox}$ mice were adoptively cotransferred via intravenous injection of 2x10^{3} antigen-specific CD8 T cells per mouse. For early (day 2.75) time points 2x10^{6} antigen-specific cells were transferred instead.

Flow cytometry

All antibodies were purchased from Biolegend (San Diego, CA, USA). Cells were stained for surface and intracellular proteins and cytokines as previously described(17). Cytokine production was assessed by direct *ex vivo* restimulation of 2x10^{6} splenocytes with 0.2μg/ml GP33-41 peptide in the presence of brefeldin A for 5h, followed by surface staining for CD8, Ly5.1, Thy1.1, or Thy1.2, and intracellular staining for IFN-γ, TNF-α, and IL-2. Flow cytometric analysis was performed on LSRII Fortessa (BD Biosciences, San Jose, CA). Single cell suspensions of spleen cells, lymph nodes, lungs, livers or PBMCs from mice were prepared and direct *ex vivo* staining was carried out as described previously(12).

Resident and circulatory cell localization was determined by IV injection of fluorescent CD8b antibody into mice 5 minutes prior to tissue collection.

Tamoxifen Treatment

IL-2 was knocked down in IL-$2^{flox/flox}$ Cre-ERT mice by treating mice with Tamoxifen (20mg/Kg) via gavage every third day for 12 days. Tamoxifen was resuspended in corn oil prior to gavage.

Statistical analysis

Paired or unpaired Student's t-test was used as indicated to evaluate differences between two group means. All statistical analyses were performed using Prism 5 and P values of statistical significance are depicted by asterisk per the Michelin guide scale: * ($P \leq 0.05$), ** ($P \leq 0.01$) and ($P > 0.05$) was considered not significant (ns).

Results

Autocrine IL-2 is lost early during chronic infections

Cytotoxic CD8 T cell rely on early autocrine IL-2 programming during priming of acute infections. Upon secondary rechallenge antigen-specific CD8 T cells rely on this previously instilled programming to properly maintain the secondary expansion to viral rechallenge. As chronic infections are by definition the prolonged activation of antigen-specific CD8 T cells, we wanted to study if autocrine IL-2 signals contributed to the programming of survival under continuous antigen stimulation. Chronic exhaustion is associated with a loss in function of antigen-specific CD8 T cells, resulting in the gradual loss of cytokine function, cytotoxicity, and degranulation; autocrine IL-2 is one of the first functions lost in this pathway. We wanted to track the evolution of IL-2 production of antigen-specific CD8 T cells to understand how it may impact exhausted CD8 T cells. For this we adoptively transferred WT LCMV specific P14 CD8 T cells into naïve B6 mice, which were subsequently infected with $LCMV_{CL\text{-}13}$ to establish a chronic infection, or $LCMV_{Arm}$ as a control acute infection. As expected, under acute conditions antigen-specific donors cells expanded vigorously to clear the virus, and following contraction formed long-lived memory cells (Figure 1A). A chronic infection resulted in significantly lower effector expansion and established a continuously contracting exhausted T cell pool (Figure 1A). Using direct *ex vivo* restimulation of antigen-specific CD8 T cells with their cognate GP33 peptide, we were able to determine the cytokine production of effector cells at different times post-infection. Following T cell priming (Day 2.75) autocrine IL-2 production is induced in antigen-specific CD8 T cells regardless of the mode of infection (Figure 1B). Following effector expansion the ability of CD8 T cells to produce autocrine IL-2 is significantly diminished in both acute and chronic infections, however, chronic infections

result in CD8 T cells with significantly lower production of IL-2. Following viral clearance, antigen-specific CD8 T cells slowly enrich for the ability to produce autocrine IL-2 as they differentiate into long-lived memory CD8 T cells (Figure 1B). During chronic infections autocrine IL-2 function is permanently lost, as the donor cells produced no significant IL-2 (Figure 1B). Thus, if autocrine IL-2 does affect CD8 T cell programming during chronic infections, it is likely also early during CD8 T cell priming.

Early priming and expansion of CD8 T cells is largely independent of autocrine IL-2

To delineate the role of autocrine IL-2 during chronic infection, WT and IL-2$^{-/-}$ CD8 T cells were cotransferred into naïve C57BL/6 mice, which were subsequently infected with $LCMV_{Cl\text{-}13}$. As autocrine IL-2 is primarily observed during CD8 T cell priming, we first focused on this time post-infection. Following antigen priming, both WT and IL-2$^{-/-}$ antigen-specific CD8 T cells underwent robust CD8 T cell proliferation resulting in a dilution of CFSE (Figure 2A). Furthermore, because the ratio of WT and IL-2$^{-/-}$ CD8 T cells didn't change significantly from the naïve to primed state, this suggested that WT and IL-2$^{-/-}$ T cells underwent similar proliferation and expansion (Figure 2A, S2A). To gauge the extent of antigen recruitment we also monitored levels of activation markers PD-1 and CD69. We observed that by day 2.75 post-infection both WT and IL-2$^{-/-}$ antigen-specific CD8 T cells were fully activated as they expressed high levels of PD-1 and CD69 (Figure 2B, S2B). We used direct *ex vivo* restimulation with GP33 peptide to compare cytokine polyfunctionality of WT and IL-2$^{-/-}$ CD8 T cells. While IL-2$^{-/-}$ T cells lacked autocrine IL-2 function (Figure S2C) they were able to produce wild-type levels of IFN-g and TNF-a (Figure 2C), suggesting

similar polyfunctionality. Thus despite lacking autocrine IL-2, priming of antigen-specific T cells was not affected.

Following priming, antigen-specific CD8 T cells undergo vigorous expansion. To assess whether autocrine IL-2 was necessary for chronic expansion we analyzed WT and IL-2$^{-/-}$ donors at day 5 post-infection, in between priming and peak effector expansion. Consistent with their similar expansion during priming, we observed a similar ratios and numbers of WT and IL-2$^{-/-}$ T cells in peripheral tissues and secondary lymphoid tissues (Figure 2D-E). As day 5 post-infection is a time of robust T cell expansion we treated mice with BrdU to compare their rate of cell cycling. Interestingly, despite having similar numbers, we observed a significant decrease in BrdU uptake by IL-2$^{-/-}$ CD8 T cells in all tissues except iLN (Figure S2D-E). In fact, IL-2$^{-/-}$ CD8 T cells in peripheral sites of infection (LNG, and LVR) displayed a more severe defect in proliferation. Collectively this data suggests that the effects of autocrine IL-2 ablation are most critical following antigen priming, and these early defects in proliferation may cause later defects in effector cell accumulation.

Decreased effector expansion in the absence of autocrine IL-2

To understand how early effector differences in BrdU uptake affected WT and IL-2$^{-/-}$ CD8 T cells effector expansion, we analyzed the peak of the effector response at day 8 post-LCMV infection. Following peak effector expansion, WT T cells accumulated in higher number compared to IL-2$^{-/-}$ in secondary lymphoid tissue and peripheral sites of infection such as lung, and similar trend in the liver of infected mice (Figure 3A-B). Important to note, despite being in the same antigenic milieu IL-2$^{-/-}$ CD8 T cells displayed a significantly

higher level of exhaustion marker PD-1, suggesting decreased expansion could be due to increased inhibitory signaling (Figure 3C). Comparing other exhaustion markers showed a decreased expression of 2B4, but similar levels of TIM3 and LAG3 (Figure S3C). However, despite a decrease in T cell accumulation and increased PD-1 expression, IL-$2^{-/-}$ did not seem defective in their effector function, as they expressed similar levels of Granzyme B (Figure 3C). When comparing polyfunctionality, as expected WT IL-2 production was dropping to IL-$2^{-/-}$ levels. Beyond that, both WT and IL-$2^{-/-}$ T cells produced similar levels of IFN-g, and only a slight decrease in TNF-a production in IL-$2^{-/-}$ T cells (Figure 3D, S3D). As decreased accumulation was the most significant defect in IL-$2^{-/-}$ donors, we wanted to see if decreased cell number could be due to differential localization. By injecting mice with fluorescent CD8b antibody prior to tissue harvesting, we were able to determine that in the absence of autocrine IL-2 CD8 T cells display no defect in tissue extravasation, and a normalization of cells by tissue number, showed that there was also no defect in localization between tissues.

As IL-$2^{-/-}$ donor CD8 T cells originate from a whole somatic knock-out strain, we wanted to confirm that the differences observed were not due to a developmental defect of an IL-$2^{-/-}$ environment. To this end, we utilized an IL-$2^{flox/flox}$ Cre-ERT P14 mouse strain in which T cells undergo standard thymic development. Then, utilizing Tamoxifen treatment (Tam Tx) we caused IL-2 ablation in mature CD8 T cells. Direct *ex vitro* stimulation of the naïve cells was used to confirm IL-2 ablation (data not shown). We then cotransferred WT and IL-$2^{fl/fl}$ Cre-ERT treated with Tamoxifen (Tam Tx: IL-$2^{-/-}$) or left untreated (UnTx: WT) into naïve C57BL6 mice. Mice were infected with $LCMV_{CL-13}$ and donors were compared at day 8 post-infection. Similar to their IL-$2^{-/-}$ counterparts, IL-$2^{fl/fl}$ Tam Tx T cells

accumulated in fewer numbers at day 8 post infection in secondary lymphoid tissues and peripheral sites of infection (Figure S3E-F). The fact that ablation prior to infection, showed similar phenotype as somatic ablation of IL-2, let us continue using the somatic knock-out strain for the remainder of the experiments.

Pronounced defect in the maintenance of IL-2$^{-/-}$ CD8 T cells

Following effector expansion, exhausted CD8 T cells undergo antigen-dependent maintenance. Exhausted CD8 T cells maintain themselves via the constant proliferation of a less exhausted stem-like subpopulation of antigen-specific T cells. Thus, we wanted to see whether decreased cell cycling observed early on continued into T cell exhaustion. Mice were adoptively transferred with WT and IL-2$^{-/-}$ donor cells and infected with $LCMV_{CL-13}$; mice were followed longitudinally through $LCMV_{CL-13}$ infection to compare exhaustion kinetics of donor CD8 T cells. In the absence of autocrine IL-2 signals, antigen-specific CD8 T cells were unable to maintain their numbers, undergoing significant contraction compared to their WT counterparts (Figure 4A-B). This increased contraction resulted in decreased peripheral T cell numbers in secondary lymphoid tissues (spleen and lymph node) as well as peripheral sites of infection (lung and liver) (Figure 4C-D). We further confirmed that this defect was not due to any minor histocompatibility issues, as IL-2$^{-/-}$ donors had no defect in maintenance under acute LCMV infections (Figure S4A). Furthermore, IL-2$^{-/-}$ donors continued to express higher levels of PD-1, and expressed slightly lower levels of Granzyme B compared to their WT counterparts (Figure 4E-F). Conversely, upon direct *ex vivo* restimulation with cognate peptide, WT and IL-2$^{-/-}$ CD8 T cells produced similarly low levels of IFN-g and TNF-a suggesting that they are undergoing similar levels of T cell exhaustion (Figure 4H, S4C). All together these data further promote

that autocrine IL-2 programs a PD-1 mediated defect in T cell maintenance. As CD4 T cells are a dominant producer of IL-2 during early effector expansion, we wanted to see if depleting early CD4 help would exacerbate the phenotype. Indeed, under these conditions, both WT and IL-$2^{-/-}$ CD8 T cells undergo precipitous decline following effector expansion (Figure S4B). However, a maintained gap between WT and IL-$2^{-/-}$ numbers suggests an autocrine-specific requirement for IL-2 in exhausted T cell maintenance (Figure S4B).

During a chronic infection a less exhausted stem-cell-like progenitor pool of cells that are $CXCR5^{hi}$ maintains peripheral T cell numbers. These $CXCR5^{hi}$ cells express lower levels of PD-1, and other inhibitory molecules. Decreased levels of T cell maintenance and increased levels of PD-1 suggested that IL-$2^{-/-}$ T cells have a defect in this pool of cells. We analyzed WT and IL-$2^{-/-}$ CD8 T cells at day 20 post-infection and observed that IL-$2^{-/-}$ CD8 T cells actually had a slight increase in the proportion of $CXCR5^{hi}$ cells compared to their WT counterparts, however both populations were a lot lower than the endogenous GP33 cells, which have a thymic pool of cells to replenish from (Figure 4G). Thus it is possible that overexpression of PD-1 in the IL-$2^{-/-}$ CD8 T cells is causing a decreased rate in conversion of $CXCR5^{hi}$ cells into the larger pool of $CXCR5^{lo}$ causing a progressive loss in T cell numbers.

PDL1 blockade provides a full rescue of IL-$2^{-/-}$ donor CD8 T cells

Checkpoint blockade has emerged as a breakthrough in rescuing exhausted CD8 T cells by blocking inhibitory ligands on CD8 T cells. Thus, the overexpression of PD-1 by exhausted IL-$2^{-/-}$ CD8 T cells suggested that releasing those inhibitory signals could provide a potent rescue of the IL-$2^{-/-}$ T cell subset. To test this theory, we adoptively cotransferred WT and IL-$2^{-/-}$ CD8 T cells into naïve mice, which were subsequently infected with $LCMV_{CL\text{-}13}$ (Figure S5A). Once chronicity was established, we started the PDL1 checkpoint blockade

therapy established in previous publications(18). As expected IL-2$^{-/-}$ CD8 T cells left untreated continued to undergo CD8 T cell contraction (Figure 5A). However, following PDL1 blockade therapy, not only did antigen-specific CD8 T cells get rescued, IL-2$^{-/-}$ CD8 T cells underwent a dramatically increased expansion over their WT P14 counterparts (Figure 5A-C, S5B). Rescue of donor CD8 T cells was met with decreased expression of exhaustion markers PD-1, 2B4 and TIM3 in both WT and IL-2$^{-/-}$ CD8 T cells (Figure 5 D). Cytokine production by the rescued donor cells shows similar rescue in IFN-g and TNF-a production in WT and IL-2$^{-/-}$ CD8 T cells (Figure 5E-C). This data is coherent with the similarities we observed in cytokine production throughout infection and shows that in the absence of autocrine IL-2 signaling, overexpression of PD-1 causes a halt in cell cycle progression, preventing the turnover of exhausted cytotoxic stem cells but not the function of the cells.

Discussion

IL-2 is a potent modulator of antigen-specific CD8 T cells, pushing effector cells to maintain their glycolytic state, and driving rapid proliferation and effector function early during infection(19, 20). However, as IL-2 function in lost early during chronic infection, and is not recovered following exhaustion, its function has been largely overlooked. On the other hand, early heterogeneity in CD25 (IL-2Ra) during acute infections plays a crucial role in the development of terminal effector CD8 T cells, which do not maintain their ability to produce autocrine IL-2***(12)***. We have demonstrated for the first time that autocrine IL-2 is vital in driving the expansion and maintenance of exhausted CD8 T cells. In fact, the decline in antigen-specific CD8 T cells lacking autocrine IL-2 could only be restored using checkpoint blockade intervention, suggesting increased susceptibility to exhaustion signals. This not only helps expand our understanding of CD8 T cell exhaustion, but supports earlier experiments showing a similar phenotype in acute CD8 T cell priming.

We utilized a P14 model of $LCMV_{CL\text{-}13}$ exhaustion in which donor CD8 T cells were IL-2 sufficient, or ablated. This allowed us to characterize the effects of autocrine IL-2 in a CD8 T cells intrinsic manner, while maintaining an identical infection milieu for both cell types. Thus, we safely determined that IL-$2^{-/-}$ T cells exhibited higher levels of PD-1 because of intrinsic difference in T cell signaling, and not due to a defect in viral clearance. We were able to further confirm that the cells were seeing similar levels of antigen by demonstrating their similar localization and extravasation into secondary lymphoid tissues and peripheral sites of infection. We were able to validate this model by confirming similar results using IL-$2^{fl/fl}$ Cre-ERT mice, in which deletion of autocrine IL-2 was performed directly prior to LCMV challenge allowing us to determine the effects to be specific to the antigen challenge and not caused by altered thymic selection. Finally, we were able to

demonstrate that the increased contraction we observed was not due to minor histocompatibility issues, as WT and IL-2$^{-/-}$ CD8 T cells were able to maintain similar number during an acute LCMV$_{Arm}$ infection.

In line with previous studies of autocrine IL-2 ablation, we did not observe major differences in Granzyme B, or IFN-g production; and only a slight decrease in TNF-a functionality in the absence of autocrine IL-2. These differences were maintained constant throughout chronic LCMV infection, demonstrating that either IL-2 is dispensable for these functions, or paracrine IL-2 is sufficient to elicit them. Similar to acute T cell priming, paracrine IL-2 was sufficient to sustain early T cell expansion. On the other hand, unlike acute infections following day 5 post-infection IL-2$^{-/-}$ CD8 T cells demonstrated a decreased capacity to proliferate. This defect was manifested in decreased effector expansion, and increased contraction of exhausted CD8 T cells. It is likely that the high viral titers during chronic infection cause an accelerated development of a similar expansion defect observed in acute during memory rechallenge.

Finally, the lack of exhausted T cell maintenance was not due to an intrinsic defect in T cell proliferation. Checkpoint blockade of WT and IL-2$^{-/-}$ donor cells resulted in at least two-fold expansion of WT cells, but over a six-fold increase in the rescue of IL-2$^{-/-}$ CD8 T cells. We hypothesize the increased capacity of IL-2$^{-/-}$ CD8 T cells to expand upon PDL1 blockade, suggests that lack of autocrine IL-2 signals instilled an increased inhibitory profile in the antigen-specific cells that preserved their T cell function by blocking cell cycling. Previous studies have shown that treating exhausted CD8 T cells with rapamycin during chronic infection, while reducing their total numbers, was able to program a better metabolic state in the exhausted CD8 T cells(21). However, continued treatment with

rapamycin in parallel with PDL1 blockade completely nullified the expansion mediated by the checkpoint blockade(22). It is possible that future studies can modulate early IL-2 signals to form a more robust population of exhausted CD8 T cells to combine with different checkpoint blockade modalities.

Acknowledgements

The authors would like to thank Dr. Kendall A. Smith for providing the conditional IL-2 knockout mice and for scientific discussions, and Ms. Laura Penny for excellent technical assistance.

Authorship and Conflict of Interest Statements

Contribution: YY carried out experiments, analyzed data, prepared figures and wrote manuscript. LAP conducted experiments and analyzed data. VK and SS conceptualized the project, designed the experiments, carried out experiments, supervised the work, analyzed data, interpreted the results and helped prepare the manuscript.

Conflict-of-interest disclosure: The authors declare no competing financial interests.

References

1. Wherry, E. J., and R. Ahmed. 2004. Memory CD8 T-cell differentiation during viral infection. *Journal of Virology* 78: 5535–5545.
2. Wherry, E. J., and M. Kurachi. 2015. Molecular and cellular insights into T cell exhaustion. *Nat Rev Immunol* 15: 486–499.
3. Penaloza-MacMaster, P., A. O. Kamphorst, A. Wieland, K. Araki, S. S. Iyer, E. E. West, L. O'Mara, S. Yang, B. T. Konieczny, A. H. Sharpe, G. J. Freeman, A. Y. Rudensky, and R. Ahmed. 2014. Interplay between regulatory T cells and PD-1 in modulating T cell exhaustion and viral control during chronic LCMV infection. *J. Exp. Med.* 211: 1905–1918.
4. Shin, H., S. D. Blackburn, A. M. Intlekofer, C. Kao, J. M. Angelosanto, S. L. Reiner, and E. J. Wherry. 2009. A Role for the Transcriptional Repressor Blimp-1 in CD8+ T Cell Exhaustion during Chronic Viral Infection. *Immunity* 31: 309–320.
5. Utzschneider, D. T., M. Charmoy, V. Chennupati, L. Pousse, D. P. Ferreira, S. Calderon-Copete, M. Danilo, F. Alfei, M. Hofmann, D. Wieland, S. Pradervand, R. Thimme, D. Zehn, and W. Held. 2016. T Cell Factor 1-Expressing Memory-like CD8(+) T Cells Sustain the Immune Response to Chronic Viral Infections. *Immunity* 45: 415–427.
6. Im, S. J., M. Hashimoto, M. Y. Gerner, J. Lee, H. T. Kissick, M. C. Burger, Q. Shan, J. S. Hale, J. Lee, T. H. Nasti, A. H. Sharpe, G. J. Freeman, R. N. Germain, H. I. Nakaya, H.-H. Xue, and R. Ahmed. 2016. Defining CD8+ T cells that provide the proliferative burst after PD-1 therapy. *Nature* 537: 417–421.
7. He, R., S. Hou, C. Liu, A. Zhang, Q. Bai, M. Han, Y. Yang, G. Wei, T. Shen, X. Yang, L. Xu, X. Chen, Y. Hao, P. Wang, C. Zhu, J. Ou, H. Liang, T. Ni, X. Zhang, X. Zhou, K. Deng, Y. Chen, Y. Luo, J. Xu, H. Qi, Y. Wu, and L. Ye. 2016. Follicular CXCR5-expressing CD8(+) T cells curtail chronic viral infection. *Nature* 537: 412–428.
8. Paley, M. A., D. C. Kroy, P. M. Odorizzi, J. B. Johnnidis, D. V. Dolfi, B. E. Barnett, E. K. Bikoff, E. J. Robertson, G. M. Lauer, S. L. Reiner, and E. J. Wherry. 2012. Progenitor and Terminal Subsets of CD8+ T Cells Cooperate to Contain Chronic Viral Infection. *Science* 338: 1220–1225.
9. Smith, K. A. 2012. Conditional IL-2 gene deletion: consequences for T cell proliferation. 1–12.
10. Janas, M. L., P. Groves, N. Kienzle, and A. Kelso. 2005. IL-2 regulates perforin and granzyme gene expression in CD8+ T cells independently of its effects on survival and proliferation. *J. Immunol.* 175: 8003–8010.
11. Sarkar, S., V. Kalia, W. N. Haining, B. T. Konieczny, S. Subramaniam, and R. Ahmed. 2008. Functional and genomic profiling of effector CD8 T cell subsets with distinct memory fates. *The Journal of* .
12. Kalia, V., S. Sarkar, S. Subramaniam, W. N. Haining, K. A. Smith, and R. Ahmed. 2010. Prolonged interleukin-2Ralpha expression on virus-specific CD8+ T cells favors terminal-effector differentiation in vivo. *Immunity* 32: 91–103.
13. Feau, S., R. Arens, S. Togher, and S. P. Schoenberger. 2011. Autocrine IL-2 is required for secondary population expansion of CD8(+) memory T cells. *Nat Immunol* 12: 908–913.
14. Matloubian, M., R. J. Concepcion, and R. Ahmed. 1994. CD4+ T cells are required to sustain CD8+ cytotoxic T-cell responses during chronic viral infection. *Journal of Virology* 68: 8056–8063.
15. Aubert, R. D., A. O. Kamphorst, S. Sarkar, V. Vezys, S.-J. Ha, D. L. Barber, L. Ye, A. H. Sharpe, G. J. Freeman, and R. Ahmed. 2011. Antigen-specific CD4 T-cell help rescues

exhausted CD8 T cells during chronic viral infection. *Proc. Natl. Acad. Sci. U.S.A.* 108: 21182–21187.
16. West, E. E., H.-T. Jin, A.-U. Rasheed, P. Penaloza-MacMaster, S.-J. Ha, W. G. Tan, Ben Youngblood, G. J. Freeman, K. A. Smith, and R. Ahmed. 2013. PD-L1 blockade synergizes with IL-2 therapy in reinvigorating exhausted T cells. *J. Clin. Invest.* 123: 2604–2615.
17. Kalia, V., L. A. Penny, Y. Yuzefpolskiy, F. M. Baumann, and S. Sarkar. 2015. Quiescence of Memory CD8+ T Cells Is Mediated by Regulatory T Cells through Inhibitory Receptor CTLA-4. *Immunity* 42: 1116–1129.
18. Barber, D. L., E. J. Wherry, D. Masopust, B. Zhu, J. P. Allison, A. H. Sharpe, G. J. Freeman, and R. Ahmed. 2006. Restoring function in exhausted CD8 T cells during chronic viral infection. *Nature* 439: 682–687.
19. Wong, P., and E. G. Pamer. 2004. Disparate in vitro and in vivo requirements for IL-2 during antigen-independent CD8 T cell expansion. *J. Immunol.* 172: 2171–2176.
20. Rollings, C. M., L. V. Sinclair, H. J. M. Brady, D. A. Cantrell, and S. H. Ross. 2018. Interleukin-2 shapes the cytotoxic T cell proteome and immune environment-sensing programs. *Science Signaling* 11: eaap8112.
21. Bengsch, B., A. L. Johnson, M. Kurachi, P. M. Odorizzi, K. E. Pauken, J. Attanasio, E. Stelekati, L. M. McLane, M. A. Paley, G. M. Delgoffe, and E. J. Wherry. 2016. Bioenergetic Insufficiencies Due to Metabolic Alterations Regulated by the Inhibitory Receptor PD-1 Are an Early Driver of CD8+ T Cell Exhaustion. *Immunity* 45: 358–373.
22. Staron, M. M., S. M. Gray, H. D. Marshall, I. A. Parish, J. H. Chen, C. J. Perry, G. Cui, M. O. Li, and S. M. Kaech. 2014. The transcription factor FoxO1 sustains expression of the inhibitory receptor PD-1 and survival of antiviral CD8(+) T cells during chronic infection. *Immunity* 41: 802–814.

Figures

Figure 1

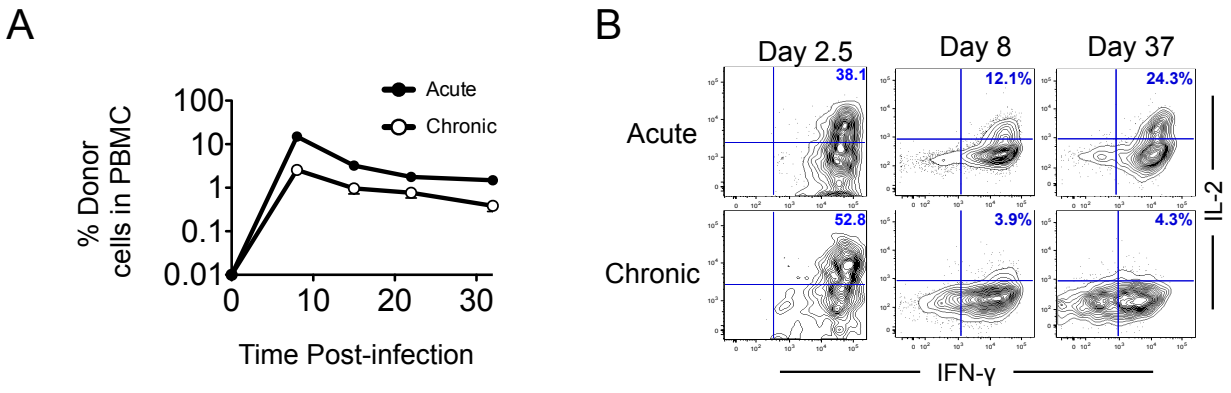

Figure 2

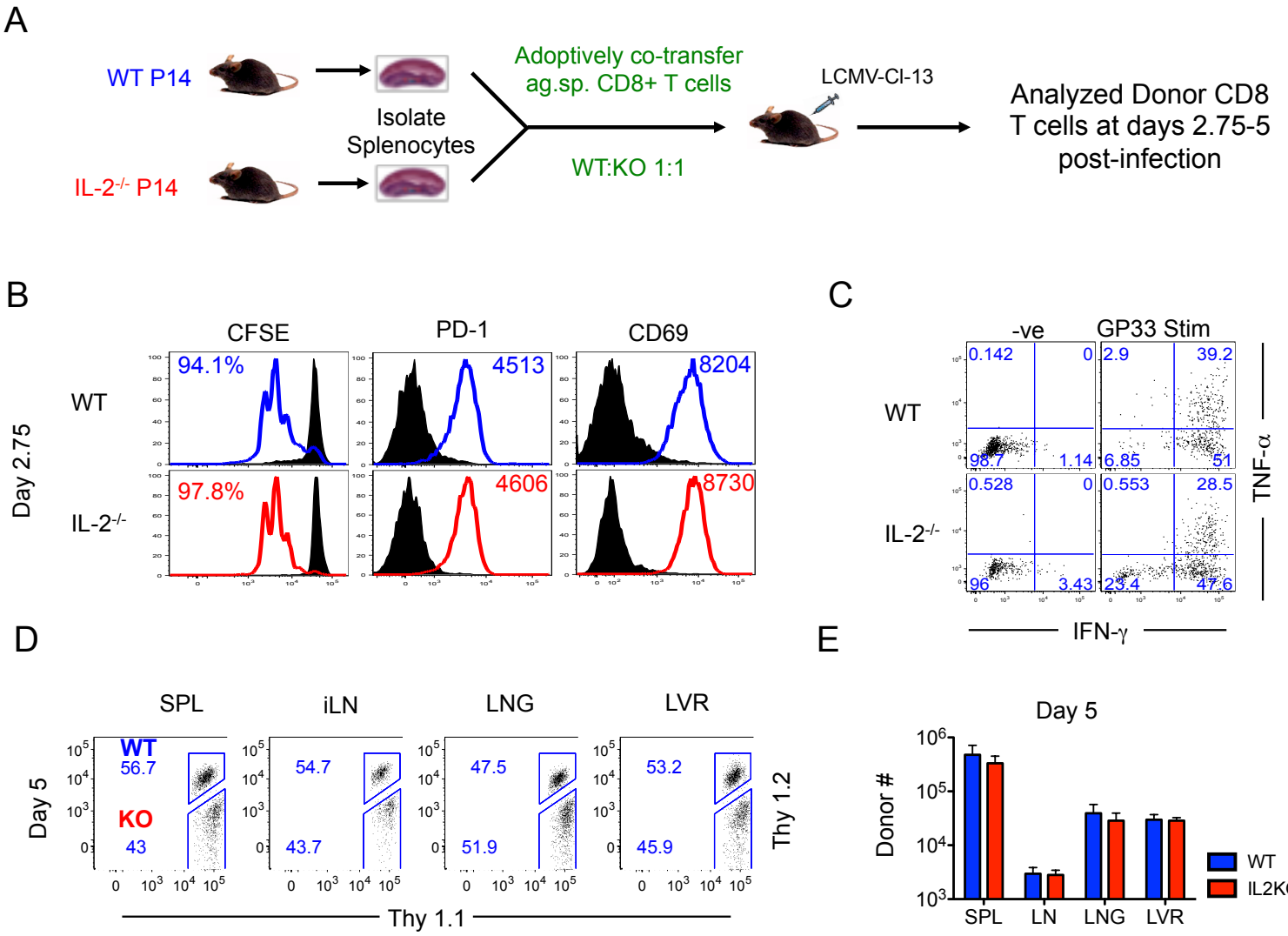
A
WT P14
IL-2-/- P14
Isolate Splenocytes
Adoptively co-transfer ag.sp. CD8+ T cells
WT:KO 1:1
LCMV-Cl-13
Analyzed Donor CD8 T cells at days 2.75-5 post-infection
B
CFSE
PD-1
CD69
Day 2.75
WT
IL-2-/-
94.1%
4513
8204
97.8%
4606
8730
C
-ve
GP33 Stim
WT
IL-2-/-
0.142
0
2.9
39.2
98.7
1.14
6.85
51
0.528
0
0.553
28.5
96
3.43
23.4
47.6
TNF-α
IFN-γ
D
SPL
iLN
LNG
LVR
Day 5
WT
56.7
KO
43
54.7
43.7
47.5
51.9
53.2
45.9
Thy 1.2
Thy 1.1
E
Day 5
Donor #
SPL
LN
LNG
LVR
WT
IL2KO

Supplemental Figure 2

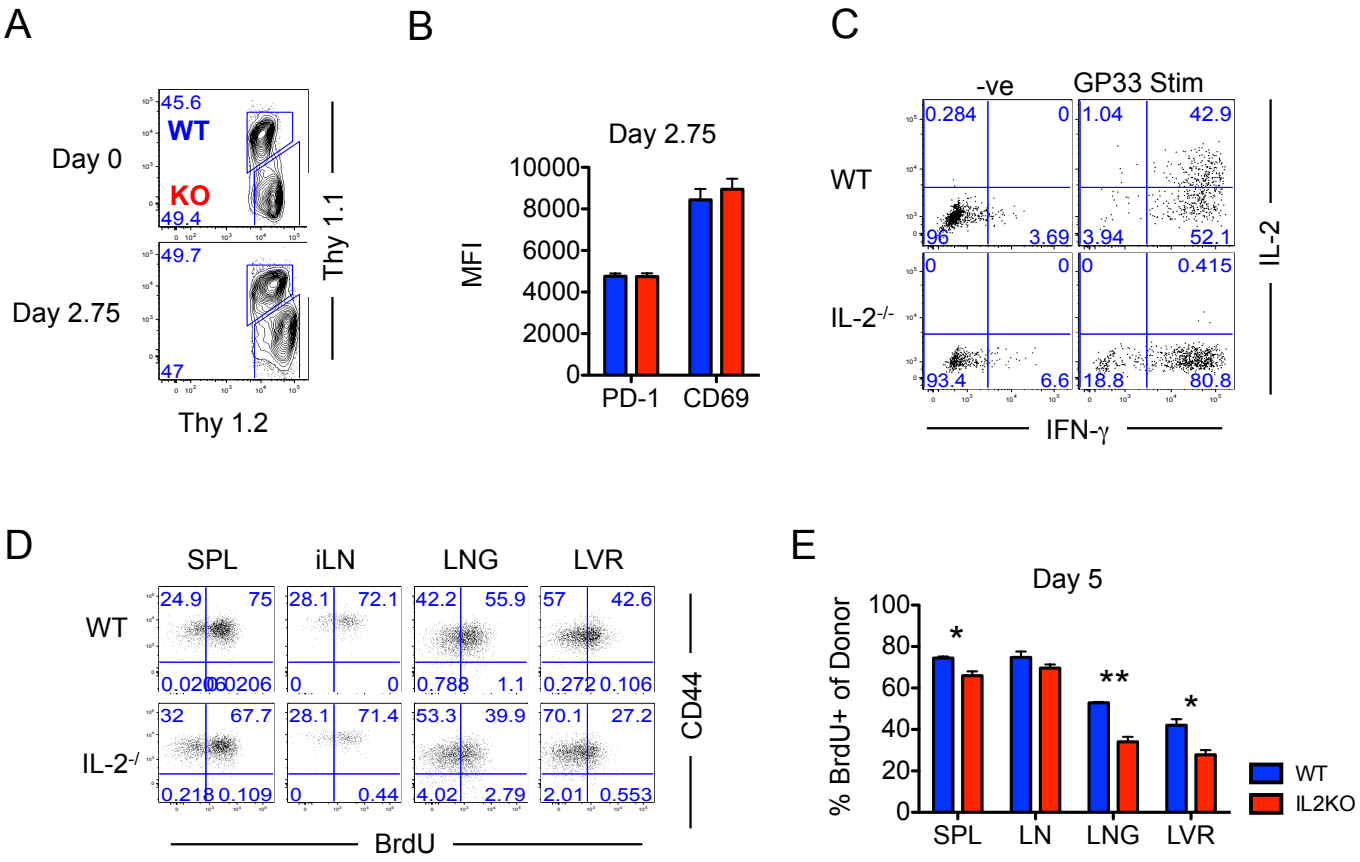

Figure 3

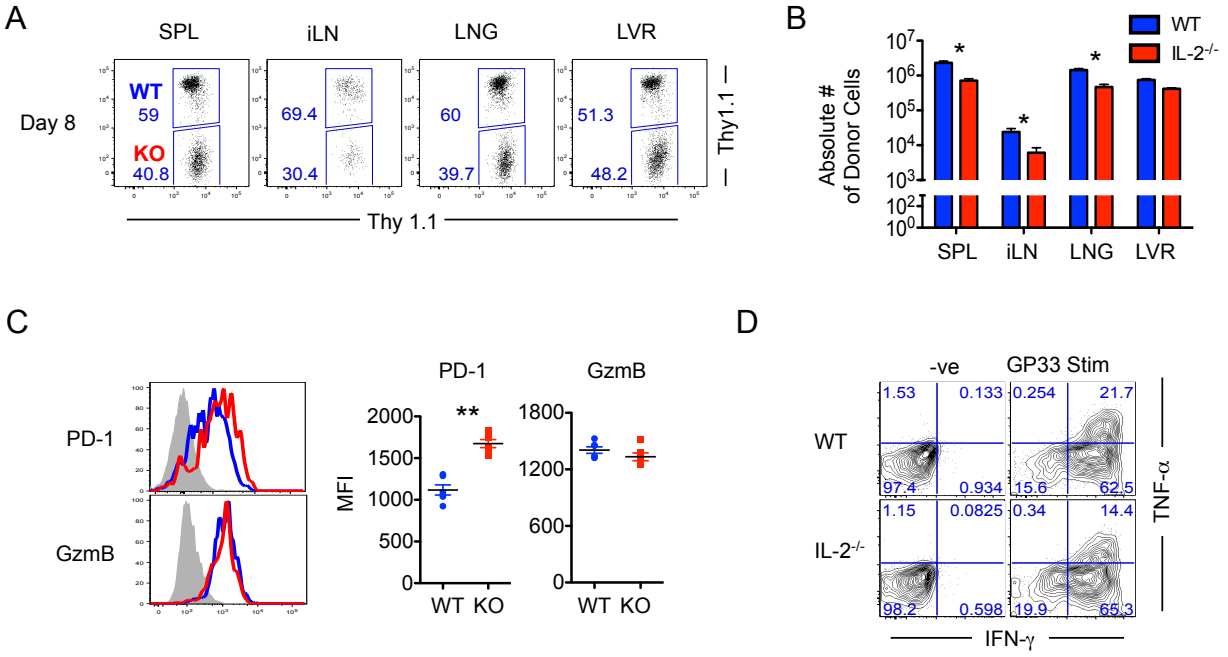
A
SPL
iLN
LNG
LVR
Day 8
WT
59
KO
40.8
69.4
30.4
60
39.7
51.3
48.2
Thy1.1
Thy 1.1
B
WT
IL-2-/-
Absolute # of Donor Cells
SPL
iLN
LNG
LVR
C
PD-1
GzmB
MFI
PD-1
GzmB
WT KO
WT KO
D
-ve
GP33 Stim
WT
IL-2-/-
1.53
0.133
0.254
21.7
97.4
0.934
15.6
62.5
1.15
0.0825
0.34
14.4
98.2
0.598
19.9
65.3
TNF-α
IFN-γ

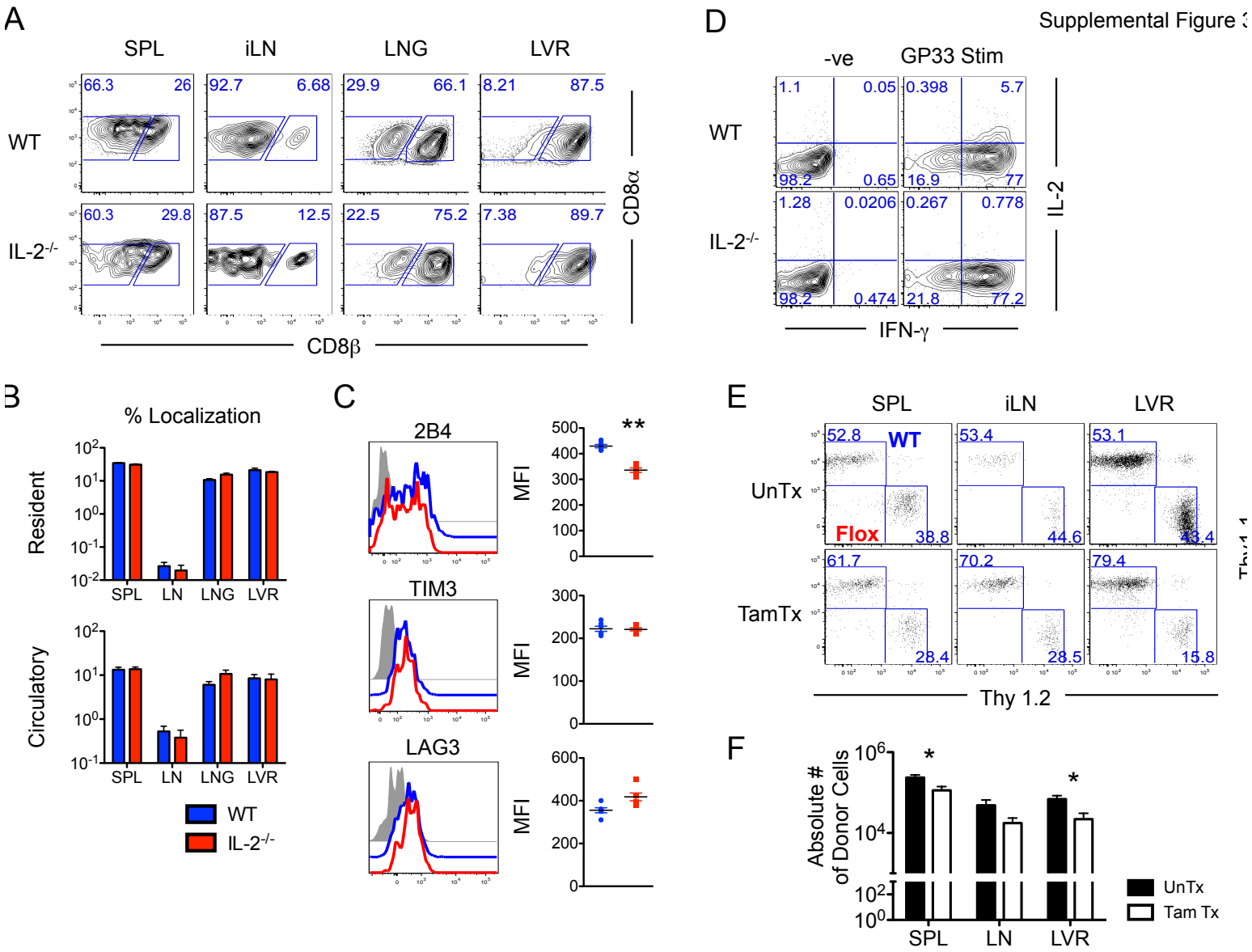
A
SPL
iLN
LNG
LVR
WT
IL-2-/-
66.3
26
92.7
6.68
29.9
66.1
8.21
87.5
60.3
29.8
87.5
12.5
22.5
75.2
7.38
89.7
CD8α
CD8β
B
% Localization
Resident
Circulatory
SPL
LN
LNG
LVR
WT
IL-2-/-
C
2B4
TIM3
LAG3
MFI
**
D
-ve
GP33 Stim
1.1
0.05
0.398
5.7
98.2
0.65
16.9
77
1.28
0.0206
0.267
0.778
98.2
0.474
21.8
77.2
IL-2
IFN-γ
E
SPL
iLN
LVR
UnTx
TamTx
52.8
WT
53.4
53.1
Flox
38.8
44.6
43.4
61.7
70.2
79.4
28.4
28.5
15.8
Thy 1.2
F
Absolute # of Donor Cells
*
*
UnTx
Tam Tx
SPL
LN
LVR

Figure 4

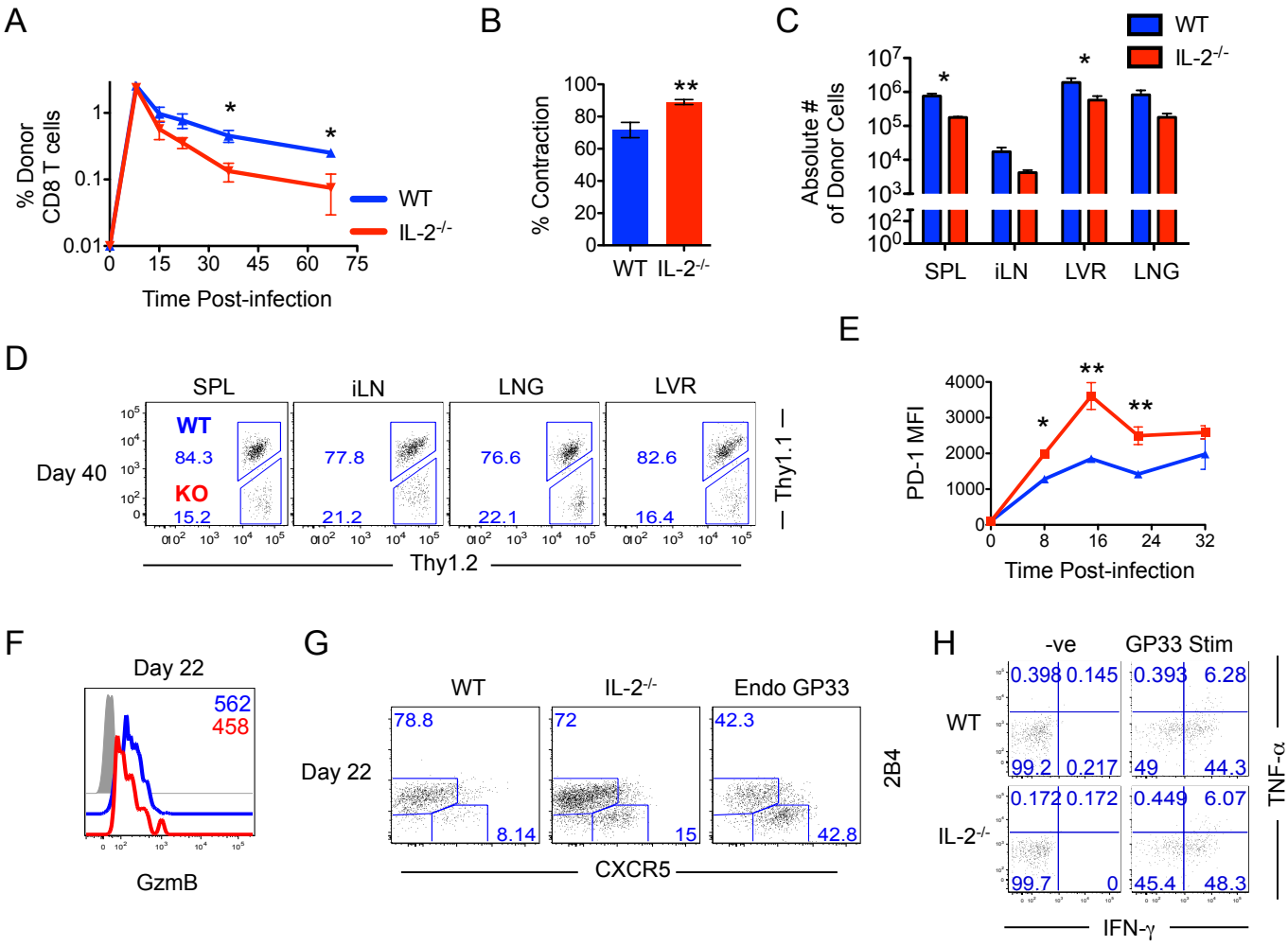
A
% Donor CD8 T cells
Time Post-infection
WT
IL-2-/-
B
% Contraction
C
Absolute # of Donor Cells
SPL
iLN
LVR
LNG
D
Day 40
WT
84.3
KO
15.2
77.8
21.2
76.6
22.1
82.6
16.4
Thy1.2
Thy1.1
E
PD-1 MFI
Time Post-infection
F
Day 22
562
458
GzmB
G
WT
IL-2-/-
Endo GP33
Day 22
78.8
8.14
72
15
42.3
42.8
CXCR5
2B4
H
-ve
GP33 Stim
WT
IL-2-/-
0.398
0.145
99.2
0.217
0.393
6.28
49
44.3
0.172
0.172
99.7
0
0.449
6.07
45.4
48.3
IFN-γ
TNF-α

Supplemental Figure 4

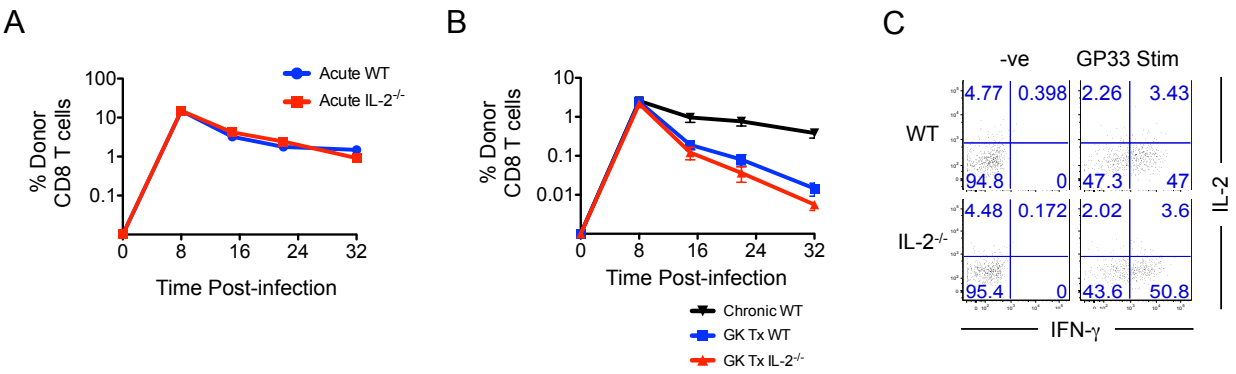

Figure 5

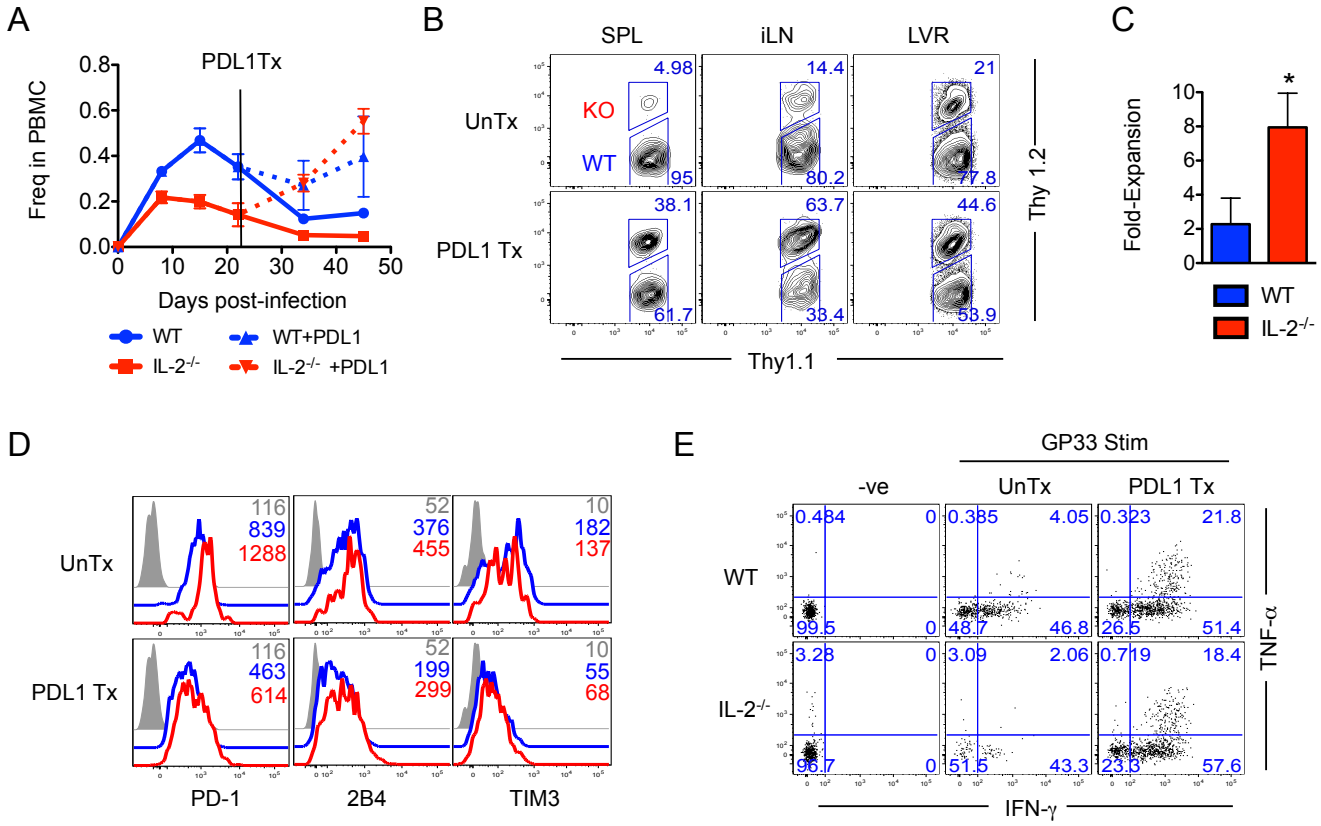
A
PDL1Tx
Freq in PBMC
0.8
0.6
0.4
0.2
0.0
0
10
20
30
40
50
Days post-infection
WT
IL-2-/-
WT+PDL1
IL-2-/- +PDL1
B
SPL
iLN
LVR
UnTx
PDL1 Tx
KO
WT
4.98
14.4
21
95
80.2
77.8
38.1
63.7
44.6
61.7
38.4
58.9
Thy 1.2
Thy1.1
C
Fold-Expansion
10
8
6
4
2
0
*
WT
IL-2-/-
D
UnTx
PDL1 Tx
116
839
1288
52
376
455
10
182
137
116
463
614
52
199
299
10
55
68
PD-1
2B4
TIM3
E
GP33 Stim
-ve
UnTx
PDL1 Tx
WT
IL-2-/-
0.484
0
99.5
0
0.385
4.05
48.7
46.8
0.323
21.8
26.5
51.4
3.28
0
96.7
0
3.09
2.06
51.5
43.3
0.719
18.4
23.3
57.6
TNF-α
IFN-γ

Supplemental Figure 5

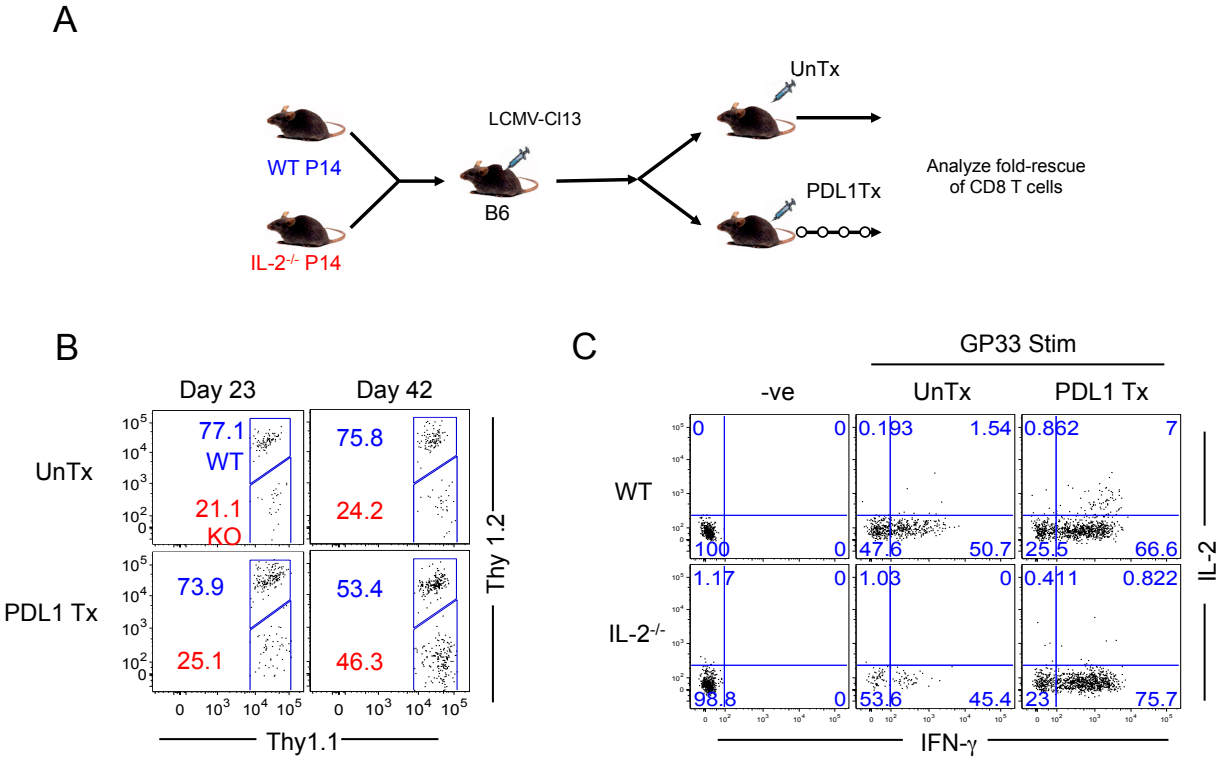

Figure Legends:

Figure 1. Cytotoxic CD8 T cells lose autocrine IL-2 function early during chronic exhaustion. A-B. GP33 specific CD8 T cells were adoptively transferred into naïve B6 mice. Mice were subsequently infected with either $LCMV_{Arm}$ (Acute) or $LCMV_{CL\text{-}13}$ (Chronic). **A**. Line-graph shows longitudinal frequency of antigen-specific CD8 T cells in blood of infected mice. **B**. Spleens were collected from infected mice at indicated times post-infection and stimulated direct ex vivo with GP33 peptide and cytokine production was assessed. FACS plots are gated on donor antigen-specific CD8 T cells. Frequencies show percent double positive donor cells. Bar graphs display mean and SEM. Data are representative of more than 5 independent experiments with n=3-5 mice per group.

Figure 2. Priming and early effector expansion is not dependent on autocrine IL-2 signals. A. Naïve WT and IL-$2^{-/-}$ GP33 specific CD8 T cells were adoptively cotransferred into naïve B6 mice. Mice were infected with $LCMV_{CL\text{-}13}$. Tissues were collected at day 2.75 and 5 post-infection. **B**. Splenocytes were analyzed at day 2.75 post-infection. Histograms are gated on donor antigen-specific CD8 T cells. Percent in histogram indicates frequency of cells past the first division. Numbers in histogram indicate MFI of given marker. **C**. Splenocytes were stimulated with GP33 direct *ex vivo* and cytokine production was assessed. FACS plots are gated on donor CD8 T cells. **D-E**. Tissues were collected at day 5 post-infection. **D**. FACS plots are gated on donor CD8 T cells. **E**. Bar graphs depict number of donor CD8 T cells in each tissue. Bar graphs display mean and SEM. Data are representative of 3 independent experiments with n=3 mice per group.

Supplemental Figure 2. Ablation of autocrine IL-2 results in decreased cell cycling during effector expansion. WT and IL-$2^{-/-}$ GP33 specific CD8 T cells were adoptively cotransferred into naïve B6 mice. Mice were infected with $LCMV_{CL\text{-}13}$. Tissues were

collected at day 2.75 (**A-C**) and 5 (**D-E**) post-infection. **A**. Splenocytes were analyzed at day 2.75 post-infection. FACS plots are gated on donor CD8 T cells. Day 0 represents control, uninfected mice. **B**. Bar graph shows MFI of markers expressed by donor T cells in spleen. **C**. Splenocytes were stimulated with GP33 direct *ex vivo* and cytokine production was assessed. FACS plots are gated on donor CD8 T cells. **D-E**. Mice were treated with BrdU 12hrs prior to tissue collection. Tissues were collected at day 5 post-infection. **D**. FACS plots are gated on donor CD8 T cells. **E**. Bar graphs show frequency of donor CD8 T cells staining positive for BrdU. Bar graphs display mean and SEM. Data are representative of 3 independent experiments with n=3 mice per group. Paired Student's t-test was used with statistical significance in difference of means represented as * ($P \leq 0.05$), ** ($P \leq 0.01$).

Figure 3. Decreased accumulation of effector CD8 T cells in the absence of autocrine IL-2. WT and IL-$2^{-/-}$ GP33 specific CD8 T cells were adoptively cotransferred into naïve B6 mice. Mice were infected with $LCMV_{CL\text{-}13}$. Tissues were collected at day 8 post-infection. **A.** FACS plots are gated on donor CD8 T cells. **B**. Bar graphs depict number of donor CD8 T cells in each tissue. **C.** Splenocytes of infected mice were analyzed for expression of exhaustion and effector markers PD-1 and GzmB, respectively. Histograms are gated on WT (Blue) or IL-$2^{-/-}$ (Red) donor CD8 T cells. Gray histograms are gated on endogenous naïve ($CD44^{lo}$)CD8 T cells. **D.** Splenocytes were stimulated with GP33 direct *ex vivo* and cytokine production was assessed. FACS plots are gated on donor CD8 T cells. Bar graphs display mean and SEM. Data are representative of 5 independent experiments with n=3-5 mice per group. Paired Student's t-test was used with statistical significance in difference of means represented as * ($P \leq 0.05$), ** ($P \leq 0.01$).

Supplemental Figure 3. Conditional ablation of autocrine IL-2 results in decreased effector accumulation. A-D. WT and IL-$2^{-/-}$ GP33 specific CD8 T cells were adoptively cotransferred into naïve B6 mice. Mice were infected with $LCMV_{CL-13}$. Tissues were collected at day 8 post-infection. **A**. Mice were injected with fluorescent CD8b antibody prior to tissue collection to determine resident and circulatory CD8 T cells. FACS plots are gated on donor CD8 T cells. **B**. Bar graphs depict percent localization of WT and IL-$2^{-/-}$ effector cells between different tissues and between circulatory and resident niches. **C**. Splenocytes of infected mice were analyzed for expression of exhaustion markers. Histograms are gated on WT (Blue) or IL-$2^{-/-}$ (Red) donor CD8 T cells. Gray histograms are gated on endogenous naïve ($CD44^{lo}$)CD8 T cells. **D**. Splenocytes were stimulated with GP33 direct *ex vivo* and cytokine production was assessed. FACS plots are gated on donor CD8 T cells. **E-F**. IL-$2^{fl/fl}$ Cre-ERT naïve P14 mice were left untreated (UnTx) or treated with Tamoxifen (Tam Tx). CD8 T cells were isolated from UnTx or Tam Tx naïve P14 mice (Thy1.2/1.2) and cotransferred with control WT CD8 T cells (Thy1.1/1.1) into naïve B6 mice. Mice were subsequently infected with $LCMV_{CL-13}$ and tissues were collected at day 8 post-infection. **E**. FACS plots are gated on donor CD8 T cells. Frequencies show ratio of Flox mice to their WT controls. **F**. Bar graph depicts number of donor UnTx or Tam Tx IL-$2^{fl/fl}$ CD8 T cells at day 8 post-infection. Bar graphs display mean and SEM. Data are representative of 2 independent experiments with n=3-5 mice per group. Unpaired Student's t-test was used with statistical significance in difference of means represented as * ($P \leq 0.05$).

Figure 4. Ablation of autocrine IL-2 results in exacerbated CD8 T cell contraction. WT and IL-$2^{-/-}$ GP33 specific CD8 T cells were adoptively cotransferred into naïve B6 mice. Mice

were infected with $LCMV_{CL-13}$. PBMC of infected mice was analyzed longitudinally throughout infection and tissues were collected following exhaustion. **A.** Line graph depicts frequency of donor CD8 T cells in PBMC of infected animals. **B**. Bar graph shows percent contraction of donor cells from peak of effector expansion (Day 8) and exhaustion (day 37). **C**. Bar graphs depict number of donor CD8 T cells in respective tissues at day 37 post-infection. **D**. FACS plots are gated on donor CD8 T cells in respective tissues at day 37 post-infection. **E.** Line graph depicts expression of donor PD-1 in PBMC. **F**. PBMC of infected mice was analyzed for expression of effector marker GzmB. Histograms are gated on WT (Blue) or IL-$2^{-/-}$ (Red) donor CD8 T cells. Gray histograms are gated on endogenous naïve ($CD44^{lo}$)CD8 T cells. **G.** FACS plots are gated on GP33 specific CD8 T cells in spleen of infected animals at day 22 post-infection. **H.** Splenocytes were stimulated with GP33 direct *ex vivo* and cytokine production was assessed. FACS plots are gated on donor CD8 T cells. Bar graphs display mean and SEM. Data are representative of 3 independent experiments with n=3-5 mice per group. Paired Student's t-test was used with statistical significance in difference of means represented as * ($P \leq 0.05$), ** ($P \leq 0.01$).

Supplemental Figure 4. Antigen-specific CD8 T cells maintain independently of autocrine IL-2 during acute infections. A. WT and IL-$2^{-/-}$ GP33 specific CD8 T cells were adoptively cotransferred into naïve B6 mice. Mice were infected with $LCMV_{Arm}$. PBMC of infected mice was analyzed longitudinally throughout infection. Line graph depicts frequency of donor CD8 T cells in PBMC of infected animals. **B**. WT and IL-$2^{-/-}$ GP33 specific CD8 T cells were adoptively cotransferred into naïve B6 mice. Mice were depleted of CD4 T cells prior to infection by GK1.5 treatment and then infected with $LCMV_{Arm}$. PBMC of infected mice was analyzed longitudinally throughout infection. Line graph depicts

frequency of donor CD8 T cells in PBMC of infected animals. Black line depicts normal frequency of WT CD8 T cells during a CD4 T cell sufficient response. **C.** Splenocytes were stimulated with GP33 direct *ex vivo* and cytokine production was assessed. FACS plots are gated on donor CD8 T cells. Bar graphs display mean and SEM. Data are representative of 2 independent experiments with n=3-5 mice per group.

Figure 5. Increased sensitivity to checkpoint blockade therapy by CD8 T cells following autocrine IL-2 ablation. A. WT and IL-$2^{-/-}$ GP33 specific CD8 T cells were adoptively cotransferred into naïve B6 mice. Mice were infected with $LCMV_{Arm}$. Following exhaustion (day 22 post-infection) mice were treated with aPDL1 antibody. PBMC of infected mice was analyzed longitudinally throughout infection. Line graph depicts frequency of donor CD8 T cells in PBMC of infected animals. **B**. Tissues were collected at day 37 post-infection. FACS plots are gated on donor CD8 T cells. Frequencies show ratio of WT and IL-$2^{-/-}$ donor CD8 T cells. **C.** Bar graph show fold-rescue over pretreated frequencies of donor cells following PDL1 checkpoint blockade. **D**. Spleens of infected mice were analyzed for exhaustion markers. Histograms are gated on WT (Blue) or IL-$2^{-/-}$ (Red) donor CD8 T cells. Gray histograms are gated on endogenous naïve ($CD44^{lo}$)CD8 T cells. **E**. Splenocytes were stimulated with GP33 direct *ex vivo* and cytokine production was assessed. FACS plots are gated on donor CD8 T cells. Bar graphs display mean and SEM. Data are representative of 2-3 independent experiments with n=3 mice per group. Paired Student's t-test was used with statistical significance in difference of means represented as * ($P \leq 0.05$).

Supplemental Figure 5. Similar rescue of function in WT and IL-$2^{-/-}$ CD8 T cells following checkpoint blockade. A. WT and IL-$2^{-/-}$ GP33 specific CD8 T cells were

adoptively cotransferred into naïve B6 mice. Mice were infected with $LCMV_{Arm}$. Following exhaustion (day 22 post-infection) mice were treated with aPDL1 antibody. **B**. FACS plots are gated on donor cells in PBMC of infected mice at indicated times post-infection. **C**. Splenocytes were stimulated with GP33 direct *ex vivo* and cytokine production was assessed. FACS plots are gated on donor CD8 T cells. Bar graphs display mean and SEM. Data are representative of 2-3 independent experiments with n=3 mice per group.